Department for Energy Security & Net Zero

LEEDS BECKETT UNIVERSITY
LEEDS SUSTAINABILITY INSTITUTE

DEEP Report 2.05

Case Study 55AD & 57AD

October 2024

Prepared for DESNZ by

Professor David Glew, Leeds Beckett University (LBU)

LBU contributing authors (alphabetically):

Mark Collett
Dr Martin Fletcher
Dr Adam Hardy
Beth Jones
Dominic Miles-Shenton
Dr Kate Morland
Dr Jim Parker
Dr Kambiz Rakhshanbabanari
Dr Felix Thomas
Dr Christopher Tsang

Any enquiries regarding this publication should be sent to us at: EnergyResearch@energysecurity.gov.uk

Contents

Executive summary

55AD and 57AD, are a pair of identical semi-detached homes, and are two of fourteen DEEP case study homes in which the comparison between a whole house and piecemeal approach to retrofit was evaluated.

The retrofit in 55AD consisted of external wall insulation (EWI), loft and ground floor insulation, new windows and external doors, and new bay roof insulation. In addition, a 'whole house approach' was adopted so discontinuities in fabric insulation were avoided. In 57AD a similar retrofit took place, but no new windows, doors, or bay roof insulation were installed. Additionally, a *'piecemeal approach'* was adopted, i.e. discontinuities were left between fabric insulation (for testing purposes) then completed later. The retrofit in 55AD and 57AD reduced the heat transfer coefficient (HTC) from (239 ± 9) W/K to (104 ± 11) W/K, and from (225 ± 9) W/K to (130 ± 13) W/K, respectively. The EWI was responsible for 70 % and 77 % of the overall savings in the homes, respectively, and was singularly responsible for their EPC improving from a D to C.

Thermal bridging calculations undertaken pre-retrofit showed almost all junctions in the homes were at risk of surface condensation. 55AD's retrofit eliminated almost all risks. In 57AD, post-retrofit, risk persisted at the discontinuities between the EWI and the bay roof, eaves, and first floor window heads. This corresponded to 57AD having 11 W/K higher modelled thermal bridging heat loss post-retrofit, i.e. 10 % of the overall measured HTC.

55AD's retrofit cost £56,161, while 57AD's retrofit cost £28,948: less than half; suggesting the piecemeal retrofit was more cost effective, given it achieved around three quarters of the HTC reductions. However, the main benefit of a whole house approach is to reduce condensation risks. This case study showed that the almost £2,000 spent to insulate 55AD's bay roof and eaves successfully removed condensation risks; and where this didn't happen in 57AD, the risk worsened. However, in some instances, the piecemeal retrofit successfully removed condensation risk at the windows in 57AD. This suggests that the £8,000 spent installing 55AD's windows in plywood boxes, so they could be moved in line with the EWI, may not have been essential.

Overheating risk was found to be significantly affected by local shading. 55AD has higher risk, since being on the south side of 57AD, it receives more solar gains. Insulating the ground floor limits the cooling effect of the sub-floor void in summer, so increases overheating risk in both homes.

Co-pressurisation highlighted that inter-dwelling air exchanges made up a third of all air leakage measured by the blower door test. Post-retrofit, the homes were found to be only just above the limiting 5 $m^3/(h \cdot m^2)$ @ 50Pa natural ventilation recommended threshold. Such potential over-reporting of inside to outside air leakage has implications for the blower door testing.

Models predict higher HTC and retrofit savings than the coheating tests measured, even when measured airtightness and U-values replaced defaults. Adding insulation tends to increase thermal bridging heat loss at junctions. In these case studies, the piecemeal retrofit increased the y-value from 0.10 to 0.18, while the whole house retrofit increased to only 0.11. The DSM model uses SAP Appendix K to calculate y-values from individual Ψ junctions, and this leads to a much higher baseline y-value of 0.25. The default y-value in RdSAP and BREDEM is 0.15, i.e. it also overestimates the predicted heat loss in 55AD, but underestimates in 57AD post-retrofit.

More appropriate y-values in EPCs, and Ψ-values in Appendix K, may be needed to better reflect bridging heat losses for different house types and retrofit stages.

1 Introduction

Case studies 55AD and 57AD are a pair of three-bedroom semi-detached, 1930s solid walled homes. As an identical pair, it offered the opportunity to install two identical deep retrofits, one in a piecemeal approach and the other as a whole house retrofit approach including external wall insulation (EWI). In 55AD, the ground floor, loft, external walls, bay window roof, external windows, and doors were all retrofitted in one go; and care was taken to ensure that a continuous insulation layer was maintained. In 57AD, the ground floor, loft, and external walls were all insulated as if they were independent fabric elements; while no new external windows, doors, or bay roof insulation were installed.

1.1 DEEP field trial objectives

55 and 57AD are two of fourteen DEEP case studies, which, collectively, will attempt to investigate research objectives listed in Table 1-1; though not all the objectives are addressed by each case study.

Table 1-1 DEEP Research objectives

Objective	Rationale
Model input accuracy	Policy relies on models with known limitations; exploring inputs and model robustness will improve policy advice.
Unintended consequence	More retrofit scenarios need modelling to confirm condensation, underperformance, air quality, and comfort risks
Cumulative impact	Piecemeal retrofits are common; clarity is needed on impact of different options including achieving EPC band C.
Fabric vs ventilation	Insulation influences fabric and ventilation heat loss, yet models currently only attribute savings to U-value changes.
Floor retrofit	80 % of homes have uninsulated floors; clarity on benefits may increase installation from 0.5 % of ECO measures.
Airtightness retrofit	Infiltration undermines retrofits; balancing airtightness and indoor air quality is an unexploited ECO opportunity.
Neighbour risk	Clarity is needed on whether whole house or staged retrofits affect condensation risk for neighbours

1.2 Case study research questions

Over the course of the three-year project and following advice from DESNZ, the wider DEEP Steering Group, and Expert QA panel, additional questions have been proposed and the objectives refined to develop seven discrete research questions. These are listed below and will be used to discuss the findings:

1. *What combinations of retrofits are needed to bring solid walled homes up to an EPC band C? Do these represent value for money and what challenges do they face?*
2. *To what extent do unintended consequences reduce energy efficiency savings and increase moisture risks, when insulating solid walled homes?*
3. *Are methods to reduce the potential risk of unintended consequences when retrofitting solid walled homes effective and appropriate?*
4. *How significant is airtightness in domestic energy efficiency, and is improving airtightness a practical, low risk retrofit measure for inclusion in domestic energy efficiency policy?*
5. *How accurate can energy modelling of retrofits be, and how can EPCs be improved for use in retrofit performance prediction?*
6. *How can thermal modelling support risk management and retrofit energy modelling predictions?*
7. *How effective are low pressure Pulse tests and QUB tests as alternatives to the blower door test and the coheating test?*

Data collected from case studies 55AD and 57AD will not answer all these research questions but will contribute to a body of evidence from the DEEP project, that may begin to address these questions.

1.3 Case study house information

55AD and 57AD, shown in Figure 1-1 and Figure 1-2, are two identical (when built) three-bedroom properties located in Loughborough, Leicestershire. They were built in the 1930s. They are a pair of two storey, semi-detached houses, of solid nine-inch brick, suspended timber ground floors, and were wet-plastered internally. They have a cold pitched roof construction, i.e. have loft insulation on the first floor ceiling and a ventilated roof space. Both houses have a rendered front elevation at first floor level and finished with brick quoins at the corners. At the front, each house also has a single storey splayed bay window and recessed entrance porch. The roof is hipped and both properties share a centrally located chimney stack. The slope of the site means that there are slightly more steps to access 55AD than 57AD. Therefore, the void under the suspended timber ground floor at 55AD is greater than that under 57AD.

There are over 2.6 million homes in England and Wales that were built between 1930 and 1949,[1] and three-bedroom semi-detached homes make up around 12 % of all homes [1]. Therefore, there may be nearly 320,000 homes that are similar to 55AD and 57AD. However, the construction of 55AD and 57AD may not be typical of the period, as cavity walls were becoming the norm. While the results from 55AD and 57AD cannot be directly transferable across all three-bedroom semi-detached properties of the era, the features of the case study do, nevertheless, enable a deeper understanding of heat loss across a party wall. The results also highlight the difference between piecemeal and whole house retrofit, particularly where the sequencing of retrofits may affect performance.

Figure 1-1 Case study house (57 on the left and 55 on the right)

Figure 1-2 Case study houses site location plan

2.05 DEEP 55 & 57AD

Floor plans, elevations and sections can be seen in Figure 1-3, Figure 1-4 and Figure 1-5 respectively.

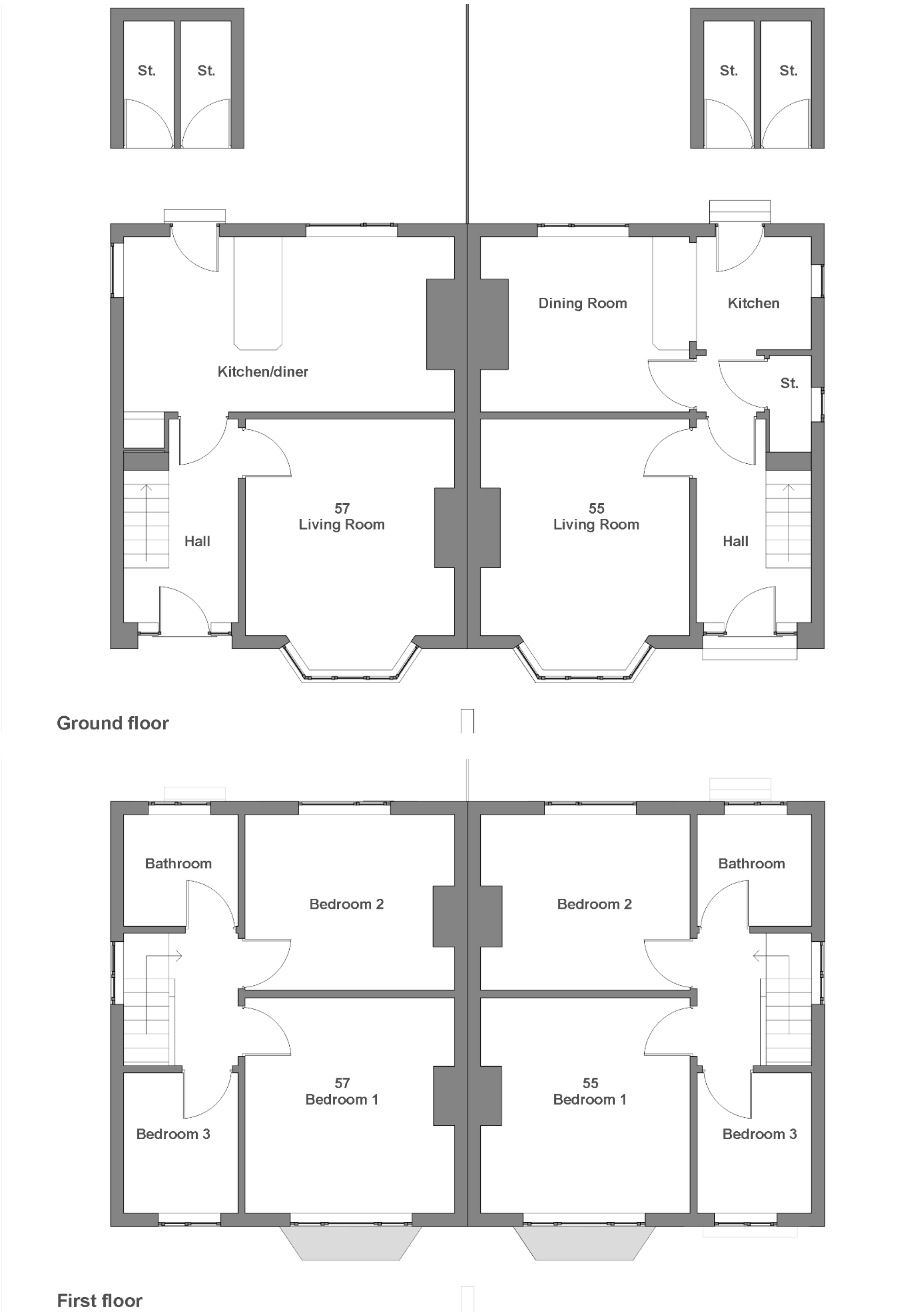

Figure 1-3 House floor plans

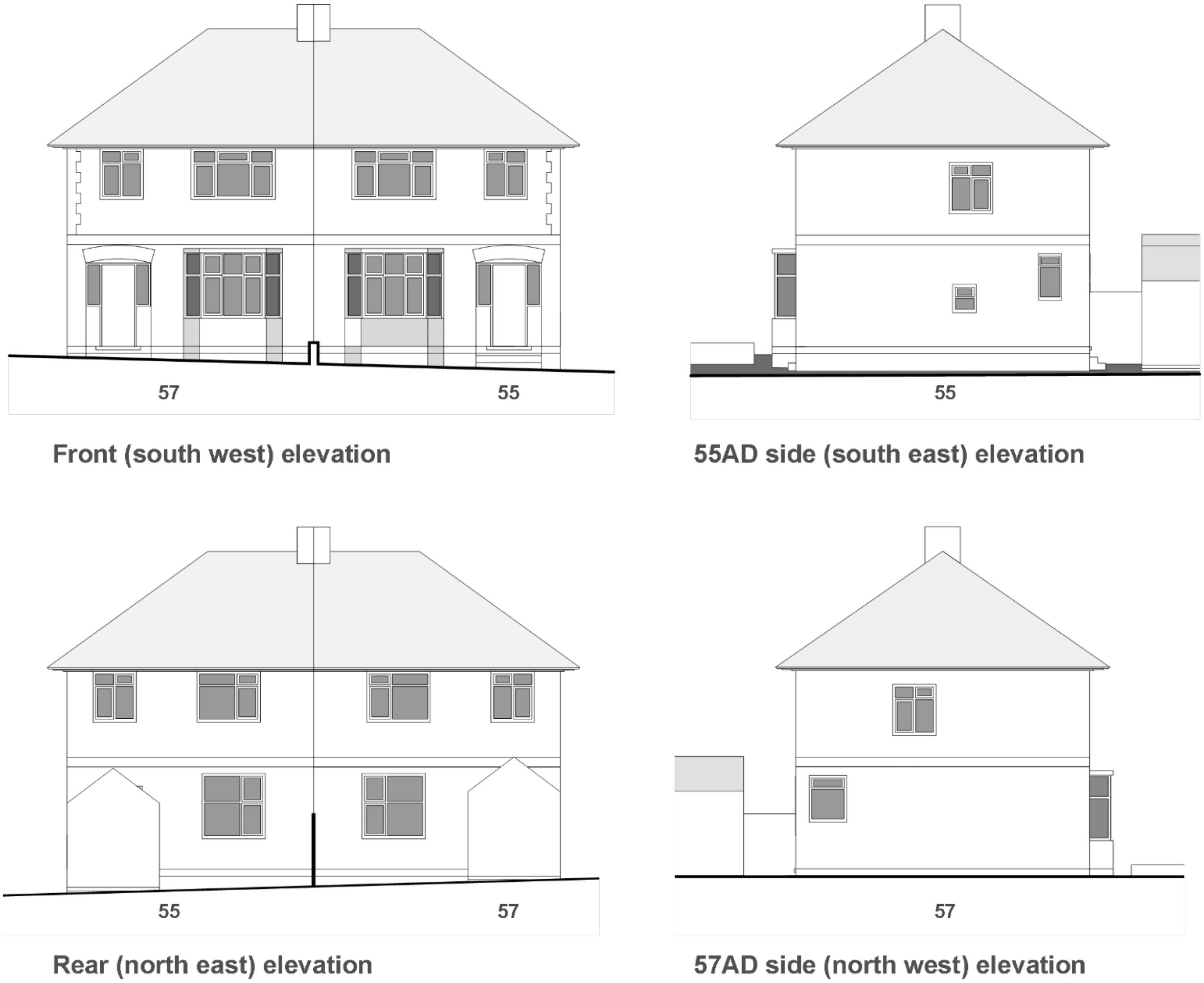

Figure 1-4 Elevations

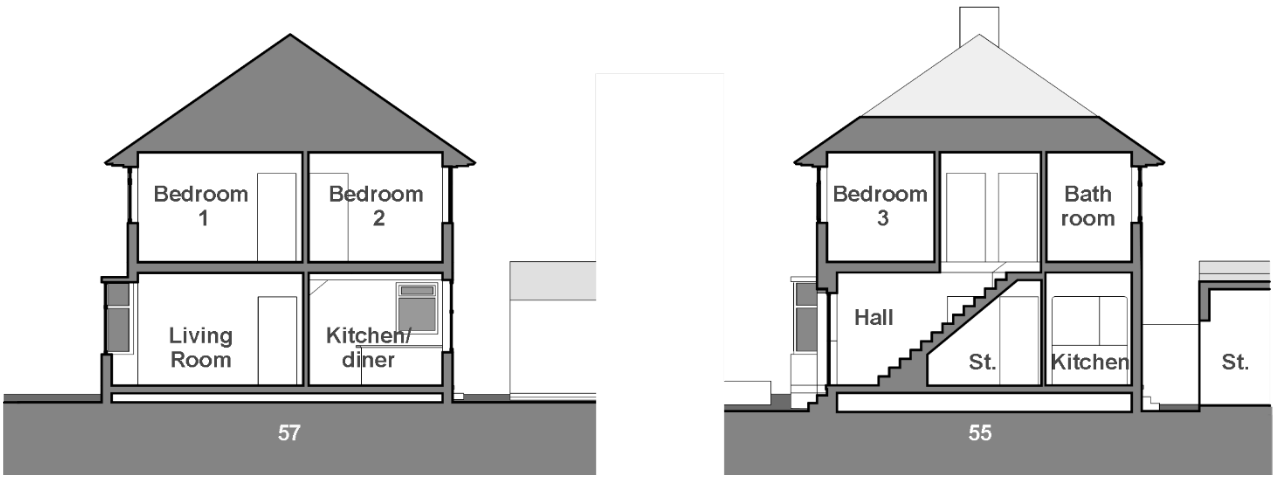

Figure 1-5 Sections through each case study house

The dimensions of each element in the home are listed in Table 12 and were used to allocate heat losses as well as generate thermal models in RdSAP, BREDEM, and DSM. The only difference in the layout and heated volume occurs at ground floor level, while 57AD also has different gable wall window positions.

In 57AD, the kitchen and dining area form one large room. Also, there is no understairs cupboard that is accessible from the hallway. Instead, there is a large storage cupboard in the kitchen that recesses into the understairs space. However, it only extends from kitchen countertop to ceiling level, meaning that the understairs space below this cupboard is inaccessible.

Conversely, at 55AD, the kitchen is reduced to accommodate a small hall which provides access to the dining room, kitchen and understairs cupboard. While there is a large opening between the kitchen and dining room, the rear of the kitchen units forms a breakfast bar.

Additionally, there was waterproof laminated foam wet room panelling in the bathroom of 55AD providing 10 mm of foam (PUR) internal wall insulation (IWI). These differences will impact on the energy calculations in the models since they impact the treated volume and heat loss.

Since there was access to both homes any inter-dwelling heat exchange and air movement across the solid party wall could also be investigated.

Table 1-2 House dimensions

Detail	Measurement
Volume	*207.27 m^3*
Total floor area	*78.00 m^2*
Total heat loss area	*176.66 m^2*
Ground floor	*38.88* m^2
Front external wall	*20.49* m^2
Rear external wall	22.24 m^2
Side external wall	*33.09* m^2
Windows	*18.49* m^2
Door	*2.97* m^2
Ceiling	*39.12* m^2
Bay window ceiling	*1.38* m^2
Party wall	*44.22* m^2

1.4 Retrofit approach

The retrofit details and U-value targets for each element are listed in Table 1-3.

Table 1-3 Construction and retrofit summary

Detail	Original construction (as found prior to DEEP retrofits)	Retrofit[1]
Airtightness	13.1 $m^3/(h.m^2)$@50Pa (55AD) 11.7 $m^3/(h.m^2)$@50Pa (57AD)	No specific retrofit
Ground floor[2]	Uninsulated suspended timber	Mineral wool between joists 150 mm x @0.032 W/(m·K) Target U-value: 0.20 $W/(m^2{\cdot}K)$
Wall type 1 (Rear, side, and front elevation at GF)[3]	Uninsulated 9-inch solid brick	EWI (8mm Render + 120 mm @ 0.036 W/(m·K) Mineral Fibre Dual Density Insulation + 2 mm Adhesive) Target U-value 0.31 $W/(m^2{\cdot}K)$
Wall type 2 (Front elevation at FF)[4]	Uninsulated rendered 9-inch solid brick	EWI (8 mm Render + 120 mm @ 0.036 W/(m·K) Mineral Fibre Dual Density Insulation + 2 mm Adhesive) Target U-value 0.26 $W/(m^2{\cdot}K)$
Wall type 3 (Side, bathroom, FF)	Uninsulated 9-inch solid brick with thin laminated foam (inside) – **55AD only**	EWI (8 mm Render + 120 mm @ 0.036 W/(m·K) Mineral Fibre Dual Density Insulation + 2 mm Adhesive) Target U-value 0.24 $W/(m^2{\cdot}K)$
Wall type 4 (Rear, bathroom, FF)	Uninsulated 9-inch solid brick with thin laminated foam and plywood (inside) – **55AD only**	EWI (8 mm Render + 120 mm @ 0.036 W/(m·K) Mineral Fibre Dual Density Insulation + 2 mm Adhesive) Target U-value 0.23 $W/(m^2{\cdot}K)$
Wall below damp proof course (DPC)	Uninsulated 9-inch solid brick	EWI (8 mm Render + 100 mm @ 0.030 W/(m·K) EPS Insulation + 2 mm Adhesive) Target U-value 0.26 $W/(m^2{\cdot}K)$
Windows (Double glazed)	uPVC Double glazed	uPVC Double glazed – **55AD only** U-value: 1.60 $W/(m^2{\cdot}K)$ Fitted inside plywood box

[1] Target U-values based on assumed construction details and may vary from Approved Document Part L maximums according to manufacturer recommendations or space limitations.
[2] In 57AD, the floor section below stairs was not insulated post-retrofit.
[3] In 57AD, the wall section above soffit was not insulated post-retrofit.
[4] In 57AD, the wall section above soffit was not insulated post-retrofit.

Detail	Original construction (as found prior to DEEP retrofits)	Retrofit[1]
External windows (single glazed)[5]	Single glazed front entrance side light	EWI (3 mm Render + 120 mm @ 0.036 W/(m·K) Mineral Fibre Dual Density Insulation + 2 mm Adhesive) + IWI (120 mm mineral wool IWI @ 0.032 W/(m·K)) Target U-value 0.19 W/(m^2·K)
External door	Timber	Composite – **55AD only** U-value: 1.8 W/(m^2·K)
Loft	Ceiling joist with mineral wool between (55AD: 100 mm, 57AD: 150 mm)	Ceiling joist with mineral wool between and above joists 300 mm @0.044 W/(m·K) Target U-value: 0.14 W/(m^2·K) Replacement loft hatch Target U-value: 0.25 W/(m^2·K)
Bay window flat roof	Uninsulated flat roof with plasterboard, joists, and lead	Foam (PIR) insulation between joists – **55AD only** 80 mm @ 0.022 W/(m·K) Target U-value: 0.33 W/(m^2·K)
Hipped roof	Rafters with felt and plain clay tiles	No retrofit
Living Room fireplace	Covered over fireplace with ceramic tiled concrete fire surround	150 mm mineral wool to base of chimney, boxed in by new ventilated timber structure

Figure 1-8 identifies where insulation was found in the homes before any retrofits were carried out. The sequence of the retrofit approach is illustrated, in Figure 1-9 to Figure 1-11. Building Performance Evaluation (BPE) tests, whole house energy modelling, and elemental thermal simulations were conducted at each retrofit stage to quantify changes in energy performance, and to assess the potential for condensation risk. The methodologies for these are described in DEEP Methods Report 2.02.

The codes in Table 1-4 and Table 1-5 are shorthand to identify the retrofit stages in order to aid the discussion and presentation of results.

While retrofits in both homes were undertaken in a single phase, the two different approaches were undertaken to compare the difference between piecemeal retrofits (57AD) and a whole house retrofit (55AD). Following the retrofits investigated in this case study, 57AD (which had the piecemeal retrofit) underwent a final retrofit, such that 57AD eventually had an identical retrofit to 55AD. This took place outside of the heating season, so it was not possible to undertake a final test to understand if the final HTC of the home matched that achieved in 55AD. However it provides useful data on the costs of undertaking these additional elements.

[5] Single glazing was removed and filled post-retrofit.

Table 1-4 Phased retrofit stages for 55AD

	Retrofit Stage	Code	Retrofit Dates
1	Baseline	55AD.B	October - December 2021
2	Whole house approach retrofit (ground floor & loft insulation, new double glazing & external door, EWI including below DPC & behind soffit, bay window roof insulation)	55AD.WH	January 2022

Table 1-5 Phased retrofit stages for 57AD

	Retrofit Stage	Code	Retrofit Dates
1	Baseline	57AD.B	October - December 2021
2	Piecemeal retrofit (ground floor insulation, loft insulation, EWI including below DPC)	57AD.R.F.W	January 2022

Some issues that are worth noting include, as shown in Figure 1-6, the glazing retrofit involved installing the windows inside a plywood box to move them into the EWI, surrounded by airtightness tape and fitted into the brickwork. This projected beyond the outer leaf of brickwork, so the windows could sit in line with the EWI. Window fitters were initially unwilling to install this design since there was a concern that it would not comply with the Fenestration Self-Assessment Scheme (FENSA) guidance. The design was later approved by FENSA, though this was considered an exception by the installer. Without the installer's compliance, the windows would have been left in line with the brickwork; suggesting greater awareness and guidance on this may be needed.

Figure 1-6 Windows and doors installed within plywood box and EWI (55AD)

The solution for 55AD, is in contrast to the conventional solution in 57AD of leaving the existing windows in-situ. This is shown in Figure 1-7, which, as can be seen, results in the window being set back deeper, in line with the existing brickwork; this was expected to cause more thermal bridging.

Figure 1-7 Existing windows and doors (not relaced) when EWI installed (57AD); also showing DPC EWI applied to door threshold

Additionally, the door retrofits were complimented with an additional layer of EWI (XPS) across the front of the door threshold (also visible in Figure 1-7) so that heat losses were minimised, though this required the doorsteps to be removed, at additional cost.

Another difference between the houses was that the existing 100 mm mineral wool loft insulation in 55AD was observed to be in good condition, so this was not removed but topped up to 300 mm. In 57AD, the existing loft insulation was completely removed and replaced with 300 mm of mineral wool (150 mm between joists and 150 mm cross-laid over joists).

Access to the understairs ground floor was available in 55AD, though not in 57AD, so it was left uninsulated in 57AD. This was done as it was assumed to be unlikely that a householder would undertake additional disruption of removing the understairs walls to insulate here. This study, therefore, investigates the impact of leaving this area uninsulated.

Finally, the single glazed side panels to the front doors in both homes were infilled to be simply walls in the post-retrofit homes. This was done since the EWI was so thick that it would have covered over the glazing and meant that it would not have been possible to retain the window.

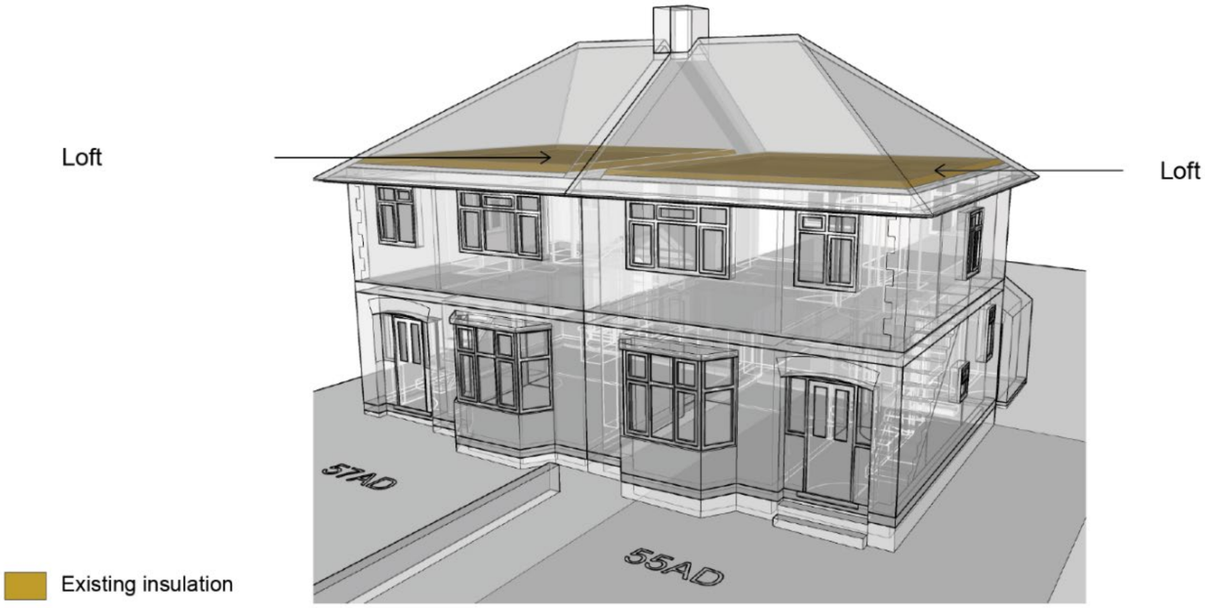

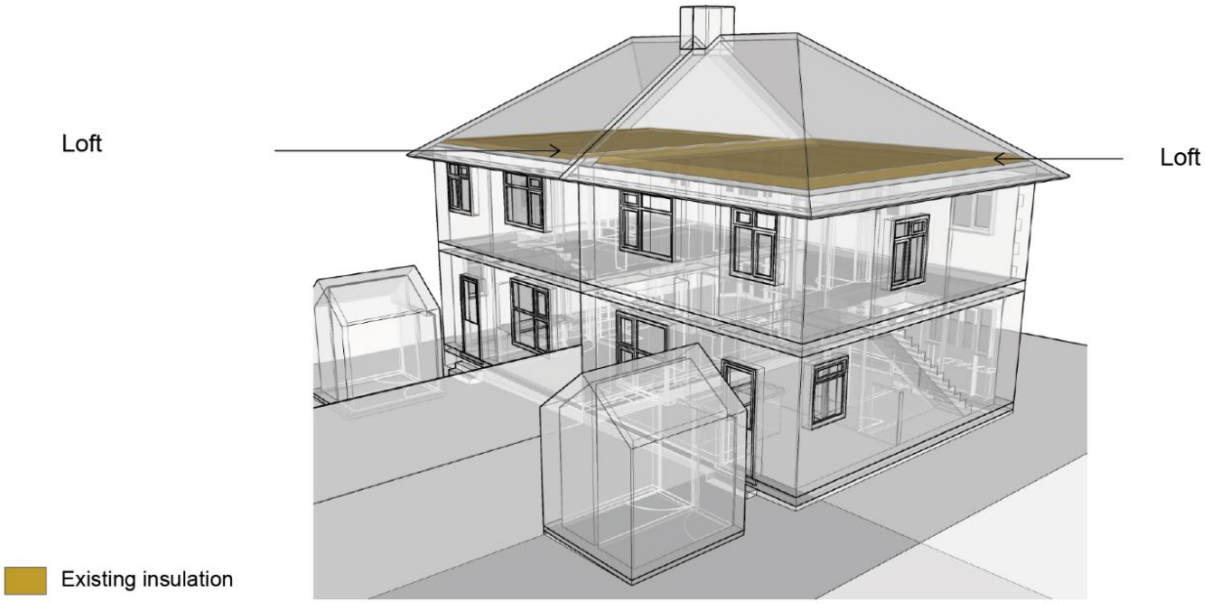

Figure 1-8 Stage 1: Insulation already in the property prior to the retrofits (55AD.B and 57AD.B). Front and rear elevations shown respectively.

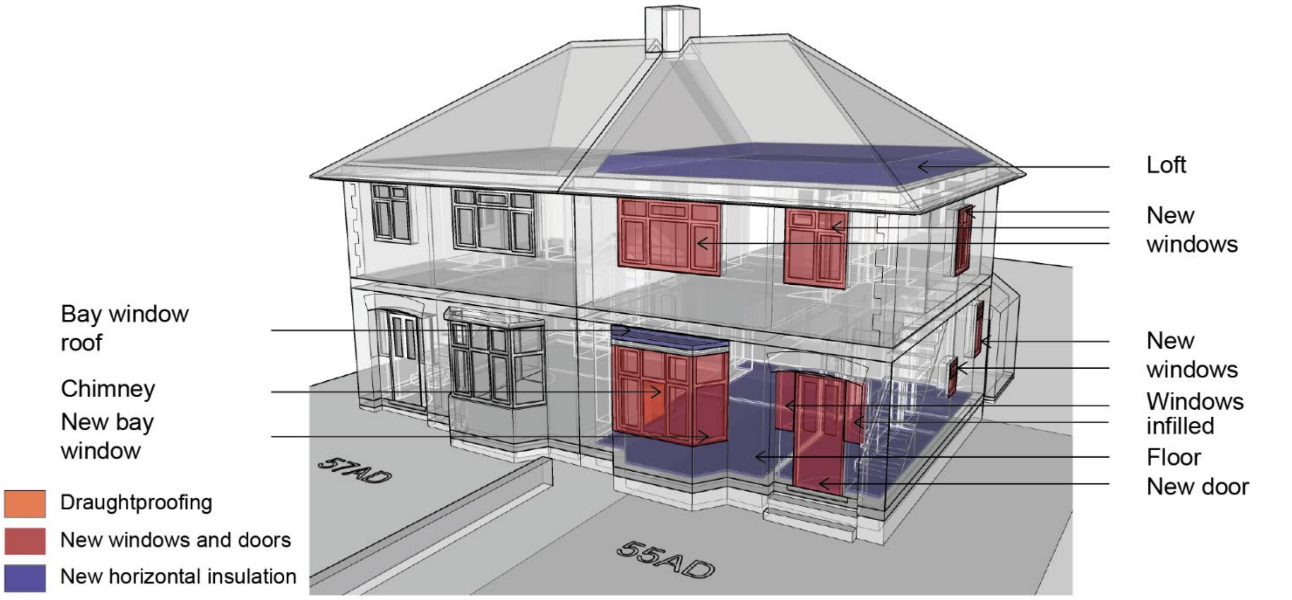

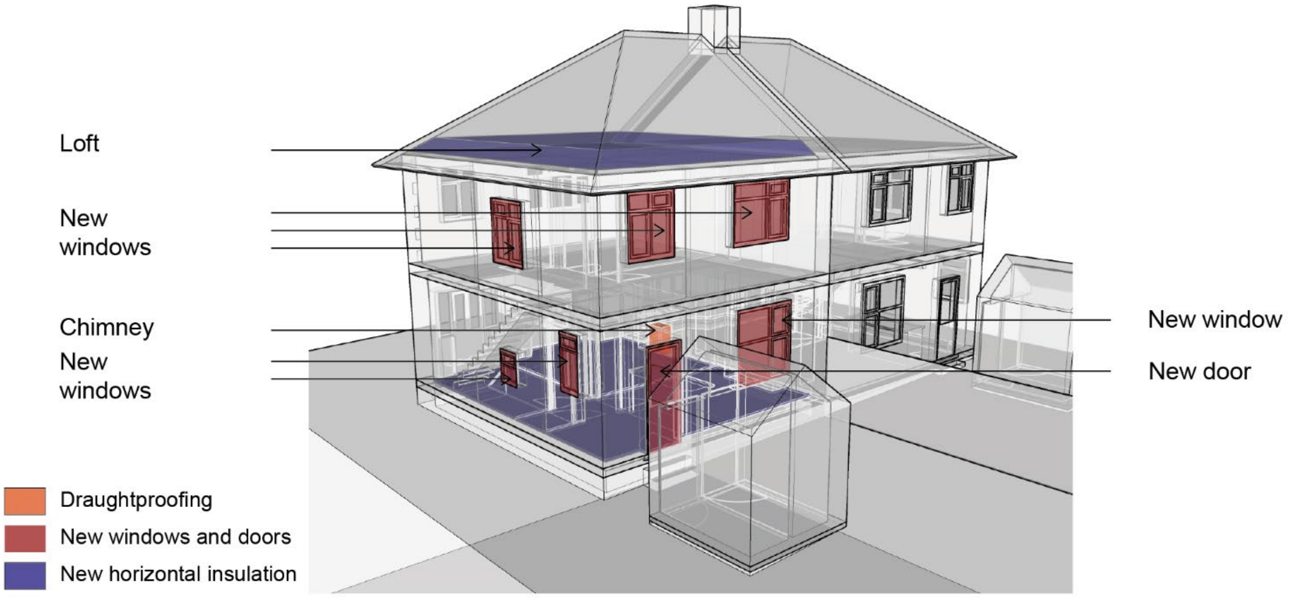

Figure 1-9 Stage 2: Roof, ground floor, glazing and external door retrofit (55AD.WH)[6]. Front and rear elevations shown respectively.

[6] The external wall insulation has been removed from the graphic for clarity and is shown in Figure 1-11

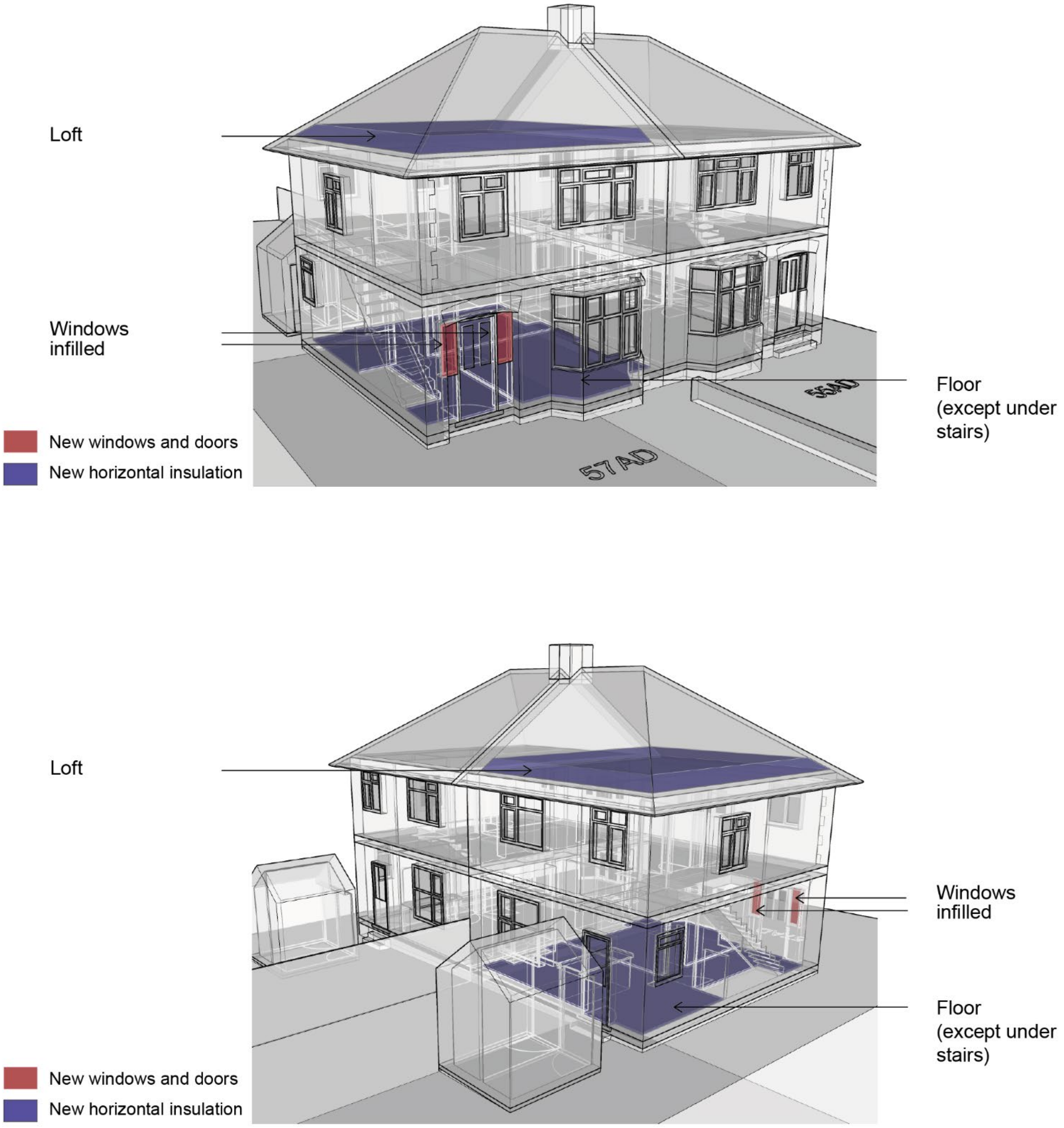

Figure 1-10 Stage 2: Roof, ground floor retrofits (57AD.RFW)[7]. Front and rear elevations shown respectively.

[7] The external wall insulation has been removed from the graphic for clarity and is shown in Figure 1-11

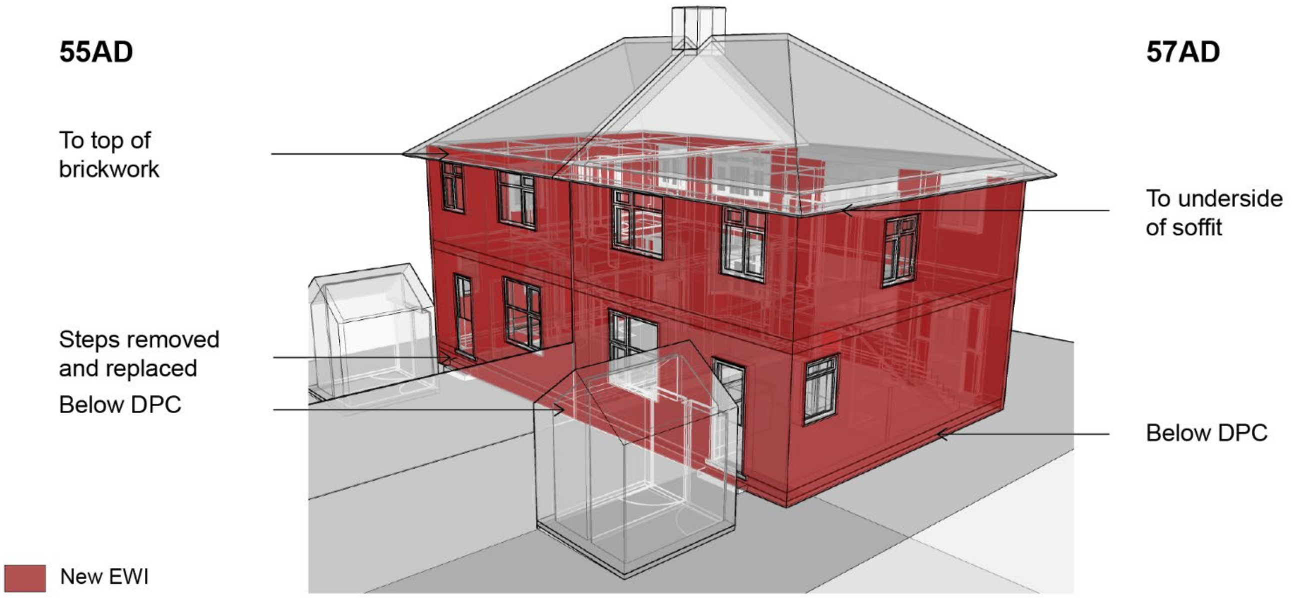

Figure 1-11 Stage 2: Wall retrofits for both 55AD (55AD.WH) and 57AD (57.RFW)[8]. The EWI was installed after the work in Figure 1-9 and Figure 1-10 was complete. Front and rear elevations shown respectively.

[8] The retrofits illustrated in Figure 1-9 and Figure 1-10 have been removed from the graphic for clarity

Case study and retrofit summary

55AD and 57AD provided an opportunity to investigate the impact of undertaking similar retrofits in two identical homes via a piecemeal, compared to a whole house, approach.

The whole house approach retrofit in 55AD includes the loft, floor, new A+ glazing and composite external doors, bay window roof, and EWI with insulation below the DPC.

The piecemeal retrofit in 57AD was similar to 55AD, except that the EWI did not extend behind the soffit and facias, the bay roof was not insulated, and existing windows and doors were left in place: i.e. discontinuities between the EWI and the loft insulation, the bay roof, and the windows and doors were deliberately created to investigate the implications of this on heat loss and condensation risks.

It was also possible to explore heat exchanges across the solid party wall and how this affects building performance evaluation (BPE) tests.

2 Fieldwork and modelling methods

BPE tests and modelling activities were undertaken on the case study homes at each retrofit stage in accordance with the methodologies listed in DEEP Report Methods 2.01. This section outlines the specific implementation of these methods, including any variations and additions.

2.1 Environmental and internal conditions data collection

Internal environmental data logging equipment is described in detail in the Methodologies Annex. Internal environmental data collected at the homes included air temperature, Relative Humidity (RH) and CO_2 levels. External environmental data was collected via a mini weather station located on site, and included vertical solar irradiance, air temperature, and wind speed.

2.2 Measured survey

A detailed survey of the building was undertaken, and from this a digital version of the house was developed using SketchUp. This model was used to calculate dimensions for each element and to draw up the plans shown in Figure 1-3. Plans, sections, and elevations were directly exported as DXFs to generate the geometry for use in Dynamic Simulation Modelling (DSM). The construction makeup of the existing building was also assessed, where access could be gained, to observe the material construction. Finally, core samples of the walls were also taken to perform lab analysis of the material properties and identify the construction layers; the method for which is described in DEEP Report 4, Brick Material Properties.

2.3 Airtightness and thermography

Blower door tests were successfully undertaken at all baseline and retrofit stages. These results were used to identify airtightness changes related to the retrofits and to be able to approximate annual average heat loss attributable to background ventilation (HTC_v). Qualitative thermography under depressurisation was undertaken and additional thermography of specific details, under normal conditions, was captured to identify changes between each retrofit stage. CO_2 tracer gas tests were also deployed during the testing program to compare with the blower door tests results.

2.4 Heat flux density measurement and U-values

64 HFPs (32 in each house) were installed on different elements in the homes. These were installed to measure the improvements in U-values achieved by the fabric upgrades as well as to quantify party wall heat loss experienced during the coheating test. The HFP locations are listed in Table 21, and for context, their locations are visualised in Figure 21 and Figure 22. Thermography was undertaken to identify the most representative HFP location for each fabric element and, where possible, multiple locations for each element were measured.

Heat flux data from individual HFPs, along with internal and external temperature recordings, were used to generate in-situ U-values for each element. Where more than one HFP was located on a single element, an average of the values was used to obtain a single U-value for the element. Where HFPs were placed on representative and non-representative areas, weighting was undertaken based upon the proportion of each across the element measured. Due to the geometry of the dwelling, a number of the HFP measurements would have been influenced by bridging.

The in-situ U-values were used to calibrate energy and thermal models, to estimate the heat loss due to the plane elements of the building fabric (HTC_f), and to compare this with the whole house HTC and disaggregation techniques. It is important to realise that the in-situ U-values are based upon a limited set of measurements, excluding non-repeating and point thermal bridges, so are not necessarily representative of the performance of the element in practice. This has implications for the results obtained using the disaggregated approach and, more importantly, the results of the modelling where in-situ measurements were used as input data.

Due to the building geometry, a number of the HFPs had to be installed in non-ideal locations. In some areas where thermal bridging may be expected, such as near corners, heat flux density measurements have been taken to provide context to the whole fabric heat loss and inform weighted average calculations.

While the BRE calculator has the capacity to calculate the U-value of windows, in these case studies the necessary manufacturer details of the windows were not available. This included the glazing U-value, the frame U-value and internal construction to estimate the linear Ψ-value. The U-values for the windows had to be assumed and this is therefore an area of uncertainty when considering accurate energy model inputs.

Table 2-1 HFP locations

HFP	Element	Room
55AD		
AD1	External wall	Bedroom 1
AD2	External wall (front)	Bedroom 3
AD3	External wall (flank)	Bedroom 3
AD4	External wall (flank)	Landing
AD5	External wall (flank)	Bathroom
AD6	External wall	Bedroom 2
AD7	External wall	Bedroom 2
AD8	Chimney breast	Bedroom 2
AD9	Chimney breast	Bedroom 1
AD10	First floor ceiling	Bedroom 1
AD11	First floor ceiling	Bedroom 1
AD12	First floor ceiling	Bedroom 2
AD13	External wall	Bedroom 2
AD14	Party wall	Bedroom 2
AD15	Party wall	Bedroom 1
AD16	First floor ceiling	Bedroom 2
AF1	Bay window wall	Living room
AF2	External wall	Living room
AF3	External wall (front)	Hall
AF4	External wall (flank)	Hall
AF5	External wall (flank)	Kitchen
AF6	Rear external door	Kitchen
AF7	External wall (rear)	Dining room
AF8	Chimney breast	Dining room
AF9	Party wall	Living room
AF10	Chimney breast	Living room

HFP	Element	Room
AF11	Ground floor	Living room
AF12	Ground floor	Dining room
AF13	External wall	Living room
AF14	Bay window ceiling	Living room
AF15	External wall (rear)	Dining room
AF16	Ground floor	Dining room
57AD		
AB1	External wall	Bedroom 1
AB2	External wall (front)	Bedroom 3
AB3	External wall (flank)	Bedroom 3
AB4	External wall (flank)	Landing
AB5	External wall (flank)	Bathroom
AB6	External wall	Bedroom 2
AB7	External wall	Bedroom 2
AB8	Chimney breast	Bedroom 2
AB9	Chimney breast	Bedroom 1
AB10	First floor ceiling	Bedroom 1
AB11	First floor ceiling	Bedroom 1
AB12	First floor ceiling	Bedroom 2
AB13	External wall	Bedroom 2
AB14	Party wall	Bedroom 2
AB15	Party wall	Bedroom 1
AB16	First floor ceiling	Bedroom 2
AA1	Bay window wall	Living room
AA2	External wall	Living room
AA3	External wall (front)	Hall
AA4	External wall (flank)	Hall
AA5	External wall (flank)	Kitchen/Diner

2.05 DEEP 55 & 57AD

HFP	Element	Room
AA6	Rear external door	Kitchen/Diner
AA7	External wall (rear)	Kitchen/Diner
AA8	Chimney breast	Kitchen/Diner
AA9	Party wall	Living room
AA10	Chimney breast	Living room
AA11	Ground floor	Living room
AA12	Ground floor	Kitchen/Diner
AA13	External wall	Living room
AA14	Bay window ceiling (post-retrofit)	Living room
AA15	External wall (rear)	Kitchen/Diner
AA16	Ground floor	Kitchen/Diner

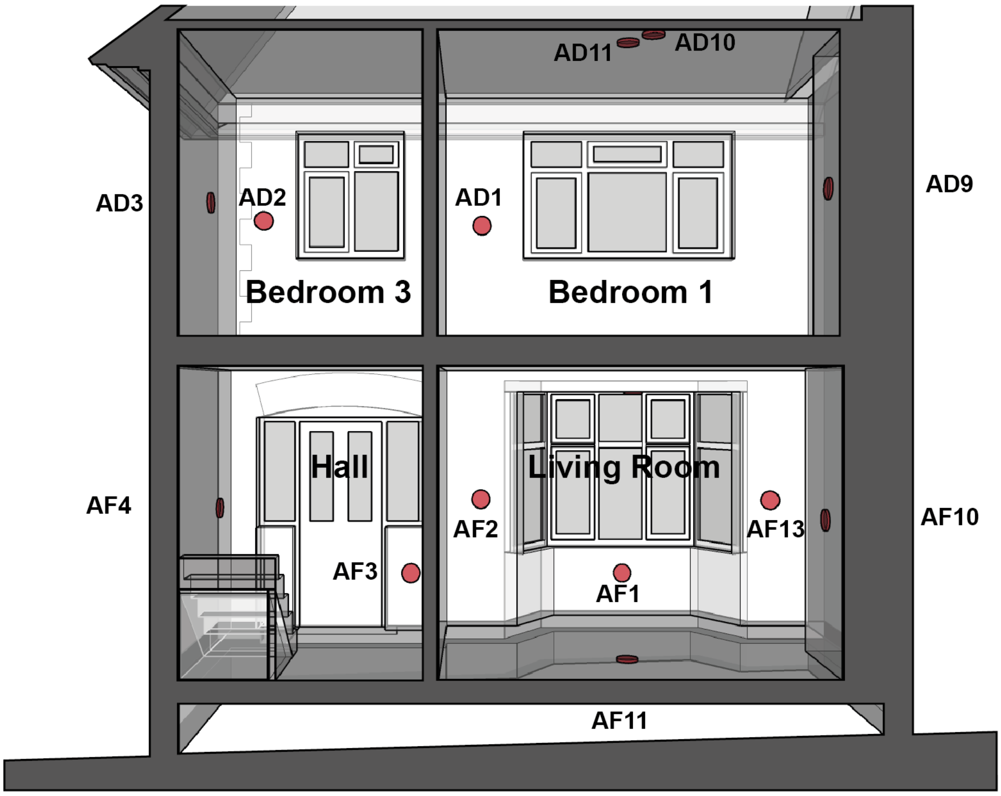
AD11
AD10
AD3
AD2
AD1
AD9
Bedroom 3
Bedroom 1
Hall
Living Room
AF4
AF2
AF13
AF10
AF3
AF1
AF11

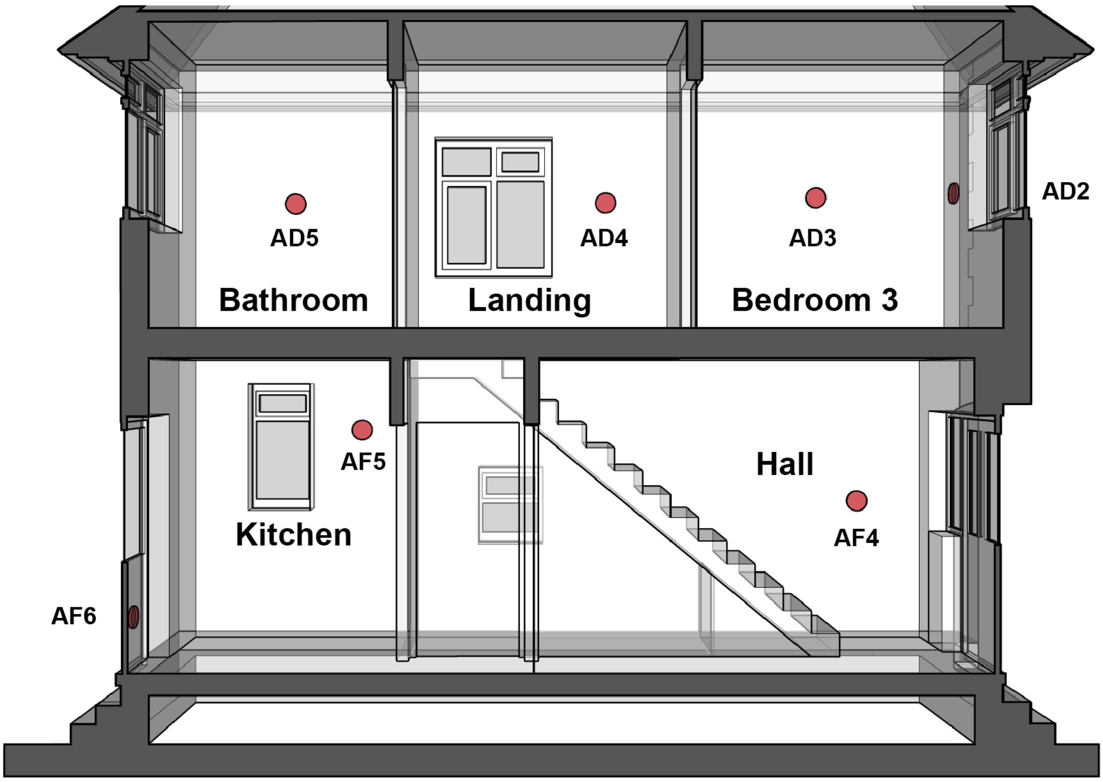
AD5
AD4
AD3
AD2
Bathroom
Landing
Bedroom 3
Kitchen
AF5
Hall
AF4
AF6

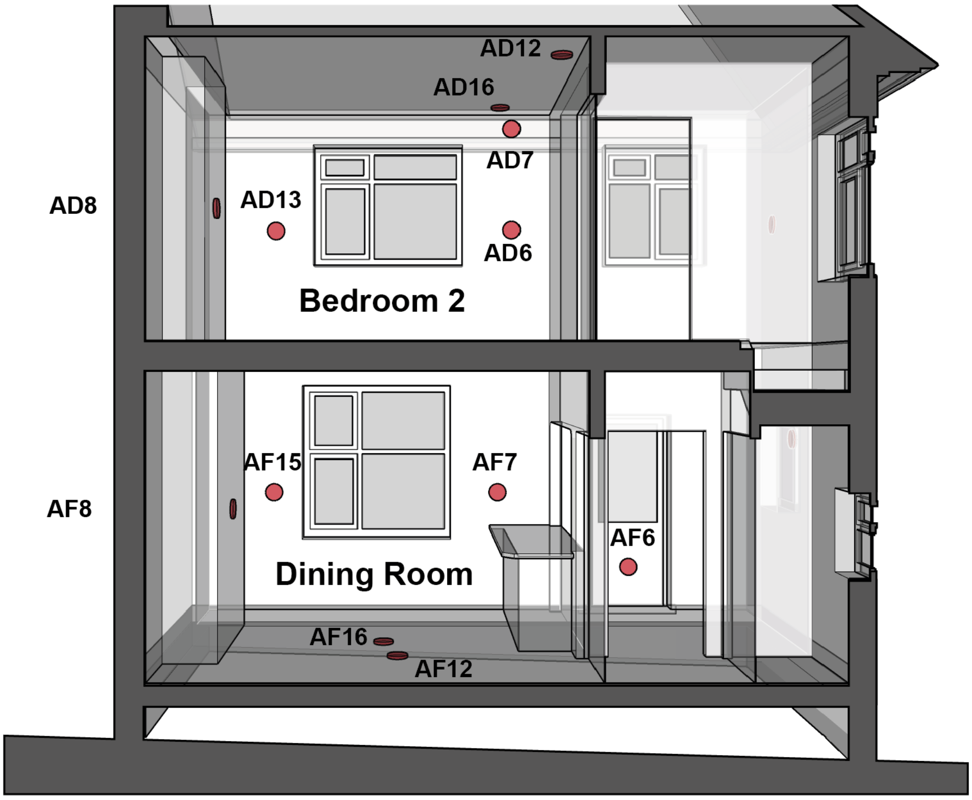

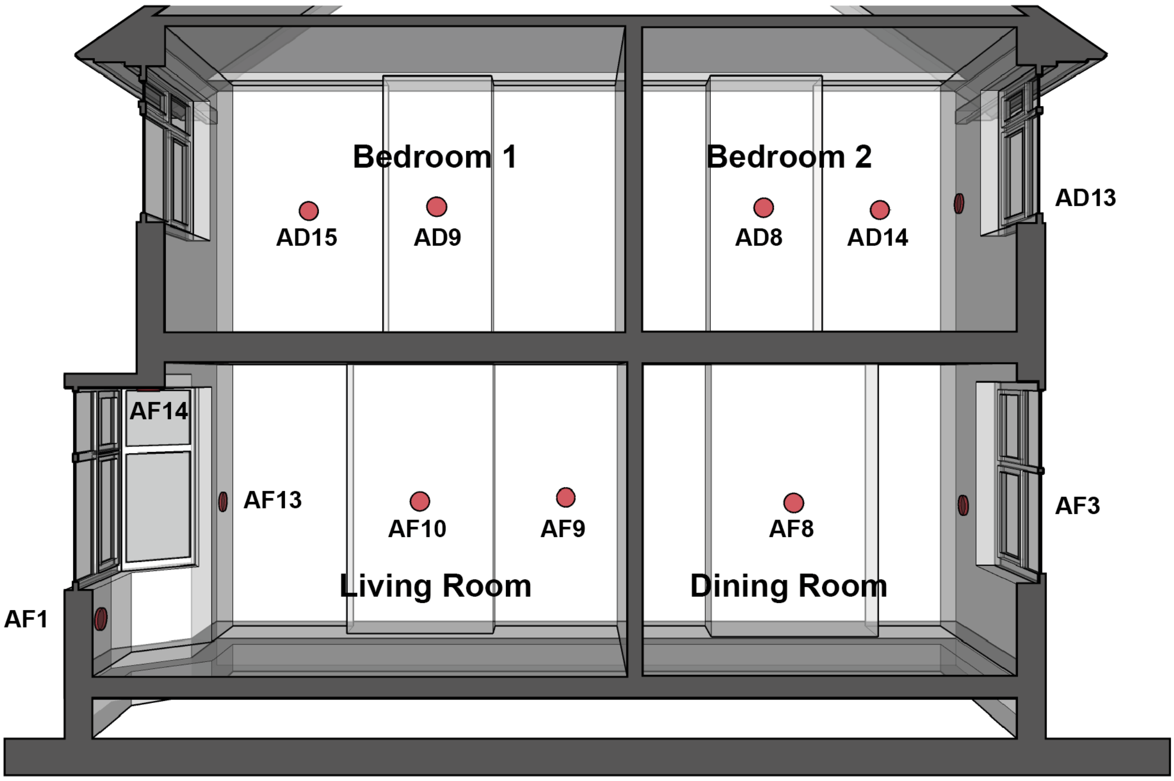

Figure 2-1 Heat flux plates in 55AD

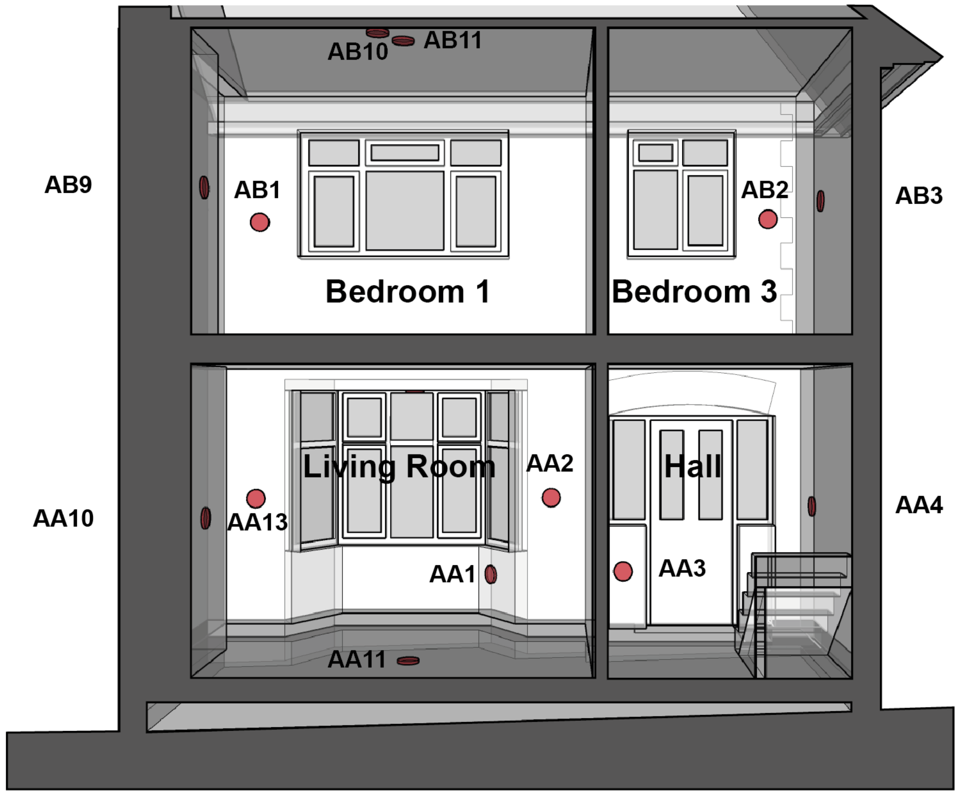
AB10
AB11
AB9
AB1
Bedroom 1
AB2
Bedroom 3
AB3
Living Room
AA2
AA10
AA13
AA1
AA11
Hall
AA4
AA3

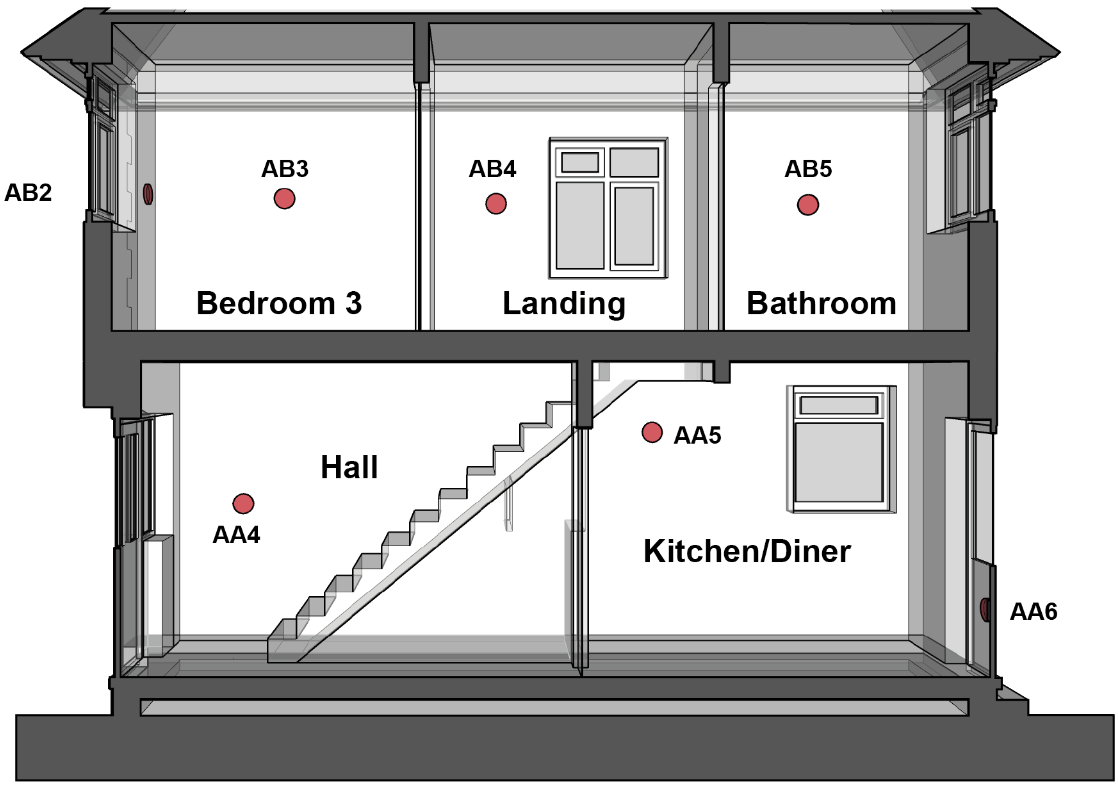
AB2
AB3
Bedroom 3
AB4
Landing
AB5
Bathroom
Hall
AA4
AA5
Kitchen/Diner
AA6

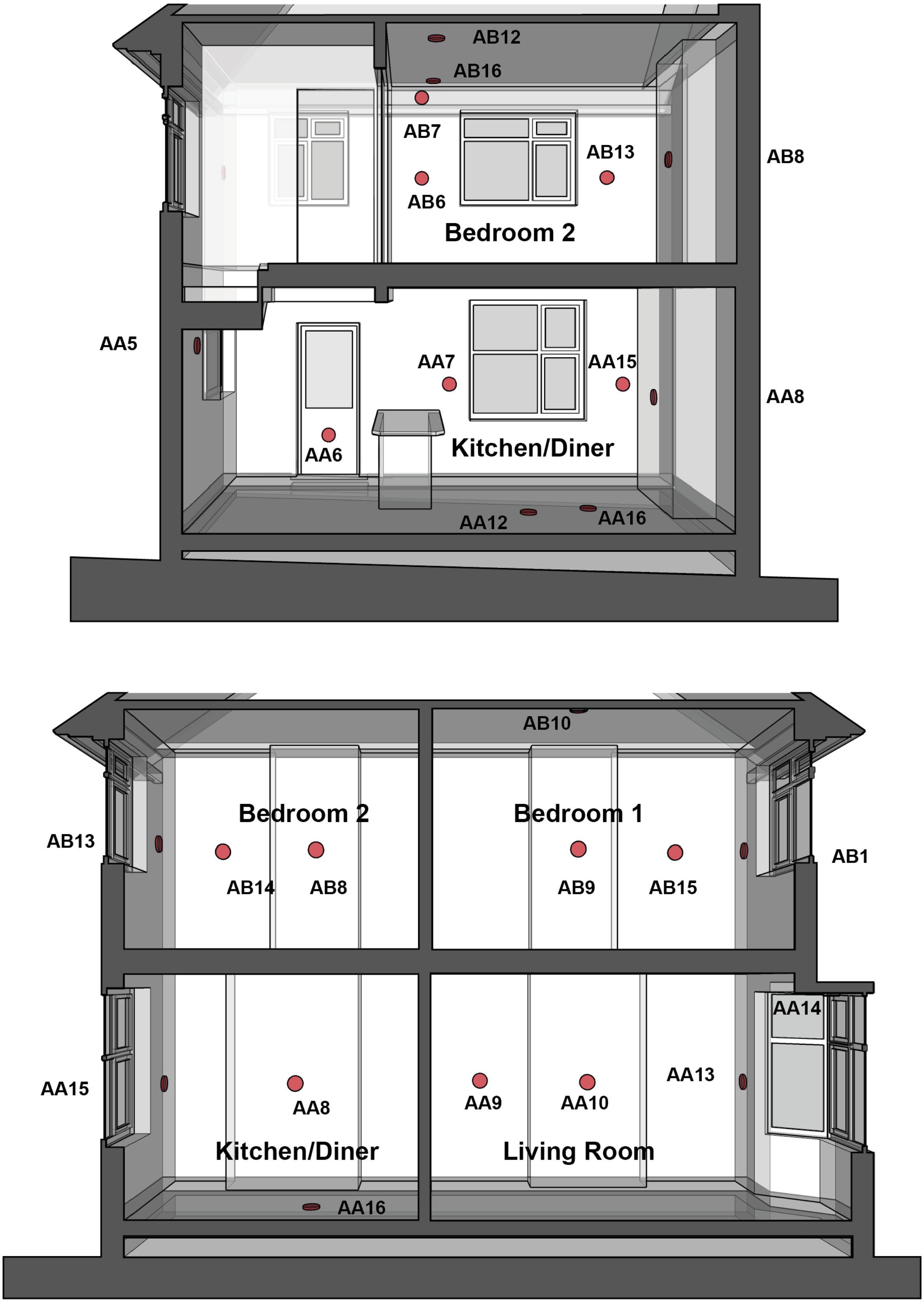

Figure 2-2 Heat flux plates in 57AD

2.5 Whole house heat transfer coefficient (HTC)

Coheating tests were successfully performed at each stage of the retrofit, as described in DEEP Report 2.01 Methods, to provide an overall measured HTC. In addition to coheating tests, QUB tests were attempted, and the results are presented for comparison where available.

2.6 Surface temperatures and thermal bridges

There were several areas of interest where there was a risk of thermal bridging. In these areas, surface temperatures were measured to calculate a temperature factor (f_{Rsi}) and assess surface condensation risk. These are described in Section 3.9, and summarised here:

- External wall to eaves junction
- External wall to ground floor junction
- External wall to window opening (head, reveal, and sill)
- External wall corner
- External wall to party wall
- Door threshold

2.7 Whole building energy modelling

The modelling methodologies undertaken are explained in detail in the Report 2.01 DEEP Methods. DEEP first used the steady-state energy model, BREDEM, which generates EPCs for existing homes via the RdSAP software. Using RdSAP means that EPC assessors interact with BREDEM using standard conventions and input defaults. DEEP compared how these restrictions affected the HTC that BREDEM predicts. These outputs were also compared with the HTC predicted by DSM (using DesignBuilder software version 7.0.0.088) at each retrofit stage. Table 22 describes the approach taken to understand how their predictions changed as default inputs were overridden.

Table 2-2 Modelling calibration stages

Calibration step	Infiltration	U-values	Bridging
1	Default[9]	Default[9]	Default[10]
2	Measured[11]	Default[9]	Default[10]
3	Measured[11]	Calculated[12]	Default[10]
4	Measured[11]	Measured[13]	Default[10]
5	Measured[11]	Measured[13]	Calculated[14]

[9] Provided by Appendix S RdSAP 2012 version 9.94
[10] Provided by Appendix K RdSAP 2012 version 9.94
[11] Derived from Blower door test
[12] Derived from BRE Calculator
[13] Derived from Heat flux plate measurements
[14] Calculated from elemental thermal simulation bridging models

Additionally, the models predict annual energy demand, annual space heating cost, carbon dioxide emissions, SAP score, and EPC band; therefore the success of the retrofits at achieving policy aims can be evaluated. In addition, along with the retrofit install costs, simple payback periods for each retrofit can also be calculated. By learning about the variability of the different models and how they compare to as-measured data, recommendations may be possible for improvements to both the models and the ways they are used. Improved understanding of modelling uncertainty may lead to better informed retrofit decision making at individual dwelling and national policy levels.

2.8 Elemental thermal modelling

In addition to the whole house energy models, elemental thermal modelling was undertaken to calculate non-repeating linear thermal bridging heat losses in each case study dwelling before and after retrofit. The modelling procedure is described in detail in Report 2.01 DEEP Case Study Methods. Modelling the Ψ-value (Psi-value) of junctions allows the non-repeating thermal bridging heat loss (HTC_b), to be calculated (point thermal bridges were not calculated). This can be useful when evaluating the appropriateness of default values in RdSAP in the context of retrofit evaluation and, specifically, how it can affect the whole house HTC.

Thermal modelling also identifies surface condensation risks, i.e. the temperature factor (f_{Rsi}), for each of the junctions in the house pre- and post-retrofit. Where different retrofit strategies are considered, thermal modelling can compare the risks associated with piecemeal vs whole house retrofits.

In 55AD and 57 AD, thermal bridging calculations were performed for all 25 unique junctions under the pre- and post-retrofit scenarios. Material properties were taken from default tabulated values found in BS EN ISO 10456-2007 [2] and BR 443 [3] and manufacturer data where available. Measured brick thermal properties were used to refine wall thermal conductivities in additional simulations, and a comparative analysis with default simulation results was undertaken.

Case study method summary

A deep dive into the 55AD and 57 AD retrofit case study was undertaken involving coheating tests, blower door tests, and 64 heat flux density measurements on fabric elements, taken before and after each of the retrofits was performed.

Steady-state and dynamic energy models were also produced, to compare against these in-situ measurements. To investigate the appropriateness of using default data in energy models, a five-step calibrated process was adopted.

Thermal models of all 25 different junction types in the house under the different retrofit scenarios were also undertaken to explore the impact of retrofits on the heat loss and surface condensation risks posed by thermal bridging. These models were refined using measured construction material properties taken from wall core samples.

These methods collectively investigated the energy performance and surface condensation risk associated with different approaches to retrofit, as well as the usefulness of models in the prediction of these factors.

3 Results

This chapter first presents results on the in-situ field trials: airtightness tests, in-situ U-values, and the whole house heat loss as measured by the coheating test. It then describes how modelled predictions compared with the measured data and how successful the five different calibration steps were at improving the predicted heat loss. The model outputs are discussed in terms of their implications for EPCs, space heating, CO_2 emissions, fuel bills, and paybacks. Finally, the potential surface condensation risks posed in the house at each retrofit stage are discussed.

3.1 Airtightness improvements

Figure 3-1 shows the airtightness results pre-retrofit were 13.12 and 11.67 $m^3/(h{\cdot}m^2)$ @ 50Pa for 55AD and 57AD respectively. Post-retrofit this dropped to 8.37 and 11.40 $m^3/(h{\cdot}m^2)$ @ 50Pa for 55AD and 57AD respectively. A third test stage is shown which represents the airtightness of the homes after the retrofit works were completed in the homes, but prior to final decoration, i.e. there was no change to 55AD between the second and third stage, but in 57AD new windows and doors had been installed, the bay window roof had been insulated and the EWI had been extended at the eaves, so that it matched 55AD.

In the baseline stage, there was no significant difference in air leakage between the homes (results were within the test error), and both homes had lower air leakage than that assumed by the RdSAP default (used in EPCs). Furthermore, measurements of air permeability under pressurisation gave results of 13.82 and 12.03 $m^3/(h.m^2)$ @ 50 Pa for 55AD and 57AD respectively (higher than the mean permeability shown in Figure 3-1). More importantly, when the homes were co-pressurised, to remove drivers for air movement through the party wall, these results fell to 10.15 & 10.02 $m^3/(h{\cdot}m^2)$ @ 50Pa respectively, indicating that the actual infiltration under normal conditions is significantly lower than assumed in EPCs, using RdSAP defaults.

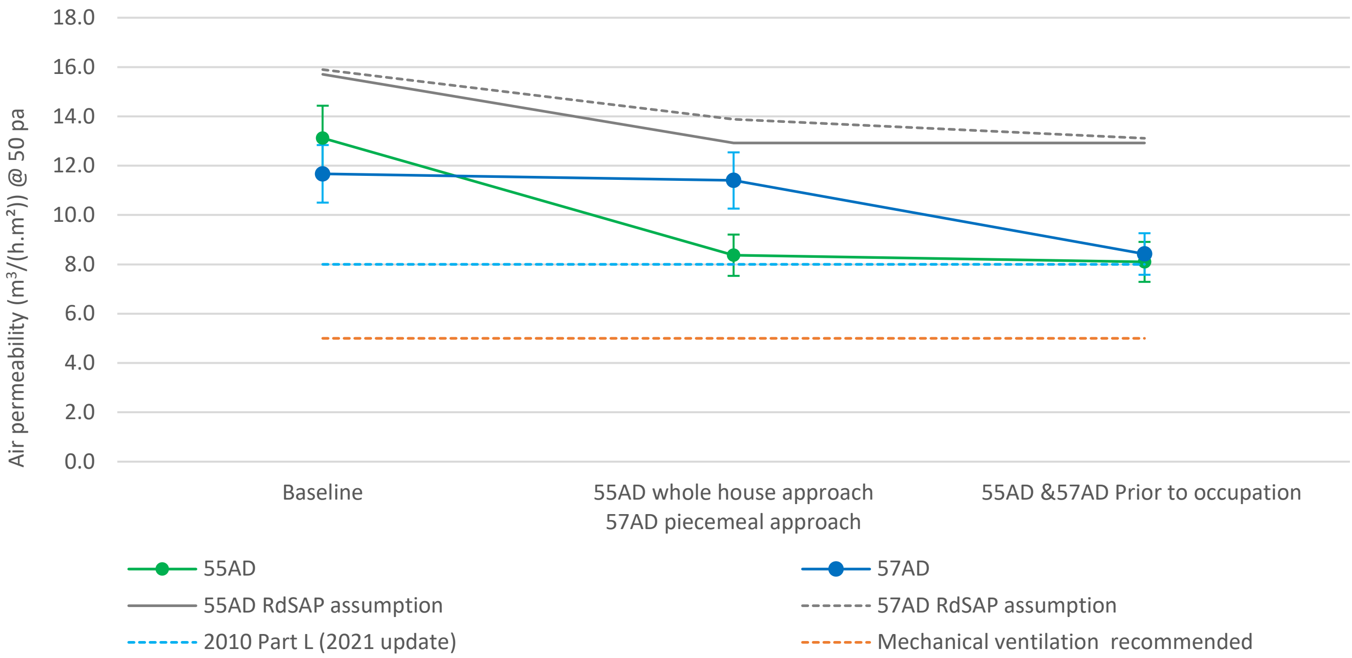

Figure 3-1 Infiltration rate of case studies

RdSAP reduces whole house air leakage when suspended timber ground floors are classified as insulated. In this case study, the reduction from the retrofit was assumed to be 2.01 $m^3/(h \cdot m^2)$ @ 50Pa. Similarly, new glazing and doors were assumed to reduced air leakage by 0.77 $m^3/(h \cdot m^2)$ @ 50Pa. However, the measured values suggest the retrofits reduced air leakage by 5 $m^3/(h \cdot m^2)$ @ 50Pa in 55AD. In 57AD the improvement from the ground floor, loft, and EWI retrofit was only measured to be 0.3 $m^3/(h \cdot m^2)$ @ 50Pa. After replacing the glazing and doors, undertaking the bay roof insulation, making good plaster work around the windows, and improving caulking to provide internal sealing around penetrations and door and window frames, the improvement was 3.3 $m^3/(h \cdot m^2)$ @ 50Pa to 8.42 $m^3/(h \cdot m^2)$ @ 50Pa. This indicates that these retrofits had much greater impact than the ground floor, loft, and wall insulation, i.e. the opposite to that assumed in RdSAP.

When co-pressurised (to remove inter-dwelling air exchange) these results fell further to 5.58 and 5.87 $m^3/(h \cdot m^2)$ @ 50Pa in 55AD and 57AD respectively, i.e. inter-dwelling air exchange was responsible for a similar amount of recorded air leakage, as that which was reduced by the retrofits. The implication of this is significant. In this case study, the retrofits had made the homes significantly more airtight, bringing them to just above the recommended infiltration rate of 5 $m^3/(h \cdot m^2)$ @ 50Pa. Below this threshold, natural ventilation alone may not provide necessary fresh air. However, without undertaking the co-pressurisation test, it would have been assumed that the homes were well above this threshold value.

The results obtained suggest that relying on a blower door test to determine if attached homes are below the recommended infiltration rate threshold may be problematic unless co-pressurisation tests are conducted. It also suggests that using the results obtained from conventional blower door tests (non-co-pressurisation tests), conducted in attached homes, to update infiltration rates used in thermal modelling, may overestimate the dwelling's air leakage rate. Consequently, this will overestimate the heat losses associated with air leakage.

The main air leakage paths identified at the baseline stage were common between both houses, although there were differences in perceived severity between the properties. Figure 3-2 shows how the fireplaces were replaced during the ground floor insulation retrofit. While a vent was left in place, this appears to be obstructed by mineral wool insulation, and will have impeded air leakage, though it is a still a breathable barrier.

Figure 3-2 Fireplace and hearth removed as part of ground floor retrofit.

Leakage through the ground floor was most severe at room perimeters and areas where a lack of floor covering revealed gaps between the plain edge floorboards, such as beneath kitchen units, in electric meter cupboards, and at the floors of the dining room cupboards.

The under-stairs cupboards on the ground floor varied; 55AD was accessible via a cupboard door, while 57AD could be accessed only via a top hatch from the kitchen. However, both were major sources of air leakage as shown in Figure 3-3 and Figure 3-4, with openings in the external wall, and unsealed service penetrations.

Figure 3-3 Unsealed penetrations in the understairs cupboard in 55AD

Figure 3-4 Air leakage via external wall opening in understairs area 57AD (hatch access only)

The ground floor to external wall junctions were particularly leaky pre-retrofit in both homes as illustrated in Figure 3-5. This also shows infiltration between the window frames and external walls, as well as unsealed boiler flues also acting as air leakage pathways. It was also observed that the external doors and windows were not draught stripped effectively and air leakage was occurring through closed trickle vents.

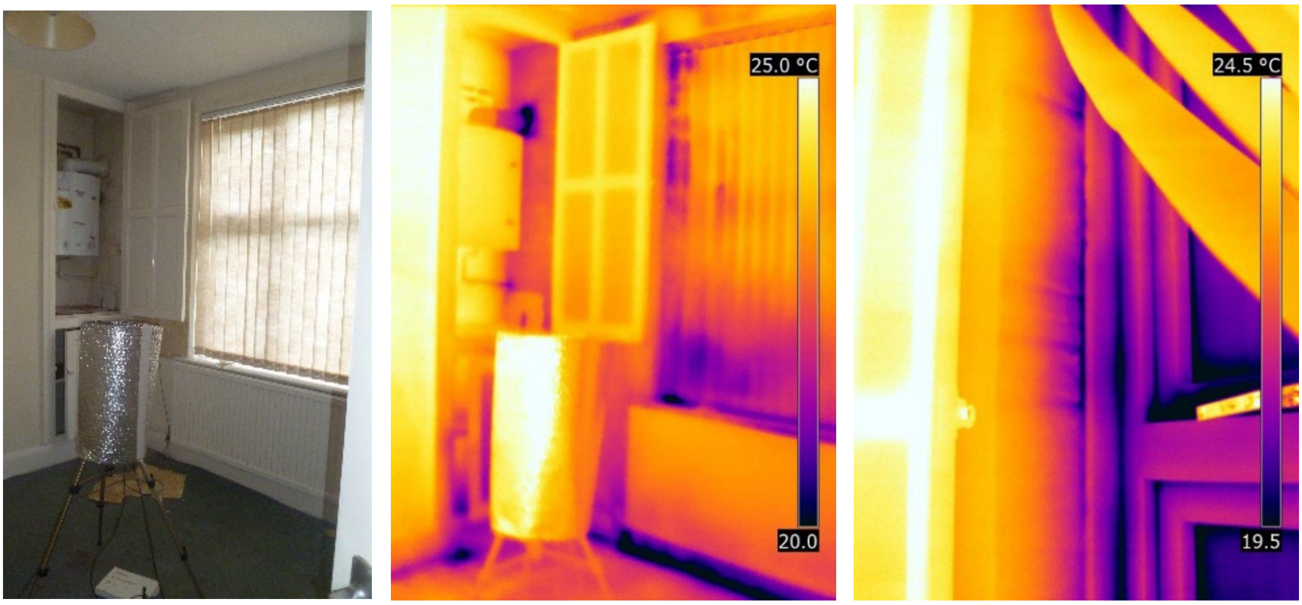

Figure 3-5 Air leakage under depressurisation at ground floor perimeter, cupboard floor, boiler flue and window in 55AD

Unsealed penetrations in both houses were a problem, for instance around extractor fans as shown in Figure 3-6, commonly due to unfinished detailing in hidden areas (inside cupboards, behind baths, and toilets etc.).

Figure 3-6 The bathroom extract grille in 57AD was not sealed to the wall

Figure 3-7 shows direct leakage paths through the ground floor at the electric meter cupboard and around the new hatch into the loft.

Figure 3-8 shows service penetrations in the bathroom that were not sealed around the toilet soil pipe and behind the bath panel.

Similarly, in the rear bedroom the cupboard had holes in the floor and around the cupboard door frames, as shown in Figure 3-9.

Figure 3-7 Lack of sealing in the hall and landing 57AD

Figure 3-8 Unfinished detailing in the bathroom of 57AD

Figure 3-9 Unfinished detailing in the rear bedroom of 57AD

In addition, indirect leakage into the first floor partition wall voids was detected. This is shown in Figure 3-10, and shows that some air infiltration was taking place, with cold air being drawn into the internal partition wall during depressurisation. It is not clear if this was being drawn direct from outside via cracks and gaps in the external solid wall, or if the air leakage pathway was indirect from the loft or the intermediate floor void, into the partition wall at its junction with the external wall.

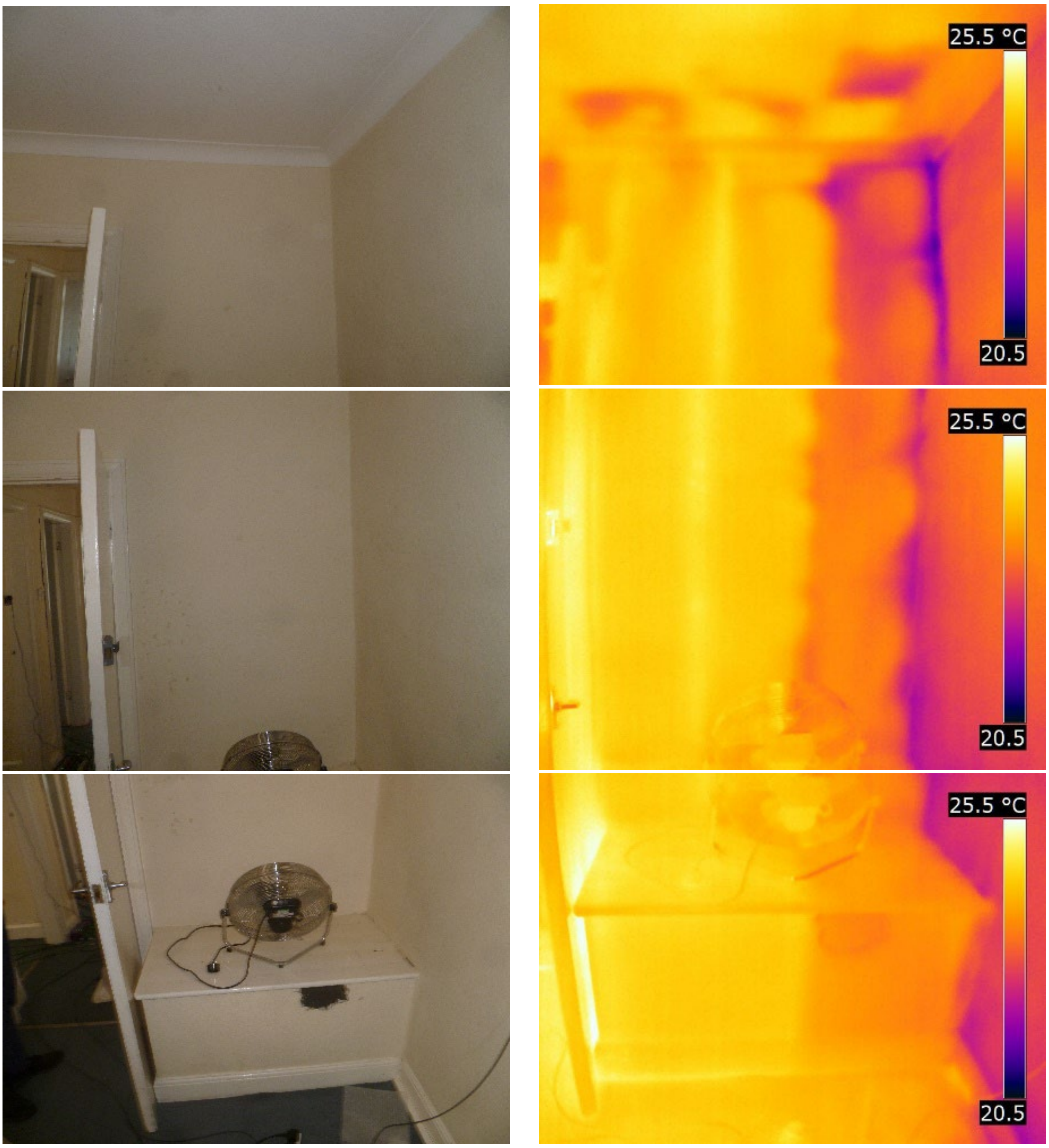

Figure 3-10 Indirect air leakage in a first floor partition wall void in 55AD

3.1.1 CO_2 decay measurement

Analysis of CO_2 decay curves proved inconsistent at the baseline stage, possibly due to the low levels of airtightness, causing the decay rates to be very susceptible to wind effects, with ventilation rates at the point of release on the ground floor varying between 0.92 and 2.20 ach^{-1}. However, while it was not possible to obtain a reliable air leakage rate from the CO_2 analysis, it was possible to see CO_2 entering 57AD from the releases in 55AD, indicating that air movement between the properties was occurring under natural conditions. No reciprocation was observed following CO_2 releases in 57AD. It is not known why there was an effect only in one direction, though it may possibly be due to the prevailing wind direction during the test period. Figure 3-11 shows CO_2 concentrations in 57AD corresponding to timed releases in 55AD, where CO_2 was discharged over 15-minute periods raising the internal concentration of CO_2 in 55AD to >2000 ppm.

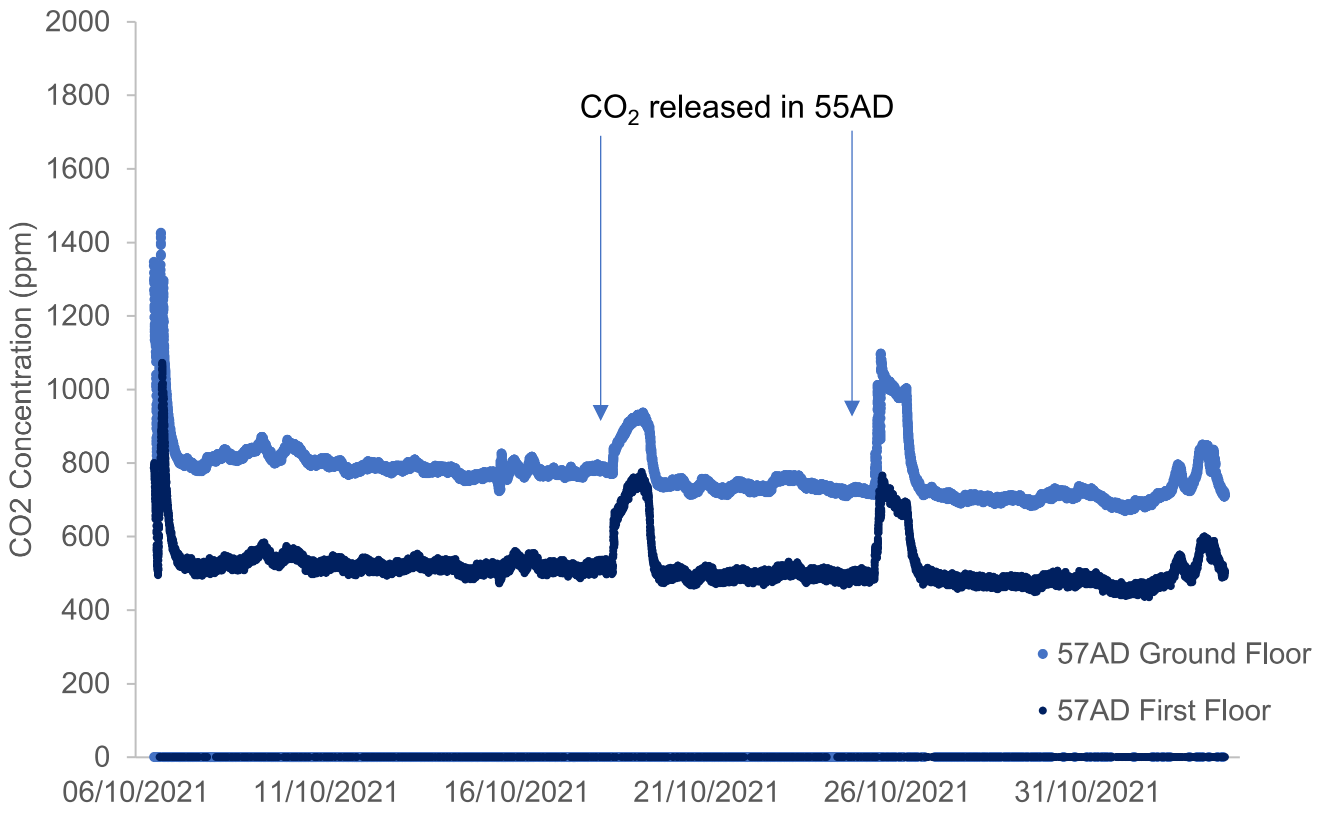

Figure 3-11 CO_2 monitoring in 57AD showed peaks corresponding to releases of gas in 55AD

Airtightness improvement summary

Common air leakage pathways were observed in both homes, around ground floor perimeters, window frames, penetrations through walls etc., though both had lower infiltration rates than assumed in RdSAP. The retrofits reduced the air leakage by 16 %, though no specific airtightness retrofit took place. Inter-dwelling air exchanges were measured to be between 16 % and 33% (qualitatively confirmed by the CO_2 measurements), indicating that fresh air provision in the homes may be lower than blower door tests suggest, and that there may be lower heat losses associated with air leakage than measured.

3.2 U-value improvements

Three methods were adopted in deriving U-values:

1. **RdSAP default U-values:** using age-related band default assumptions provided in SAP Appendix S, the most common approach used in EPCs for existing homes.
2. **Calculated U-values:** used where construction details are known and a calculation is undertaken in separate approved software (e.g. the BRE U-value calculator).
3. **Measured U-values:** used where in-situ heat flux density measurements were undertaken using an approved methodology. This approach is the most specialist and costly to undertake and so is the least likely to be undertaken in retrofit projects.

All three methods were used in DEEP for comparison and this section reports on the difference between them. The report considers implications of the method selected on accuracy of energy and heat loss predictions, the contribution of fabric elements to the HTC, and the predicted benefit achieved by retrofits.

First, a summary of the pre- and post-U-value measurements undertaken in 55AD are discussed, then the findings from 57AD are presented. Finally, the implications with respect to the heat loss in both homes is discussed.

The U-values for each home are presented below and this is followed by summary tables listing the U-values and how these changed post-retrofit.

3.2.1 55AD U-values

A summary of the pre- and post-retrofit U-values for each of the ground floor, external windows, external doors, and the first floor ceilings in 55AD is presented in Figure 3-12. As can be seen, the pre-retrofit measurements for the ground floor, the external door, and the bay window ceiling had large uncertainties. This was due to a ground loop issue with the Datatakker DT85 HFP data logger used in the dwelling, which resulted in erratic readings being recorded. While it was possible to some degree to correct the data to account for this, after this correction, the results still had higher than normal uncertainty values. We have therefore not used the values for the ground floor, bay wall, bay ceiling, or doors in the heat loss calculations, but instead relied on calculated values.

Despite this, the pre-retrofit U-values for the external doors and bay roof align relatively well with the calculated values for the elements, though the ground floor U-value is significantly higher than default RdSAP values and the values that the BRE calculator predicted. This figure is unexpected, since the HFPs were not located near to the edges of the ground floor and so were not subject to additional heat losses associated with edge effects, which are accounted for in the BRE calculator. Thus, the uncertainty associated with the measured ground floor pre-retrofit U-values is a limitation.

In almost all instances, the measured U-values post-retrofit were in line with the predicted calculated U-values, as well as the Building Regulations limiting values for retained elements. In the case of the external door replacement, the post-retrofit U-value was measured to have exceeded the predictions. In the case of the bay window retrofit a lack of space limited the amount of insulation that could be installed, and so the limiting value was not quite achieved.

No HFP was located on the windows meaning that there could be no measurements of the centre pane U-value. No post-retrofit value for the single glazing is shown since, as mentioned previously, these side panels to the front doors were converted into external wall as part of the retrofit.

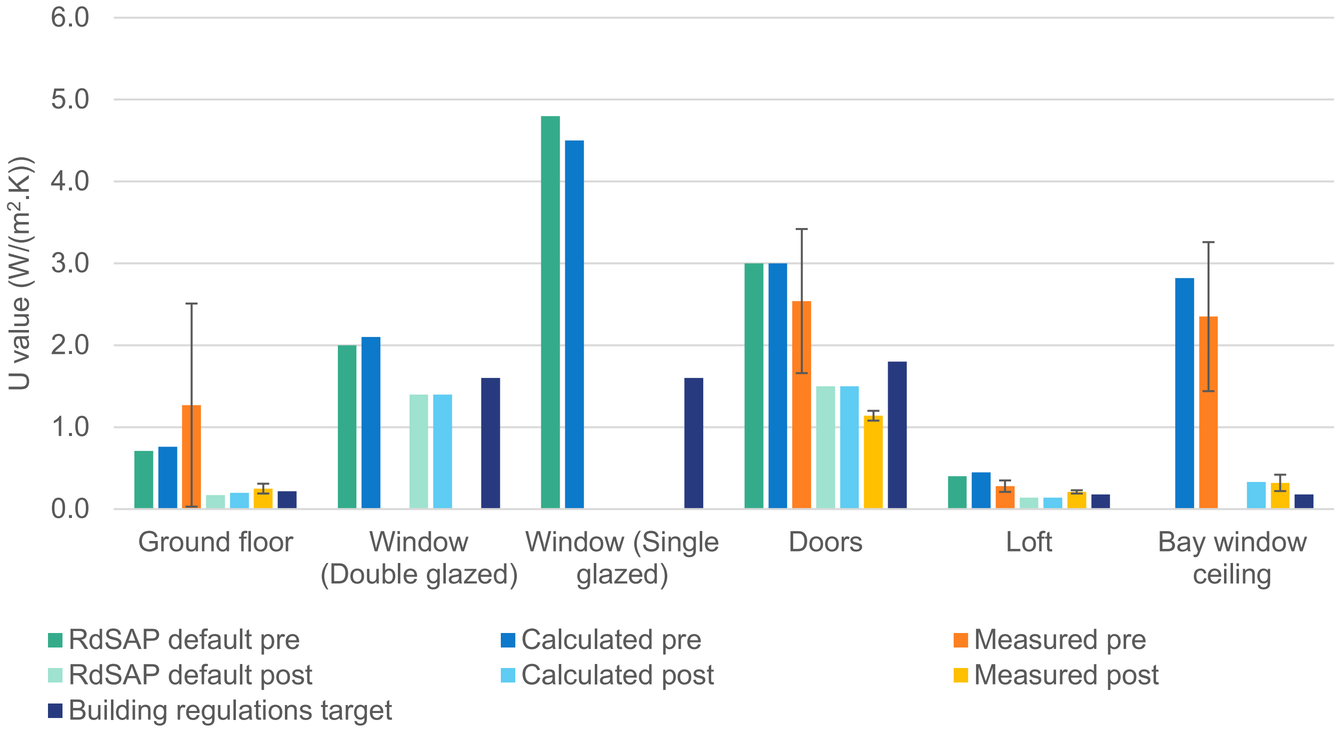

Figure 3-12 Pre- and post-retrofit fabric U-values (55AD) (excluding walls) (W/(m²·K))

The U-values for the external walls, presented in Figure 313, illustrate again that the DT85 ground loop issues caused large uncertainty values, this time with the pre-retrofit bay window external wall U-value measurements. Specifically, the error reported for this element is large because of the necessary corrections that were made to correct the ground loop issue, and so this is an area of uncertainty in the assessment. The bay wall is only a small proportion of the overall heat loss area (<1 %) so this is not a large limitation. The rest of the pre-retrofit external wall U-values were measured using a DT80 and so not subject to the ground loop phenomenon.

Three separate area-weighted external wall U-values are presented since these have slight variations in their construction. The front external wall had an area of double brickwork as an architectural feature above the front door, the bathroom's side external wall had an internal thin wall insulation board, and the bathroom's rear external wall had a 12 mm plywood and an internal thin wall insulation board. However, these differences caused negligible variations in the pre-retrofit U-values predicted by the BRE calculator.

Post-retrofit, the measured U-value for the external walls shows a significant reduction, of (77 ± 11) %. The U-value, however, was slightly higher than predicted by the RdSAP defaults and BRE calculator and didn't quite achieve the Building Regulations limiting value. It is probable that this was due to the uninsulated wall having a higher measured U-value than was predicted.

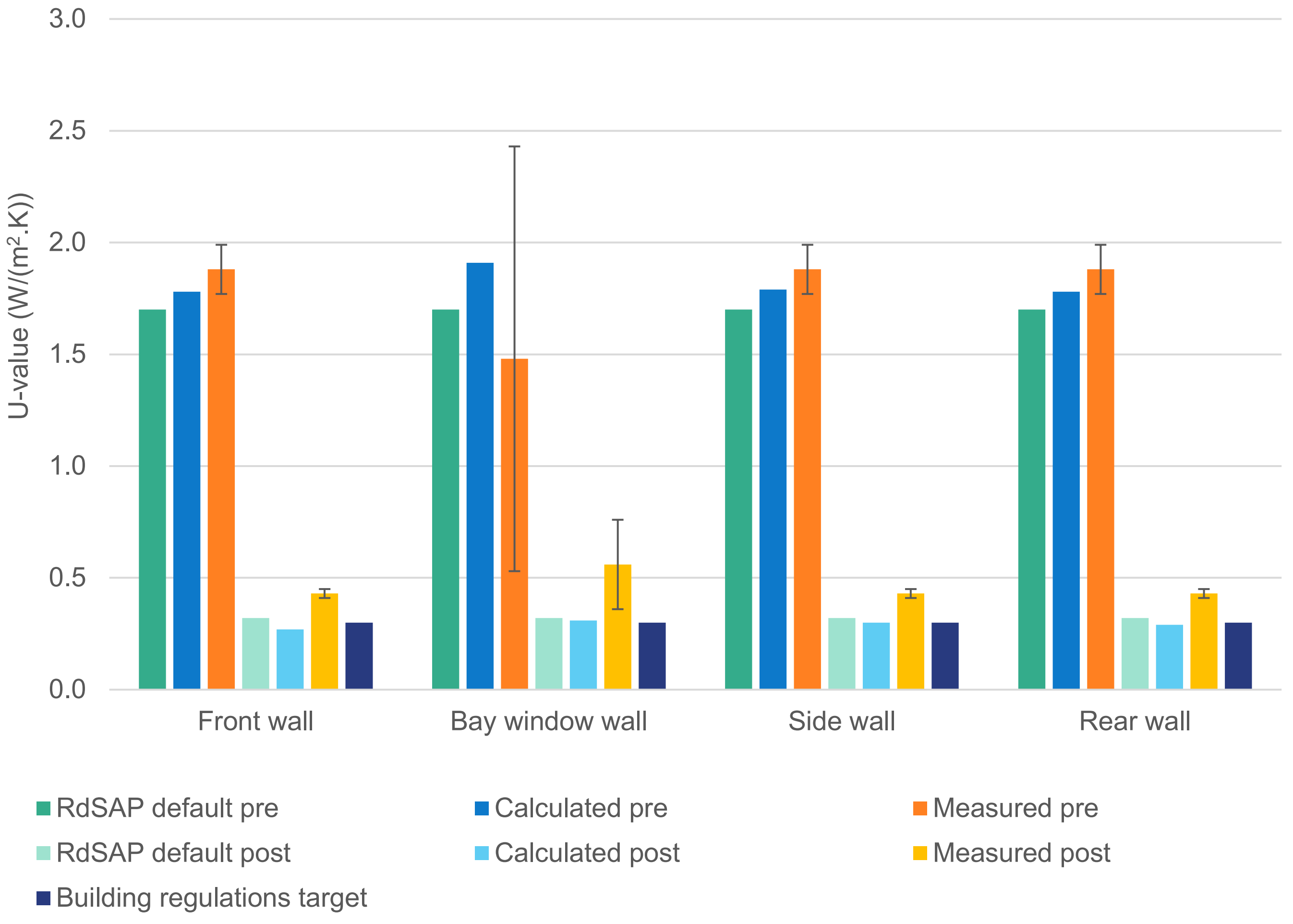

Figure 3-13 Pre- and post- U-values (55AD) (Walls) (W/(m²·K))

3.2.2 57AD U-values

In 57AD, ground loop issues also existed for the pre- and post-retrofit ground floor and bay window external wall U-value measurements, as shown in Figure 314 and Figure 315. This caused higher than normal uncertainty, and so as in 55AD, these were not used in the heat loss calculations, rather the calculated U-values were used.

The measured U-values of the ground floor were, as observed in 55AD, higher than the calculated and default U-values. It is probable that this is again due to the ground loop problem. It was expected that the ground floor U-values derived from centre room HFPs would measure lower heat losses than the RdSAP defaults and the BRE calculator, since the latter methods account for additional heat losses associated with the edges of floors, which do not affect the centre room HFPs. It is likely therefore that the ground floor heat losses in 57AD represent a large area of uncertainty and as such, as in 55AD, it is more appropriate to use the calculated U-values to predict heat losses.

The replacement loft retrofit was measured to have only a marginal impact on the absolute U-value (0.21 ± 0.02) W/(m^{2}K), though proportionally this represents a (50 ± 7) % reduction. Post-retrofit the loft retrofit was measured to exceed the limiting U-value in the Building Regulations and was in line with the calculated and RdSAP U-values.

The pre-retrofit data recorded for the bay window ceiling in 57AD did not meet the quality standard required by ISO9869 for the calculation of U-values and therefore the calculated value has been used for the heat loss calculations. However, post-retrofit, the measurement was compliant and so the pre-retrofit U-value was assumed to be the same, as this element was not altered during the retrofit.

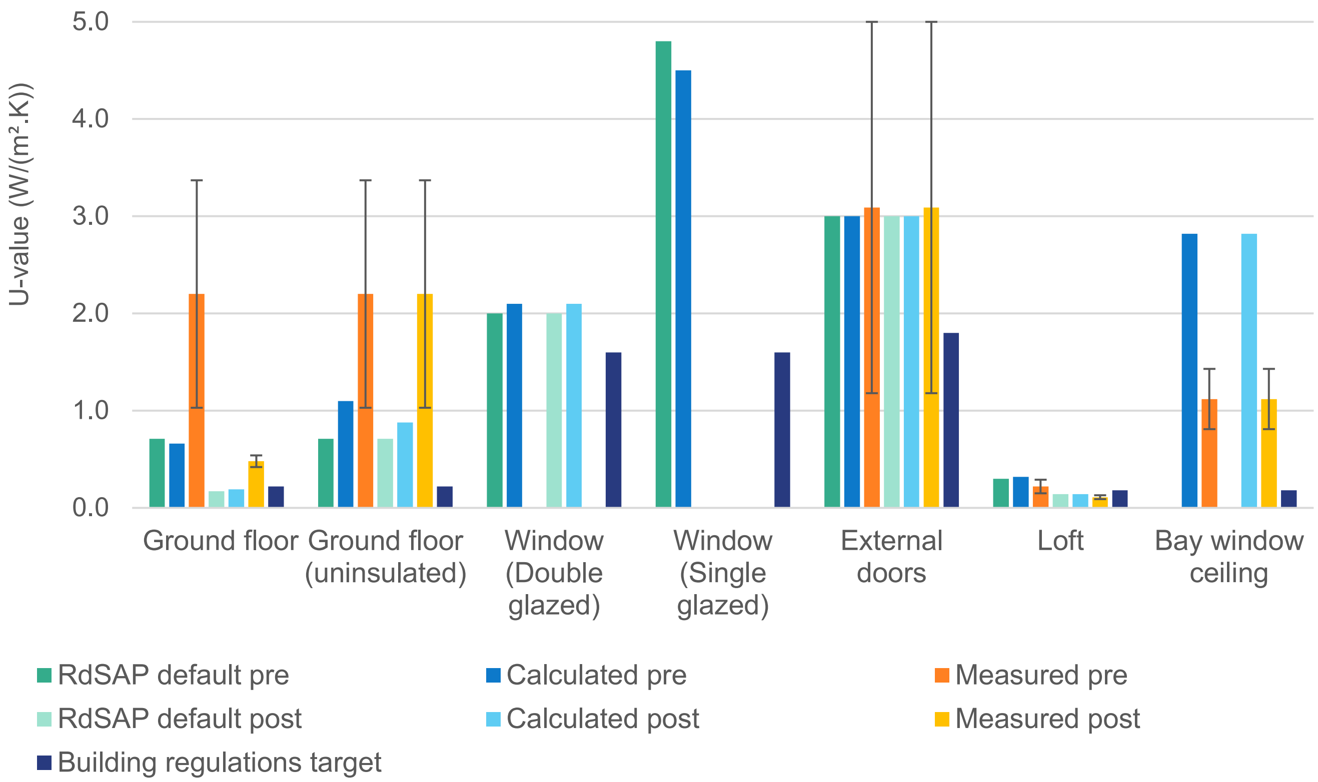

Figure 3-14 Pre- and post-retrofit fabric U-values (57AD) (excluding walls) (W/(m^2·K))

Again, several external wall U-values are shown in Figure 3-15, since slight variations were observed that may affect heat losses. The front external wall, as at 55AD, had a double brick element above the front door, and there was thin internal wall insulation (IWI) observed on the side and rear external walls in the bathroom, which again affected the area weighted U-value. The IWI only made a small difference in the area weighted calculated U-value, since the bathroom external wall area was very small. The RdSAP and measured U-values only have a single U-value for all the walls.

Unlike 55AD, the uninsulated external wall U-values were measured to be slightly lower than the BRE calculator predictions; the reason for this is not known. However, the post-retrofit U-values for those areas that were retrofitted were higher than the predictions, indicating a performance gap, though it is not known what caused this. Despite this, the savings achieved by the wall insulation were significant (72 ± 12) %, though the insulation did not quite achieve the same performance level as that predicted by the RdSAP defaults or BRE calculator, nor the limiting U-value in the Building Regulations for retained elements.

As in 55AD, the bay window external wall had a much higher uncertainty, and a much higher U-value was measured compared to the other external walls. Additionally, the bay window wall in 57AD post-retrofit was measured to be significantly worse performing and achieved much lower savings; only halving the U-value. The uncertainty, however, is too high to have confidence in the measured saving (52 ± 99) %, and so is a limitation in the study. Therefore, despite the small area of heat loss that this wall represents, for consistency, the calculated U-values have been used to predict the heat losses associated with this element.

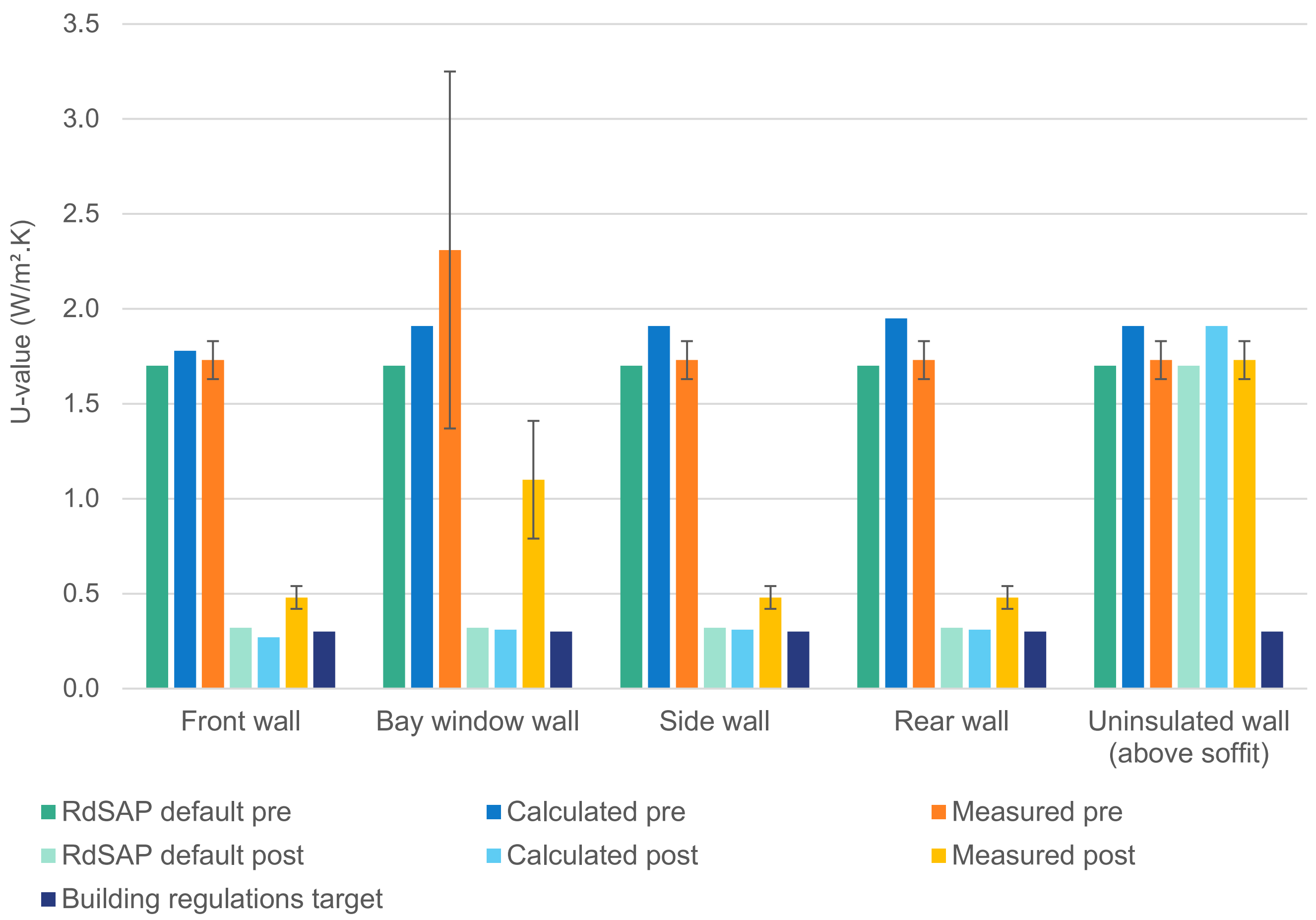

Figure 3-15 Pre- and post-retrofit U-values (57AD) (Walls) (W/(m^2·K))

3.2.3 U-values summary

Table 3-1 shows the area weighted U-values achieved by each of the fabric elements pre- and post-retrofit including the improvement achieved by the addition of insulation.

As can be seen, significant improvements in fabric U-values were achieved in both homes: a reduction in heat loss of over three quarters for the ground floors (though this had a very large uncertainty); a reduction of between a half and two thirds for the lofts; heat loss for the doors was again cut in half; and most significantly, since it represents the largest heat loss area, heat loss through the external walls was seen to be reduced by around three quarters.

Table 3-1 55AD and 57AD RdSAP Default, calculated and measured U-values (W/(m²·K))

	Pre-retrofit			Post-retrofit U-value (% improvement)		
	RdSAP Default	Calculated	Measured	RdSAP Default	Calculated	Measured
55AD						
Ground floor	0.71	0.76	1.27 ± 1.24	0.17 (76 %)	0.20 (74 %)	0.25 ± 0.06 (80 ± 124) %
External front wall	1.70	1.78	1.88 ± 0.11	0.32 (81 %)	0.27 (85 %)	0.43 ± 0.02 (77 ± 11) %
Bay window external wall	1.70	1.91	1.48 ± 0.95	0.32 (81 %)	0.31 (84 %)	0.56 ± 0.20 (62 ± 97) %
External side wall	1.70	1.79	1.88 ± 0.11	0.32 (81 %)	0.30 (83 %)	0.43 ± 0.02 (77 ± 11) %
External rear wall	1.70	1.78	1.88 ± 0.11	0.32 (81 %)	0.29 (84 %)	0.43 ± 0.02 (77 ± 11) %
Window (double glazed)[15]	2.00	2.10	-	1.40 (30 %)	1.40 (33 %)	-
Window (single glazed)[16]	4.80	4.50	-	-	-	-
External door	3.00	3.00	2.54 ± 0.88	1.50 (50 %)	1.50 (50 %)	1.14 ± 0.06 (55 ± 88)%
Loft	0.40	0.45	0.28 ± 0.07	0.14 (65 %)	0.14 (69 %)	0.21 ± 0.02 (25 ± 7)%
Bay window ceiling	2.30	2.82	2.35 ± 0.91	0.50 (78 %)	0.33 (88 %)	0.32 ± 0.10 (86 ± 92)%

[15] No HFP recordings were obtained for the Windows.
[16] No HFP recordings were obtained for the Windows. Single glazing was removed and filled post-retrofit.

	Pre-retrofit			Post-retrofit U-value (% improvement)		
	RdSAP Default	Calculated	Measured	RdSAP Default	Calculated	Measured
57AD						
Ground floor	0.71	0.66	2.20 ± 1.17	0.17 (76 %)	0.19 (71 %)	0.48 ± 0.06 (78 ± 117) %
Ground floor (uninsulated)[17]	0.71	1.10	2.20 ± 1.17	-	0.88 (20 %)	-
External front wall	1.70	1.78	1.73 ± 0.10	0.32 (81 %)	0.27 (85 %)	0.48 ± 0.06 (72 ± 12) %
Bay window external wall	1.70	1.91	2.31 ± 0.94	0.32 (81 %)	0.31 (84 %)	1.10 ± 0.31 (52 ± 99) %
External side wall	1.70	1.91	1.73 ± 0.10	0.32 (81 %)	0.31 (84 %)	0.48 ± 0.06 (72 ± 12) %
External rear wall	1.70	1.95	1.73 ± 0.10	0.32 (81 %)	0.31 (84 %)	0.48 ± 0.06 (78 ± 117) %
Uninsulated external wall (behind soffit)	1.70	1.91	1.73 ± 0.10	-	-	-
Window (double glazed)[18]	2.00	2.10	-	-	-	-
Window (single glazed)[19]	4.80	4.50	-	-	-	-
External door	3.00	3.00	3.09 ± 1.91	-	-	-
Loft	0.30	0.32	0.22 ± 0.07	0.14 (53 %)	0.14 (56 %)	0.11 ± 0.02 (50 ± 7)%
Bay window ceiling[20]	2.30	2.82	1.13 ± 0.03	-	-	-

The improvements in U-values achieved for each element are summarised in Table 3-2 for each approach to acquiring the U-values. The results suggest that there are considerable gaps between what EPCs assume and the BRE calculator predicts, compared to what is experienced in-situ. Conventionally, a performance gap is observed where there is an underperformance of the known construction details. However, perceived gaps can also occur due to the use of defaults in RdSAP.

There are therefore not only 'performance gaps', but also 'prediction (or modelling) gaps'. We define these two gaps and calculate their values in Table 3-2.

[17] Post-retrofit calculated U-value improvement is the result of the external wall thickness increase.
[18] No HFP recordings were obtained for the Windows.
[19] No HFP recordings were obtained for the Windows. Single glazing was removed and filled post-retrofit.
[20] No HFP recordings were obtained for the Bay window ceiling in 57AD.

RdSAP defaults prediction gap = difference between the predicted reduction in U-value from RdSAP compared to the measured reduction in U-value.

Performance gap = difference between the predicted reduction in U-value from a calculation method (e.g. the BRE U-value calculator) compared to the measured reduction in U-value.

Table 3-2 Summary of measured U-value reductions and gaps in performance. Numbers in red show a statistically significant gap.

Element	RdSAP default predicted reduction	Calculated predicted reduction	Measured reduction	RdSAP defaults prediction gap	'As-built' performance gap
55AD					
Ground floor	0.54	0.56	1.02 ± 1.24	-0.48 ± 1.24	-0.46 ± 1.24
External front wall	1.38	1.51	1.45 ± 0.11	-0.07 ± 0.11	0.06 ± 0.11
Bay window wall	1.38	1.60	0.92 ± 0.97	0.46 ± 0.97	0.68 ± 0.97
External side wall	1.38	1.49	1.45 ± 0.11	-0.07 ± 0.11	0.04 ± 0.11
External rear wall	1.38	1.49	1.45 ± 0.11	-0.07 ± 0.11	0.04 ± 0.11
Double glazing	0.60	0.70	-	-	-
External door	1.50	1.50	1.40 ± 0.88	0.10 ± 0.88	0.10 ± 0.88
Loft	0.26	0.31	0.07 ± 0.07	0.19 ± 0.07	0.24 ± 0.07
Bay window ceiling	1.80	2.49	2.03 ± 0.92	-0.23 ± 0.92	0.46 ± 0.92
57AD					
Ground floor	0.54	0.47	1.72 ± 1.17	-1.18 ± 1.17	-1.25 ± 1.17
Ground floor (uninsulated)[21]	-	0.22	-	-	-
External front wall	1.38	1.51	1.25 ± 0.12	0.13 ± 0.12	0.26 ± 0.12
Bay window wall	1.38	1.60	1.21 ± 0.99	0.17 ± 0.99	0.39 ± 0.99
External side wall	1.38	1.60	1.25 ± 0.12	0.13 ± 0.12	0.35 ± 0.12
External rear wall	1.38	1.64	1.25 ± 0.12	0.13 ± 0.12	0.39 ± 0.12
Loft	0.16	0.18	0.11 ± 0.07	0.05 ± 0.07	0.07 ± 0.07

[21] Post-retrofit calculated U-value improvement is the result of the external wall thickness increase.

The gaps predicted for the ground floor, bay window external wall, and bay window ceiling U-values can to some extent be disregarded, due to the uncertainty in the U-value measurements caused by the necessary ground loop corrections.

Despite this, in most instances, there was a negligible prediction gap, suggesting that the scale of the reduction predicted by RdSAP, in the main, matched the measured reductions. This means that even if a different pre- and post- U-value was predicted by RdSAP compared to the measured values, a similar reduction in U-value was achieved. The exceptions were the loft insulation in 55AD as well as the EWI in 57AD.

It is not known why performance gaps were observed in the walls of 57AD, but not 55AD, since the same system and installer team were responsible for fitting the EWI in both homes during a single retrofit. There may have been some difference caused by environmental conditions during the U-value measurements. The performance gap found for 57AD is, however, only just significant. Therefore, it may be that a gap also exists for 55AD but was not detectable within the sensitivity of our tests.

3.2.4 Contribution of individual elements to plane element fabric heat loss (HTCf)

Table 3-3 shows the impact the improvement in U-values have had on plane element fabric heat loss, i.e. considering the average U-values and relative size of heat loss area of each element.

Table 3-3 Impact of retrofit on fabric plane element heat loss (excluding thermal bridging)

Element	Pre-retrofit (W / K)	Proportion of heat loss	Post-retrofit (W / K)	Proportion of heat loss
55AD				
Roof	11 ± 3	(5 ± 1) %	8 ± 1	(10 ± 1) %
Floor[22]	30	13 %	10	12 %
Doors & windows[22]	50	21 %	28	35 %
Walls	142 ± 10	(60 ± 4) %	33 ± 2	(42 ± 2) %
Bay window roof	3 ± 1	1 %	0.4	(1 ± 1) %
Total	**235 ± 11**	**-**	**80 ± 2**	**-**
57AD				
Roof	9 ± 3	(4 ± 1) %	4 ± 1	(4 ± 1) %
Floor[22]	26	12 %	9	8 %
Doors & windows[22]	51	23 %	46	42 %
Walls	133 ± 10	(60 ± 4) %	39 ± 6	(42 ± 5) %
Bay window roof	4 ± 1	2 %	3 ± 1	(4 ± 1) %
Total	**222 ± 11**	**-**	**109 ± 6**	**-**

Cumulatively, the retrofits in 55AD reduced plane element fabric heat loss by around two thirds, and in 57AD by around a half. The difference in fabric heat loss according to these assessments between the homes is estimated to be 29 W/K ± 11 W/K, over half of which was predicted to be attributable to the new external windows and doors in 55AD.

Most of the plane element fabric heat loss in both homes pre-retrofit was through the external walls, and the EWI was responsible for most of fabric heat loss reductions. Lower heat loss savings were achieved by the EWI in 57AD because of the uninsulated wall behind the eaves soffit, which was calculated to be responsible for around 10 W/K by thermal bridging calculations undertaken in Section 3.3.

[22] Based on calculated U-values so no uncertainty is presented

Other differences were that the 3 W/K heat loss through the bay window roof in 55AD was almost eliminated when insulated, but it was still present in 57AD. The area of uninsulated ground floor under the stairs in 57AD was calculated to be causing an additional 5 W/K, while this was insulated in 55AD.

The external windows and doors were not upgraded in 57AD and as a result, in the post-retrofit home, these constituted a similar amount of heat loss (46 W/K) as the external walls (39 ± 6 W/K); while in 55AD the new external windows and doors reduced this to only 28 W/K. The U-value measurements suggest that the new external doors may have reduced 55AD's HTC by around 4 W/K and the BRE calculator predicts the new windows in 55AD may have reduced the HTC by a further 11 W/K. This means the glazing may be responsible for a large proportion, but not all the measured difference. However, caution needs to be taken around the glazing U-values, since the performance of the pre-retrofit windows was unknown and assumed to be equivalent to the age band defaults in RdSAP.

The loft retrofit in 57AD was a 'top-up' as the existing insulation was in good condition, while in 55AD it was completely replaced. Both were laid with the insulation in two layers of quilt 'between and over' the ceiling joists. As mentioned, however, the replacement in 55AD exhibited a performance gap while the loft top-up in 57AD did not.

The top-up loft resulted in roughly double the heat loss reduction ((5 ± 3) W/K) arising from a (50 ± 7) % improvement in U-values. Conversely, the full loft insulation replacement did not lead to a significant reduction in heat loss ((3 ± 3) W/K) and only a (25 ± 7) % reduction in U-value was measured. This highlights how the installation of loft insulation can significantly affect its performance. It also suggests that loft top-up insulation could be an effective retrofit measure if installed correctly, and conversely that if there are issues with the installation of the full loft replacement, it may not provide the expected performance.

The measured U-values for the ground floor were not reliable and so calculated U-values were used to estimate the heat loss reductions associated with the plane elements shown in Figure 316 and Figure 317. Similarly, the glazing values shown are based on calculations, and the bay window roof in 57AD was assumed to be equal to the measured values in 55AD. The external wall U-values were measured to be higher than predicted by the RdSAP and BRE calculator for 55AD, and as a result, the heat loss is higher than it was expected to be. In 57AD, the measured values more closely matched the predictions, and so the associated measured heat losses are closer to the predicted values.

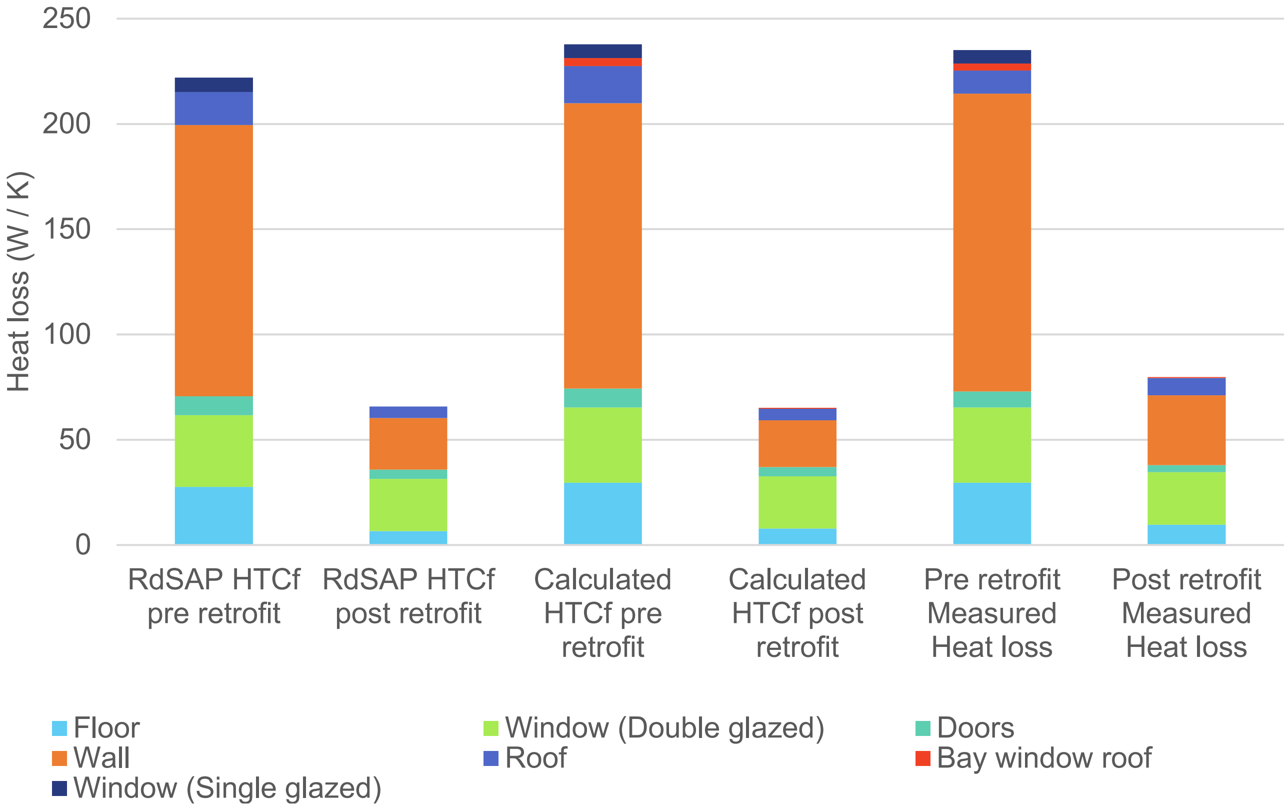

Figure 3-16 Heat loss of fabric elements pre and post-retrofit, (55AD)

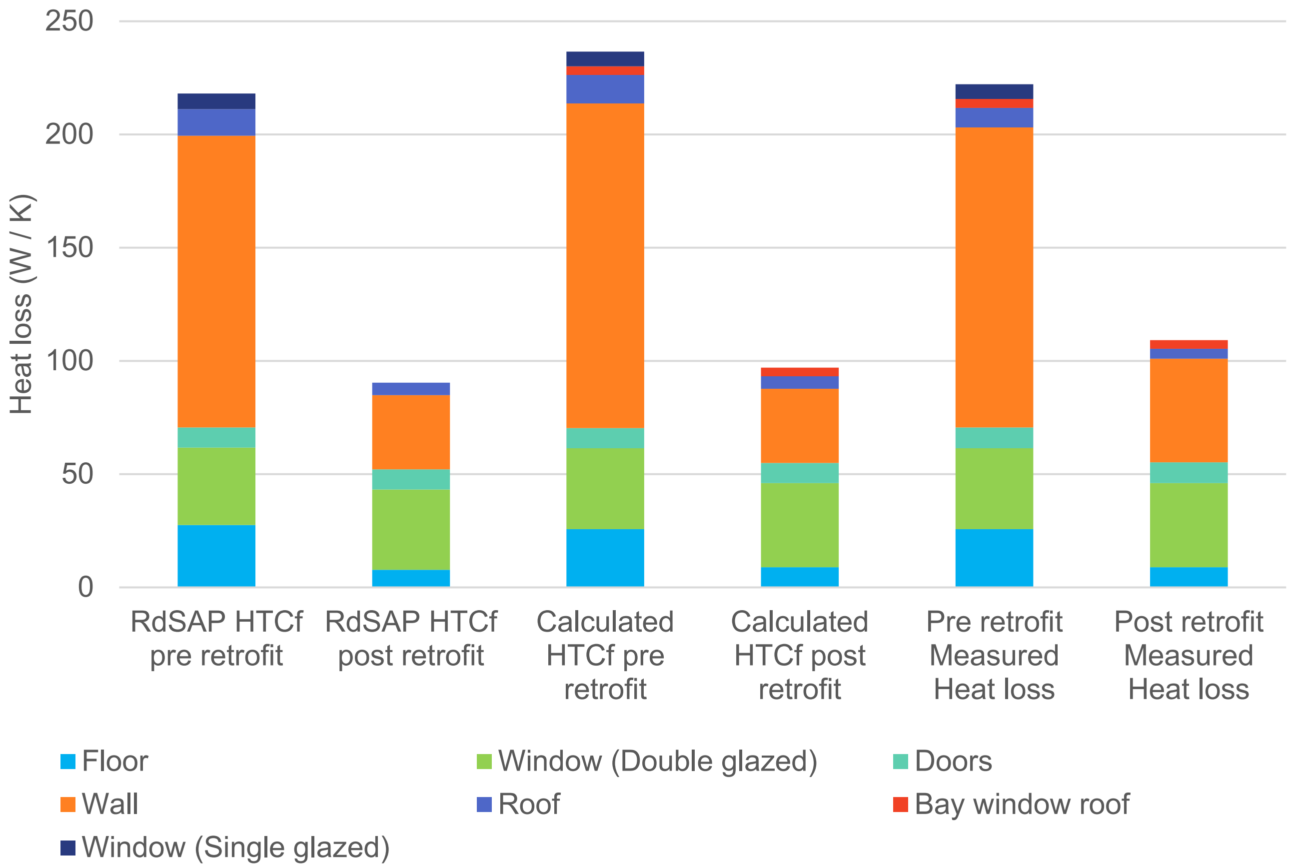

Figure 3-17 Heat loss of fabric elements pre and post-retrofit 57AD

U-value improvement summary

In-situ U-value measurements suggest that the retrofits undertaken in 55AD achieved a much larger HTC reduction than in 57AD, by (29 ± 11) W/K. This is not surprising, given that a number of the elements retrofitted in 55AD were not retrofitted in 57AD. The results also indicate that all the fabric retrofits were effective in reducing U-values, resulting in the plane element fabric heat losses being reduced by around two thirds in 55AD and half in 57AD. 70 % of the plane element heat loss reduction in 55AD and 77 % in 57AD is predicted to be from the EWI, between 13 % and 15 % respectively comes from the ground floor, and the glazing and doors saved around 12 % in 55AD (these were not upgraded in 57AD).

Despite this, post-insulation the external walls were still responsible for the majority of the plane element heat loss in 55AD homes. In 57AD, predicted heat lost via the existing external glazing and doors (46 W/K) was marginally greater than that measured via the external wall (39 ± 6 W/K). There is some uncertainty over the glazing heat losses and savings, since the existing window U-values are based on the default age bands, as the manufacturer's details were not available.

A performance gap in the 57AD external wall U-values was observed due to the uninsulated baseline wall having a better measured U-value than predicted, though the reason for this was not known. An additional 10 W/K (almost a quarter of the total external wall heat loss) was assumed to be lost by not insulating the wall behind the soffit, which makes the underperformance even more significant. This impact may be greater in detached homes and lower in terraced homes, as the scale of heat loss is proportional to the length of the junction.

Insulating the bay roof has reduced heat losses by 3 W/K in 55AD, though this heat loss is ignored in RdSAP, while leaving the understairs ground floor uninsulated may have resulted in an additional 5 W/K. Despite replacing the loft insulation completely in 55AD, post-retrofit it had higher heat loss (8 ± 1 W/K) of the loft than in 57AD (4 ± 1 W/K) which was only topped up; it is not known why this was the case or if this was linked to an irregularity in the installation technique.

Ground loop corrections increased the uncertainty in some U-value measurements affecting the ground floor, bay roof, and bay external walls. Consequently, the measured values relating to these elements were not included in the analysis and the calculated values from the BRE calculator were used instead. Additionally, the ground floor U-values did not account for edge effects and so are only indicative, and not used in heat loss calculations.

3.3 Non-repeating linear thermal bridges heat losses

Non-repeating linear thermal bridging at all junctions in 55AD and 57AD, identified in Figure 3-18 and Figure 3-19 below, was assessed with numerical simulation techniques, using TRISCO software. The outputs from the software were used to calculate junction Ψ-values and surface temperature factors. Each junction was assessed under uninsulated and retrofitted scenarios.

21 individual junctions were identified in the base case; following retrofit, two junctions were eliminated and four added, due to the infilling of window lights flanking the external front door. The resulting Ψ-values were then used to calculate the whole building thermal bridging heat transfer coefficient (HTC_b) at each stage. It is important to note that this figure does not include the thermal bridges attributable to point thermal bridges, which is assumed to be negligible in both dwellings.

A brick sample was taken for analysis so that the default thermal conductivity of the bricks could be compared to the actual thermal conductivity found on site and the implications of any disparity in thermal bridging and condensation risk at junctions could be considered.

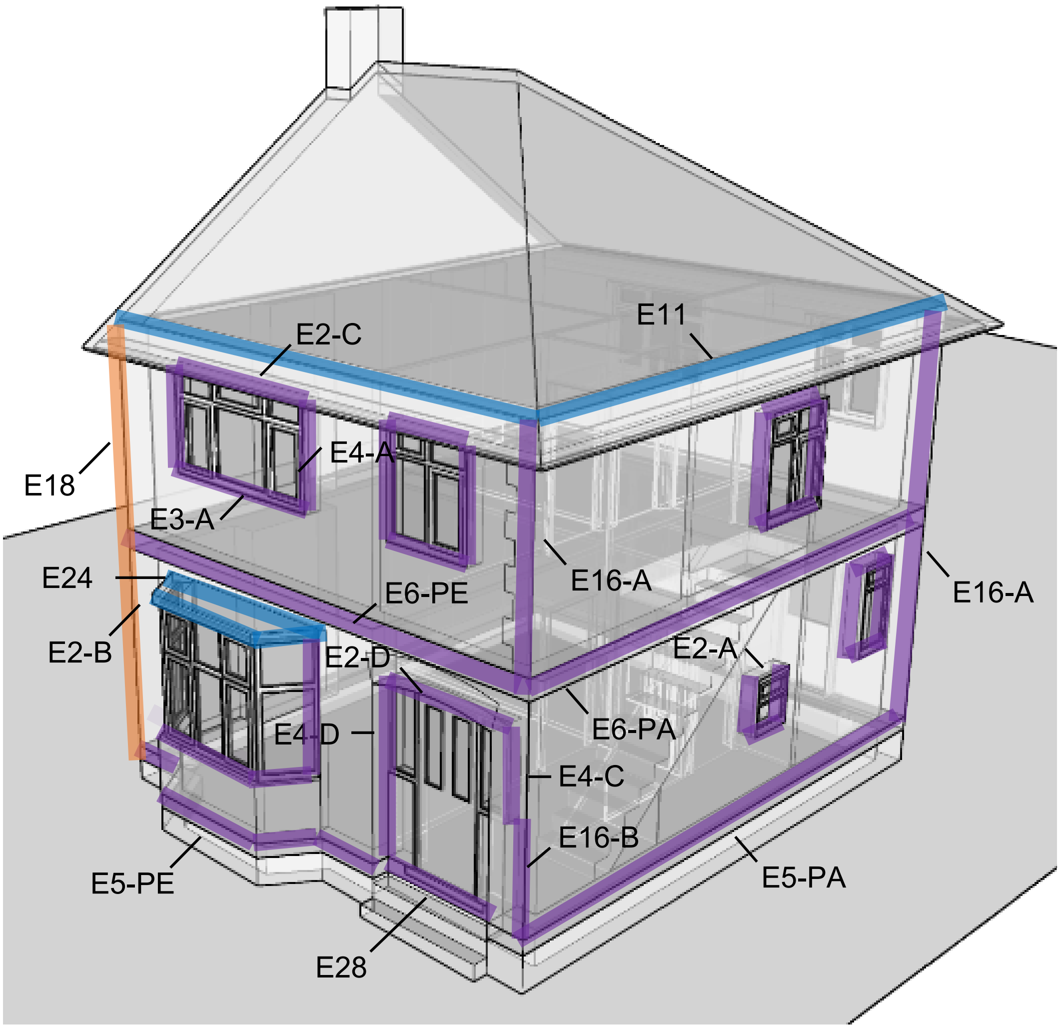

Figure 3-18 Frontal view of 55AD junctions. 57AD is a mirror image of 55 AD. (Purple: wall junctions, blue: roof junctions, orange: party junctions)

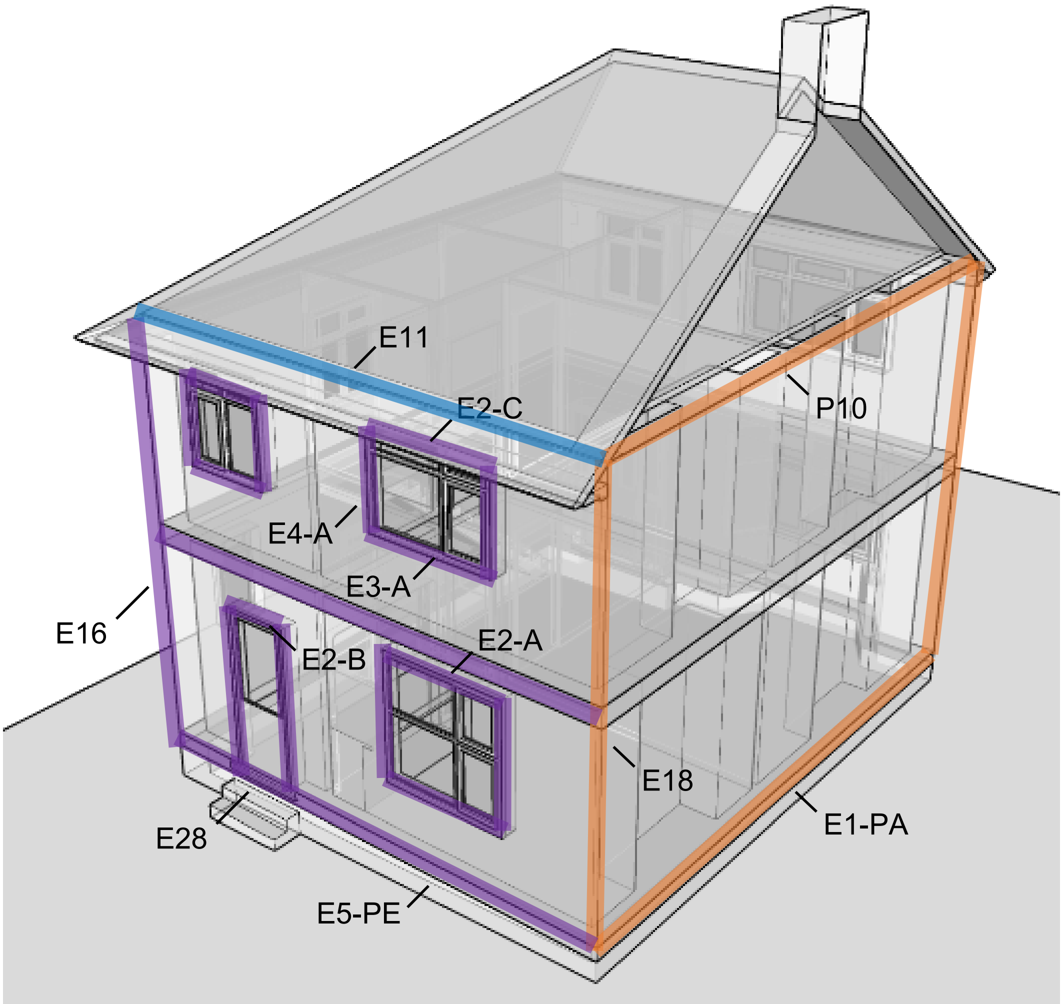

Figure 3-19 Rear view of 55AD junctions. 57AD is a mirror image of 55 AD. (Purple: wall junctions, blue: roof junctions, orange: party junctions)

Each junction highlighted and labelled in Figure 3-18 and Figure 3-19 is described in Table 3-4. There is no standardised catalogue of junctions and Ψ-values for categorising and assessing linear non-repeating thermal bridging in existing buildings. Instead, the newbuild junctions list contained in SAP Appendix K were used. Appendix K contains a list of building junctions for newbuild homes along with Ψ-values, which were used to provide a comparison in the absence of any other available data.

As no default Ψ-values are available for existing buildings, SAP assumes a default y-value (0.15 W/(m^2·K)) which is used in RdSAP calculations to account for thermal bridging heat loss. The default value of 0.15 W/(m^2·K) is compared here with the y-values derived from Ψ-values calculated at each stage of the 55AD and 57AD retrofits.

Table 3-4 Thermal bridging junction codes

Code	Description
E11	Eaves - external wall
P10	Flat ceiling - party wall
E24	Bay roof - external wall
E5-PE	Suspended ground floor - front wall, joists perpendicular
E5-PA	Suspended ground floor - gable wall, joists parallel
E28	Door threshold
P1-PA	Ground floor - party wall, joists parallel
E16-A	External wall, normal corner
E17	External wall, inverted corner
E18	External wall - party wall
E19-A	Infill wall - window head
E19-B	Infill wall - gable wall
E19-C	Infill wall - front external wall
E19-D	Infill wall - window sill
E16-B	Normal corner, gable wall - half wall.
E6-PE	Intermediate floor - external wall, joists perpendicular
E6-PA	Intermediate floor - external wall, joists parallel
E2-A	Window head
E2-B	Window head - bay window roof
E2-C	Window head, first floor
E2-D	Front door head
E3-A	Window sill - external wall
E4-A	Window Jamb - external wall
E4-C	Window jamb - gable wall
E4-D	Window jamb - external wall, inverted corner

3.3.1 Ψ-values; SAP Appendix K vs Simulation

Figure 3-20 compares Ψ-values between Appendix K of SAP and those calculated, showing there is no correlation between the calculated values and the default values found in Appendix K, i.e. the defaults are not representative of the junctions in these homes.

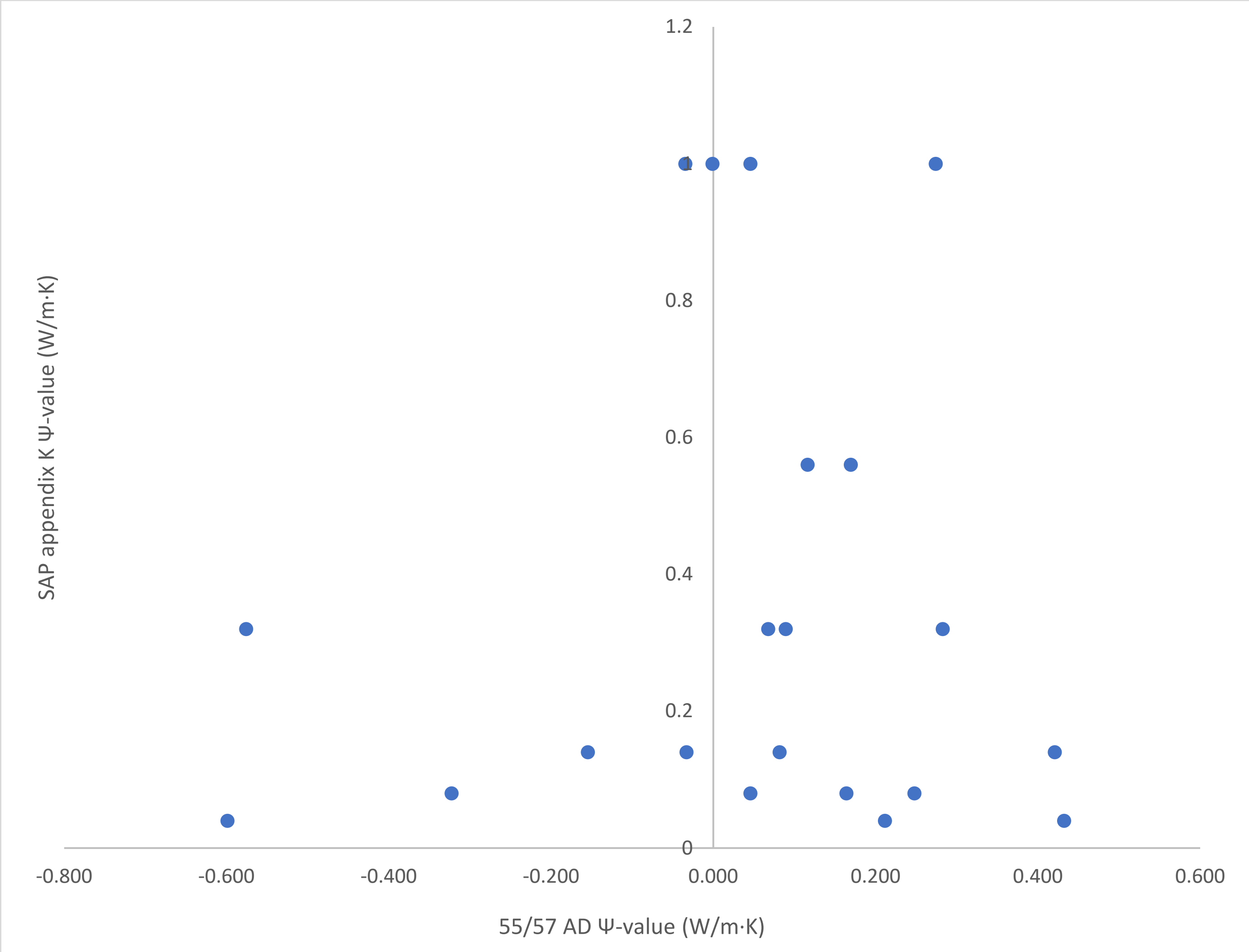

Figure 3-20 comparison of 55AD and 57AD Ψ-values to SAP Appendix K Ψ-values

The lack of relationship is likely due to the differences in building fabric assumptions and junction build-ups, as Appendix K values are based on a typical new build house. This assessment suggests that Appendix K may not be suitable and an alternative Appendix specific to existing solid walled buildings would be needed. Thus, refined Ψ-values could form the basis of a revised y-value that can be incorporated into RdSAP. Table 3-5 contains Ψ-values for each junction assessed.

Table 3-5 Summary of Ψ-values for 55AD & 57AD

Junction	Ψ-value			
	Appendix K	Base case	57AD	55AD
Eaves - external wall	0.14	0.421	0.918	0.379
Flat ceiling - party wall	0.56	0.170	0.129	0.129
Bay roof - external wall	0.04	-0.599	0.024	0.295
Suspended ground floor- front wall, joists perpendicular	0.32	0.068	0.542	0.505
Suspended ground floor - gable wall, joists parallel	0.14	-0.033	0.465	0.380
Door threshold	0.04	0.432	0.443	0.443
Ground floor - party wall, joists parallel	0.56	0.116	-0.032	-0.032
External wall, normal corner	0.32	0.068	0.542	0.505
External wall, inverted corner	0.14	-0.033	0.465	0.380
External wall - party wall	0.04	0.432	0.443	0.443
Infill wall - window head	N/A	N/A	-0.032	-0.032
Infill wall - gable wall	N/A	N/A	0.542	0.505
Infill wall - front external wall	N/A	N/A	0.465	0.380
Infill wall - window sill	N/A	N/A	0.443	0.443
Normal corner, gable wall - half wall.	0.56	0.116	-0.032	-0.032
Intermediate floor - external wall, joists perpendicular	0.14	0.082	0.018	0.018
Intermediate floor - external wall, joists parallel	0.14	-0.155	-0.049	-0.049
Window head	1	-0.034	0.034	0.026
Window head - bay window roof	1	0.046	0.046	0.054
Window head, first floor	1	0.274	0.274	0.100
Front door head	1	-0.001	0.097	0.104
Window sill - external wall	0.08	0.046	0.030	0.022
Window Jamb - external wall	0.32	0.089	0.036	0.029
Window jamb - gable wall	0.32	0.283	N/A	N/A
Window jamb - external wall, inverted corner	0.32	-0.576	N/A	N/A

The base case Ψ-values vary from those in appendix K by a wide margin: in almost all cases. Some of the greatest divergences include:

- Bay roof external wall where the inverted corner of the bay roof meets the front external wall. This junction was predicted to experience negative thermal bridging. The appendix K equivalent has a low, but positive Ψ-value.

Door thresholds. The concrete door thresholds present at the front and back external doors in both houses were found to have much higher Ψ-values that the equivalent in appendix K. This is most likely due to the high thermal conductivity of the concrete and short heat flow path underneath the doorframe.

- Window and door openings: junctions around window and door openings were found to have much lower Ψ-values than the equivalents in Appendix K. Window heads featured the greatest divergence. This is likely due to the differences in construction make-up between the new build Appendix K junctions and those found in the case study homes which featured timber lintels above window openings.

- Eaves junctions and first floor window heads: The eaves featured boxed soffits that extended to first floor window head height. No brickwork was present above the first floor window heads at the front and back of each house. This construction led to greater thermal bridging than found in Appendix K.

3.3.2 Non-repeating thermal bridging heat loss; HTCb pre- vs post-retrofit

Absolute heat loss from a non-repeating thermal bridge (HTC_b) is calculated by multiplying the Ψ-value by the length of the junction. Figure 3-21 shows the change in HTC_b for individual junctions, comparing post-retrofit values with the pre-retrofit baseline case.

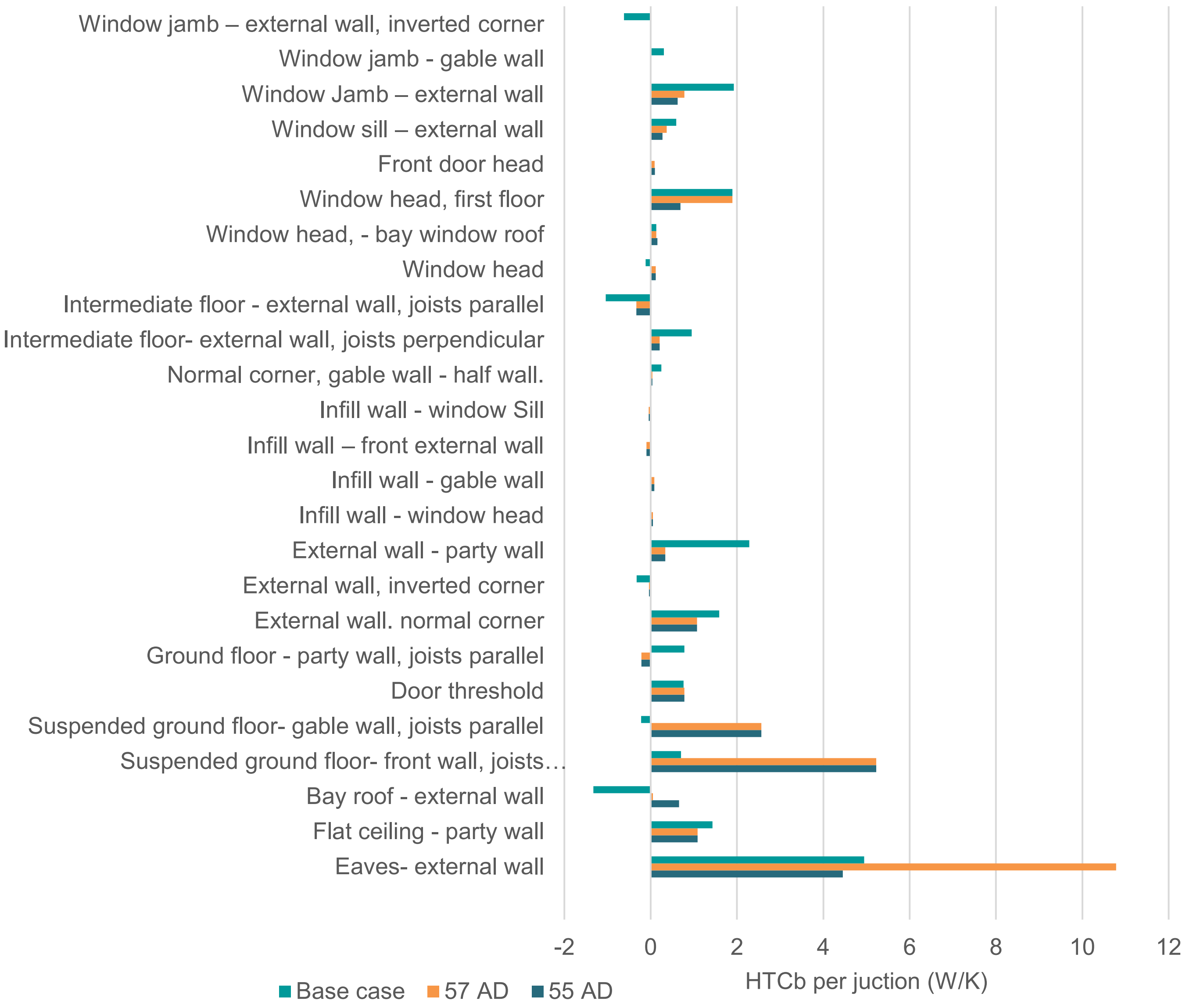

Figure 3-21 HTC_b per junction in 55AD (whole house approach) and 57AD (piecemeal approach)

Figure 3-21 shows that following retrofit, HTC_b increased at the majority of junctions, with some differences between the different approaches to the retrofits:

- Sill and jamb junctions at openings saw a reduction in thermal bridging following retrofit in both 55AD and 57AD, with 55AD experiencing a greater reduction. Ground floor window and door head junctions experienced a small increase in thermal bridging post-retrofit.
- Junctions that received full EWI coverage, including the external wall corners and intermediate floors resulted in an overall reduction in HTC_b, due to the uninterrupted insulation coverage.
- Party junctions, including the party wall to external wall, ground floor, and first floor ceiling all experienced a reduction in HTC_b, as both sides of these junctions were insulated, and no increased thermal bridging was imposed upon the neighbouring building.
- Both ground floor to external wall junctions experienced an increase in HTC_b following retrofit.
- The eaves to external wall junction experienced an increase in HTC_b in 57AD, where no additional EWI was added within the boxed soffits. In 55AD the EWI was fitted to the top of the external wall within the soffits, reducing HTC_b at the eaves below the base case.
- First floor window heads were of an unusual construction, with no outer leaf of brickwork above the window heads. Mineral wool was placed above the window heads in 55AD which had the effect of reducing the HTC_b of the junction to below base case levels.

3.3.3 Thermal bridging heat loss; y-values

RdSAP (and therefore EPCs for existing homes) does not use HTC_b to attribute heat loss for non-repeating thermal bridges (repeating thermal bridges are already included within U-values). instead, a simplified thermal bridging factor, called a y-value, is applied to the entire external heat loss area of a building. The default y-value in RdSAP is 0.15 W/(m^2·K). These y-values are calculated as the sum of HTC_b for all junctions, divided by the total heat loss area (i.e. excluding the party wall). It is therefore possible to generate a y-value from all the individually calculated HTC_b values for both the base case and post-retrofit for 55AD and 57AD, and then compare these with the RdSAP default of 0.15 W/(m^2·K).

HTC_b and y-values for 55AD and 57AD are shown in Table 36. The default value of 0.15 W/(m^2·K) overestimates heat loss in the uninsulated base case. Following the retrofit, 55AD has a y-value below the default, whilst 57AD exceeded the default y-value. More research would be needed to investigate if this scenario is common to different building types and retrofit designs, i.e. those with and without discontinuities in insulation. The results suggest that having a wider range of default y-values could improve the accuracy of EPCs and predictions around retrofit savings.

Comparing the post-retrofit y-values of the two houses allows the differences in thermal bridging heat loss between the different retrofit approaches to be compared. The approach taken in 55AD, where discontinuities in the insulation were minimised, resulted in 31.27 W/K heat loss. This is around a third lower than for 57AD where discontinuities at the windows, the eaves, and the bay window roof were left in the home. The most significant reduction in 55AD's HTC_b was at the eaves junction, where insulation was fitted within the boxed soffits. Reductions were also achieved at window openings, particularly the first-floor window heads and bay roof to wall junction.

To investigate the default thermal properties found in BR 443 [3], the calculations were repeated using the thermal conductivity of the actual bricks used in the case study home. A sample was taken from 55AD and tested in laboratories to derive this value, as described in DEEP Report 4 Brick Material Properties. This resulted in further reductions in HTC_b and y-values in all scenarios, i.e. the bricks had lower conductivity than was originally assumed.

Table 3-6 Calculated HTC_b and y-value after each retrofit stage comparing the standard calculations (default values) with calculations using conductivity values derived from laboratory tests of wall core brick samples taken at the homes (lab values)

Retrofit stage	HTC_b (W/K) (book values)	HTC_b (W/K) (lab values)	y-value (book values)	y-value (lab values)
RdSAP default	26.64	N/A	0.15	N/A
Appendix K	41.85	N/A	0.24	N/A
Base case	17.79	13.06	0.10	0.07
57AD	31.27	25.67	0.18	0.14
55AD	20.29	18.83	0.11	0.11

3.3.4 Surface temperature factor analysis

Thermal bridges also pose problems in the form of cold surfaces and surface condensation risk in homes. Temperature factors were used to indicate whether a location is at risk of surface condensation. A temperature factor below the critical value of 0.75 is deemed to be at risk. The temperature factor (f_{Rsi}) is calculated using Equation 1:

Equation 1 Temperature factor calculation method

$$f_{Rsi} = \frac{T_{si} - T_e}{T_i - T_e}$$

Where: T_{si} is internal surface temperature (°C)

T_e is external air temperature (°C).

T_i is internal air temperature (°C).

Each numerical thermal simulation that was performed yields a minimum internal surface temperature in addition to heat flow, which was used to perform the temperature factor calculation using Equation 1.

In the pre-retrofit base case, 18 of the 21 base case junctions in 55AD and 57AD were assessed to be at risk of surface condensation formation. Following the piecemeal retrofit in 57AD, only 4 of 23 post-retrofit junctions were identified as being at risk. The whole house approach retrofit in 55AD was even more effective at eliminating condensation risk, as only the door threshold junction remained below the critical temperature factor of 0.75. The temperature factor found at the door threshold was lowered by the retrofit in both houses, likely due to the introduction of ground floor insulation lowering the underfloor void air temperature. The nature of this junction makes the addition of insulation on top of the doorstep difficult without introducing a change in the floor level at the door threshold.

Table 3-7 shows the temperature factor (f_{Rsi}) of the 25 junctions modelled for each retrofit stage. The junctions with f_{Rsi} below 0.75 are highlighted red, indicating that they may be at risk of surface condensation.

In the pre-retrofit base case, 18 of the 21 base case junctions in 55AD and 57AD were assessed to be at risk of surface condensation formation. Following the piecemeal retrofit in 57AD, only four of 23 post-retrofit junctions were identified as being at risk. The whole house approach retrofit in 55AD was even more effective at eliminating condensation risk, as only the door threshold junction remained below the critical temperature factor of 0.75. The temperature factor found at the door threshold was lowered by the retrofit in both houses, likely due to the introduction of ground floor insulation lowering the underfloor void air temperature. The nature of this junction makes the addition of insulation on top of the doorstep difficult without introducing a change in the floor level at the door threshold.

Table 3-7 Temperature factor (f_{Rsi}) after each retrofit stage (red = potential risk)

Element	Junction	Base case	57AD	55AD
Roof	Eaves - external wall	0.685	0.698	0.857
	Flat ceiling - party wall	0.839	0.889	0.889
	Bay roof - external wall	0.736	0.792	0.861
Wall	External wall, normal corner	0.589	0.912	0.912
	External wall, inverted corner	0.670	0.946	0.946
	External wall - party wall	0.728	0.963	0.963
	Infill wall - window head (retrofit only)	N/A	0.925	0.925
	Infill wall - gable wall (retrofit only)	N/A	0.885	0.885
	Infill wall - front external wall (retrofit only)	N/A	0.935	0.935
	Infill wall - window sill (retrofit only)	N/A	0.943	0.943
	Normal corner, gable wall - half wall.	0.603	0.906	0.906
Window/ opening	Window head	0.746	0.959	0.895
	Window head - bay window roof	0.649	0.649	0.788
	Window head, first floor	0.544	0.544	0.752
	Front door head	0.838	0.948	0.908
	Window sill - external wall	0.746	0.960	0.966
	Window Jamb - external wall	0.556	0.902	0.913
	Window jamb - gable wall	0.620	N/A	N/A
	Window jamb - external wall, inverted corner	0.683	N/A	N/A
Ground floor	Suspended ground floor - front wall, joists perpendicular	0.698	0.759	0.775
	Suspended ground floor - gable wall, joists parallel	0.698	0.766	0.799
	Door threshold	0.306	0.258	0.258
	Ground floor - party wall, joists parallel	0.927	0.774	0.774
	Intermediate floor - external wall, joists perpendicular	0.714	0.961	0.961
	Intermediate floor - external wall, joists parallel	0.709	0.963	0.963

3.3.4.1 Gas pipe cut-outs

Due to retrofit scheduling issues, the external gas pipe that runs into both 55AD and 57AD was not moved. The presence of external gas pipes required cut-outs to be made in the EWI, creating a discontinuity in the insulation layer. The gas pipe cut-outs were recognised as potential surface condensation risks due to thermal bridging, so numerical thermal simulations were carried out to assess if any potential risk was posed.

The gas pipe at 55AD is located on the gable wall (see Figure 3-22), extending to just above ground floor level, and does not intersect any other junctions in the building envelope. Simulations of the insulation cut-out around the gas pipe in 55AD resulted in a temperature factor of 0.85, indicating that the cut-out does not pose a risk of surface condensation on the inside surface and that no remedial action was required. The temperature distribution isotherm from the thermal bridging modelling is also shown in Figure 3-22.

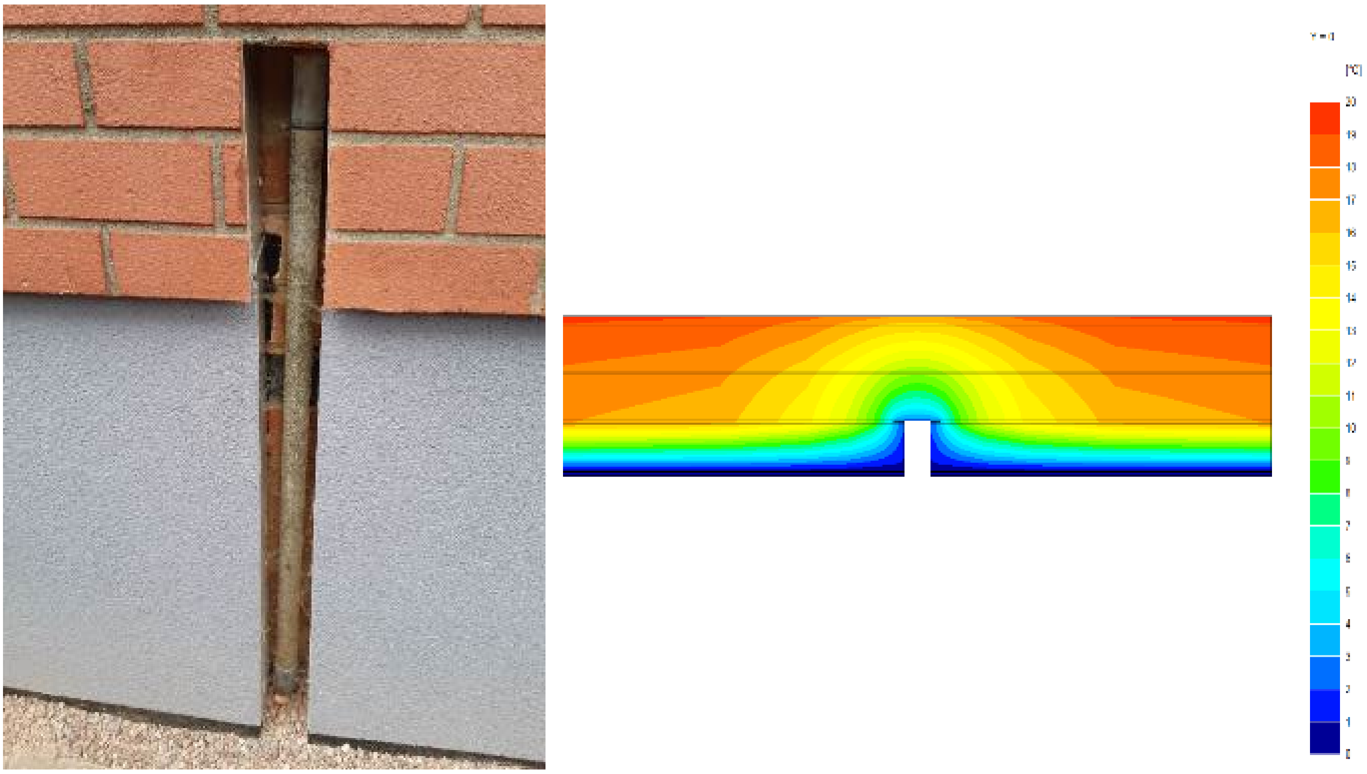

Figure 3-22 Left: Gas pipe cut-out at 55 AD. Right: thermal simulation temperature distribution at 55 AD gas pipe cut-out.

The external gas pipe at 57AD is located on the gable wall (Figure 3-23), between the gable wall to rear wall corner and a window jamb. It also extends much further up the wall than in 55AD and terminates just below the first-floor ground level. The proximity of these junctions, as well as the length of the cut-out and the discontinuity of EWI due to the cut-out, was found to pose a risk of surface condensation. The temperature distribution isotherm from the thermal bridging modelling is also shown in Figure 3-23 and the results of several assessments are contained in Table 3-8.

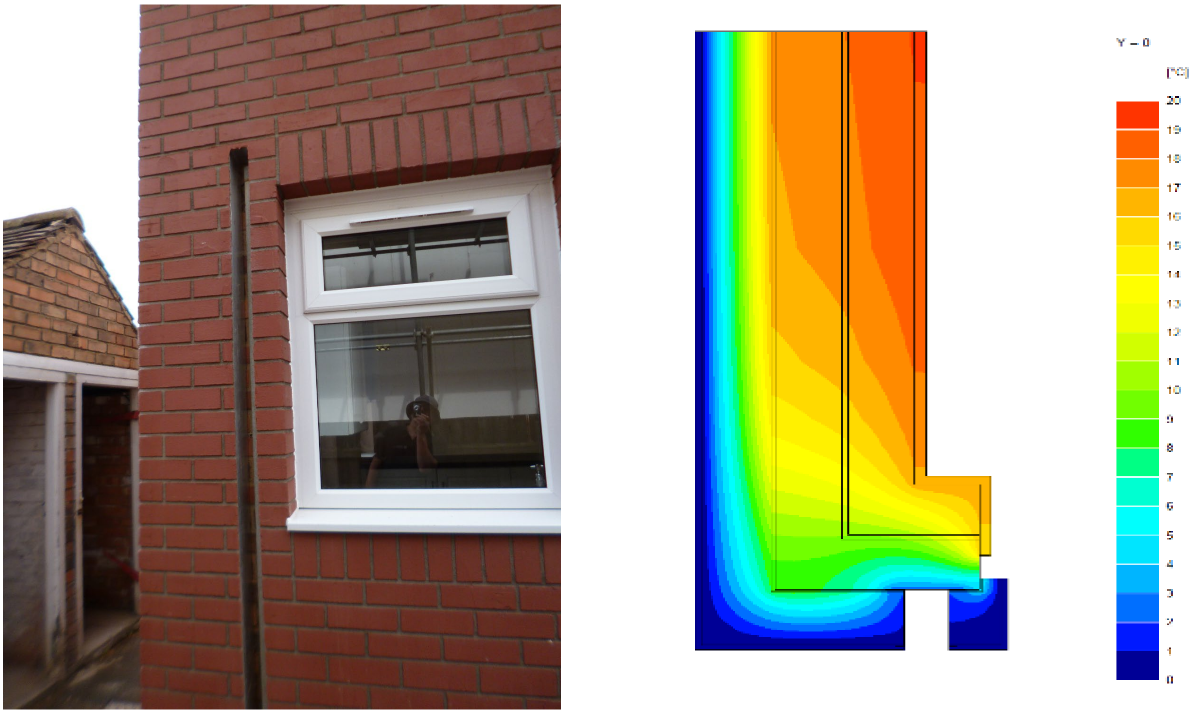

Figure 3-23 Left: Gas pipe cut out at 57 AD. Right: thermal simulation temperature distribution of 57 AD gap pipe cut-out

As shown in Table 3-8, the decision to not move the external gas pipes lead to surface condensation risk at the internal surface in 57AD, indicated by a temperature factor below 0.75. The condensation risk was found to persist even after the new windows were installed. Adding thermal laminate plasterboard, including 10 mm of EPS insulation to the internal window jamb, was found to increase the temperature factor to an acceptable level. Simplified risk reduction strategies can avoid costly remedial work, however, understanding where risk exists may require thermal modelling of junctions. The creation of best practice allowable solutions to these issues, which have been assessed to be safe, may be a way of ensuring installers without access to thermal bridging software can ensure risk mitigation is undertaken.

Table 3-8 57AD gas pipe temperature factors

Scenario	Temperature factor (f_{Rsi})
Whole house, non-PAS retrofit - without gas pipe cut out	0.93
Whole house, non-PAS retrofit - with gas pipe cut out	0.66
Post testing PAS upgrade - with gap pipe cut out	0.66
Post testing PAS upgrade - gap pipe cut out, plus remedy IWI	0.77

3.3.5 Thermal bridging alternative scenarios

Additional thermal bridging analysis was carried out to explore the impact of alternative retrofit scenarios for the suspended timber ground floor junction with the gable wall and front wall, with and without insulation. The results are shown in Table 3-9 :

Table 3-9 Alternative scenario model results: suspended timber ground floor to external wall junctions with and without floor insulation (red = risk of condensation).

	Ground floor	Wall	DPC	Ψ-value W/(m·K)	Heat loss W/K	Temperature factor
EWI (front external wall)	Un-insulated	Uninsulated	Uninsulated	0.068	0.701	0.698
	Insulated	Uninsulated	Uninsulated	0.219	2.271	0.685
	Insulated	EWI	Uninsulated	0.542	5.613	0.759
	Un-insulated	EWI	Uninsulated	0.381	3.941	0.803
	Insulated	EWI	Insulated	0.505	5.227	0.775
	Un-insulated	EWI	Insulated	0.336	3.482	0.817
EWI (gable external wall)	Un-insulated	Uninsulated	Uninsulated	-0.033	-0.222	0.698
	Insulated	Uninsulated	Uninsulated	0.076	0.514	0.685
	Insulated	EWI	Uninsulated	0.465	3.138	0.766
	Un-insulated	EWI	Uninsulated	0.349	2.352	0.803
	Insulated	EWI	Insulated	0.380	2.562	0.799
	Un-insulated	EWI	Insulated	0.255	1.722	0.829

The front external wall has a higher Ψ-value when compared to the gable wall equivalents, due to the joist location for the front external wall (joist perpendicular) and gable external wall (joist parallel); which affects how much heat escapes from the ground floor. Additionally, the front external wall has a slightly higher condensation risk (lower temperature factor) than the gable wall equivalents.

In the uninsulated base case scenario, the ground floor to external wall junction is at risk of surface condensation, but the thermal bridging heat loss is small. Installing EWI causes a marginal increase in thermal bridging heat loss but eliminates surface condensation risk. Conversely, insulating the ground floor without installing EWI results in both a minor increase in thermal bridging heat loss and a marginal increase in surface condensation risk. Therefore, a risk-based approach to retrofit in solid walled homes like 55AD may be required to ensure that the suspended ground floor insulation takes place after EWI is installed.

Introducing a strip of EWI below the DPC level further reduces heat loss and surface condensation risk, though the improvement is negligible. These results further suggest that, for some homes with suspended timber ground floors, it may not be necessary to extend EWI below DPC to remove surface condensation risk, which is counter to best practice guidance [4].

In these scenarios, the DPC started (and therefore the EWI stopped) at ground floor level, which is a relatively common detail. Homes with different constructions and different relative ground floor and DPC positions, however, could have differing risks related to ground floor insulation and insulating below the DPC. Additionally, internal surface condensation risk is not the only moisture risk associated with this junction. Thus, more investigations of different ground floor types would be needed to understand how applicable the results found here are to the UK housing stock.

Thermal bridging heat loss improvement summary

Both 55AD and 57AD had higher thermal bridging heat losses (HTC_b) post-retrofit than pre-retrofit (17.79 W/K). However, 55AD, which had EWI extended behind the soffits, its bay window roof insulated, and new windows fitted in-line with the EWI, had lower thermal bridging heat losses (20.29 W/K) compared to 57AD (31.27 W/K) which did not have these details.

The y-value default of 0.15 W/(m^2·K) contained within RdSAP was found to be an overestimate for the pre-retrofit base case, which both had a y-value of 0.10 W/(m^2·K). Post-retrofit the y-value was not substantially changed in 55AD, moving to 0.11 W/(m^2·K), while in 57AD where there were more discontinuities in the insulation layer, the y-value increased to 0.18 W/(m^2·K). This means that post-retrofit, the y-value in RdSAP was overpredicting the HTC_b in 55AD, but under predicting it in 57AD.

Using actual measured material properties of the bricks had the effect of further lowering the HTC_b, resulting in the y-value dropping to 0.07 for the uninsulated homes, exacerbating the overprediction by EPCs using RdSAP. Post-retrofit, the y-value also fell to 0.11 and 0.14 for 55AD and 57AD, respectively. It may therefore be beneficial to revisit and expand the range of default y-values available for EPC inputs for existing homes, specifically to account for which elements are insulated and the presence of thermal bridges.

Pre-retrofit the homes were assessed to have surface condensation risks at almost all junctions. Adding the EWI in 57AD removed the risk in almost all the junctions in the home, except the junction between the bay window to bay roof (which was uninsulated), and the external wall to eaves and first floor window head junctions. However, when both the bay window roof and the external wall behind the soffit at the eaves were insulated in 55AD, these risks were also removed. The only junction post-retrofit in both homes that persisted was the door threshold, as has been found in other DEEP case studies.

The additional whole house approach retrofit therefore may be considered a lower risk retrofit. Notably though, in this case study, relocating the windows to ensure they were in-line with the EWI did not materially reduce risks or heat losses. This means that there needs to be greater guidance on which interactions between fabric elements are critical to a risk-based approach to retrofit, and which may not be in specific situations.

Commonly, cut-outs in the EWI are undertaken to avoid costs associated with arranging for utility companies to relocate gas pipes. In this study, the cut-outs were not deemed to cause a surface condensation risk by themselves. However, where cut outs are large, and located in proximity to a window and a wall corner, the discontinuity of insulation did cause a surface condensation risk on the internal wall surface. This was countered by applying thin IWI to the affected window reveal, which is considered a cost-effective approach to reducing risk, and could be employed more widely with appropriate guidance.

3.4 Whole house heat loss (HTC) improvement

The total measured heat loss for each dwelling following the retrofits is shown in Table 3-10.

Table 3-10 Test house HTC after each retrofit stage

Retrofit stage	HTC (W/K)	HTC uncertainty	HTC reduction (W/K)	Percentage reduction
55AD.B Baseline	239	9 (4 %)	-	-
55AD.WH Whole house approach	104	11 (11 %)	135 ± 14	(56 ± 6) %
57AD.B Baseline	225	9 (4 %)	-	
57AD.R.F.W Floors, EWI, loft insulation	130	13 (10 %)	95 ± 16	(42 ± 7) %

As can be seen, pre-retrofit, the two homes had roughly the same measured HTC, between (225 ± 9) W/K and (239 ± 9) W/K. The whole house approach retrofit in 55AD was found to have a made significantly larger HTC reduction, (40 ± 17) W/K more than the piecemeal retrofit in 55AD. This is illustrated in Figure 3-24.

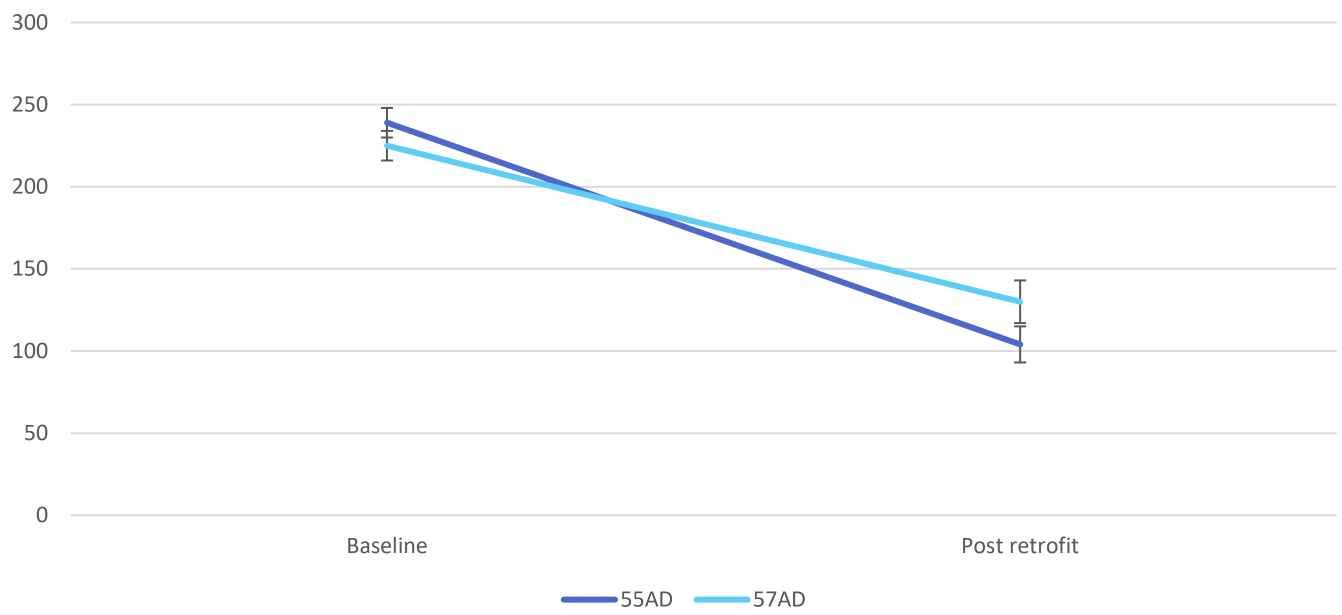

Figure 3-24 Coheating HTC at each retrofit stage

The uncertainty in the coheating test result for the pre-retrofit in both homes is low (4 %), however, post-retrofit it is relatively high (11 % for 55AD and 10 % for 57AD). In part, this was linked to higher levels of solar radiation in the post-retrofit test (taking place later in the heating season), but also linked to ground loop corrections affecting U-value measurements on party walls.

3.4.1 Comparing whole house and piecemeal retrofit approaches

The homes pre- and post-EWI retrofit are shown in Figure 3-25.

Figure 3-25 55AD & 57AD pre- (top) and post- (bottom) retrofit

The EWI mineral fibre boards were mechanically fixed to the walls, then rendered over, as shown in Figure 3-26. Additional layers of render were applied in place of the original brick courses on the ground floor and corners, and the beige render details on the first floor.

Figure 3-26 Mechanical fixing to wood fibre EWI board (left) followed by render (right)

Figure 3-27 shows the difference in the EWI at the eaves between the whole house approach (extend EWI behind the soffit) and the piecemeal approach (EWI stops at soffit) to compare the extent of thermal bridging taking place at the eaves, for each approach.

Figure 3-27 EWI stops at soffit level in 57AD (left) but continues behind soffit in 55AD (centre); view behind the soffit (right) at the party wall showing EWI on 55AD eaves but not 57AD

The implications of the discontinuities indicated in Figure 3-27 are shown in Figure 3-28, where a clear thermal bridge is observed at the eaves junction in all the upstairs rooms in 57AD. This was not observed in 55AD. The extent to which this causes additional thermal bringing heat losses was discussed in Section 3.3 and the implications this has for surface condensation risk are discussed in Section 3.9.

Figure 3-28 Top: thermal bridge at eaves in 57AD where EWI is not installed behind the soffit Bottom: equivalent view in 55AD, with EWI behind the soffit

On further investigation, a smaller discontinuity in the EWI and loft insulation was also observed in 55AD, as shown in Figure 3-29. In the case of the window to eaves detail, the loft insulation continued through to meet the window head. However, at the external wall eaves junction, the loft insulation did not continue to overlap with the EWI, leaving a discontinuity. It is not known if this was due to a buildability issue, such as: contractors could not install a small section of mineral wool here owing to the space being too narrow; if it was left to ensure that ventilation at the eaves could be preserved; or if it was unintentionally omitted.

Thus, despite the EWI being extended to ensure it could meet with the loft insulation in the whole house approach retrofit, a small discontinuity still occurred here. It is not known if this was the case for the entire eaves of both homes or just at this inspection point. However, thermal bridging calculations have considered this the 'as-built' detail to estimate thermal bridging heat loss and condensation risk.

Figure 3-29 55AD EWI continuity with loft insulation at window heads junction (left), compared to EWI discontinuity at the external wall to ceiling junction (right)

The loft hatches in both homes were retrofitted with insulated and sealed units, replacing unsealed and uninsulated timber hatches. As can be seen in Figure 3-30, this resulted in much less air leakage and warmer loft hatch temperatures. This not only reduces the chance of surface condensation occurring on the underside of the loft hatch, but it also limited the potential for warm moist air to enter the cold loft space, thus reducing the chance of surface condensation occurring on the roof timbers.

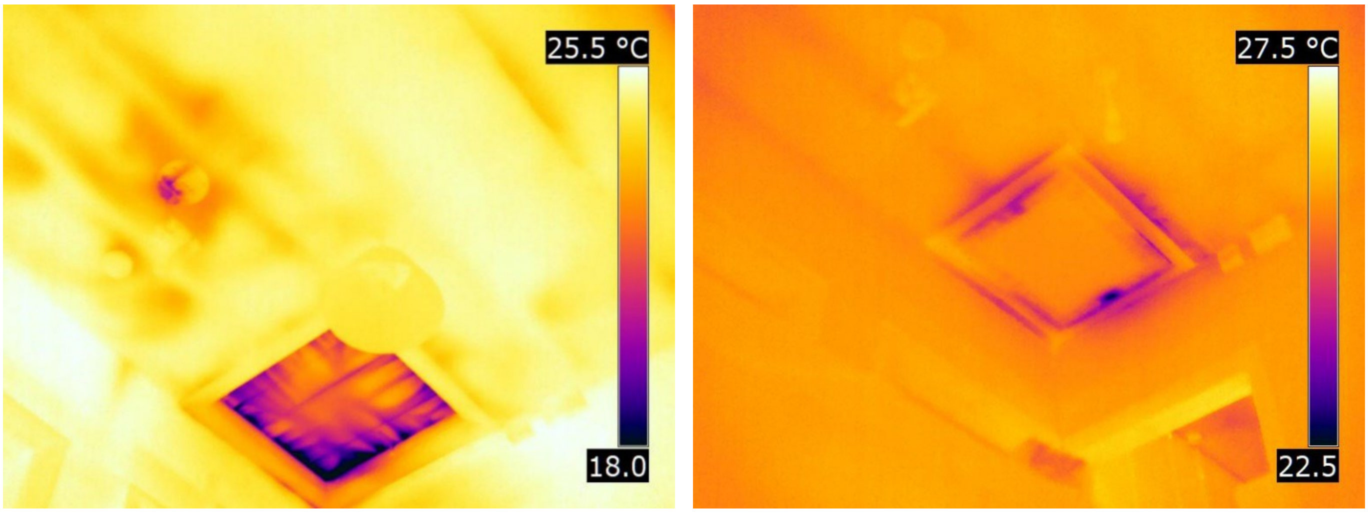

Figure 3-30 Uninsulated (left) and insulated (right) loft hatches under depressurisation

Figure 3-31, shows another whole house approach consideration in 55AD: bay roof insulation was fitted, and new bay windows installed (this did not take place in the piecemeal approach to 57AD). As can be seen, additional construction to pull out the bay window from the existing opening was needed to ensure that the EWI would not cover over the window frame and to ensure that the windows could remain installed in-line with the EWI.

Figure 3-31 Bay roof insulated in 55AD (left) and bay walls and sills extended to accommodate new windows in-line with EWI (right)

Similarly, to ensure that the new glazing and external doors installed in 55AD were installed in-line with the EWI, plywood boxes were used. These boxes extended beyond the external face of the existing external solid wall, into which the windows could be fitted, as shown in Figure 3-32.

Figure 3-32 Plywood boxes in 55AD to accommodate new external windows and doors in-line with the proposed EWI

Both homes had their suspended ground floor retrofitted including having membrane fitted over the floor joists, infilled with mineral wool, and taped to the walls, as shown in Figure 3-33, before new tongue and groove floorboards were laid.

Figure 3-33 Ground floor retrofit with air barrier membrane (left) and mineral wool (right)

However, it was not possible to access the understairs suspended timber ground floor in 57AD. This meant that this section of the ground floor remained uninsulated. As can be seen in Figure 3-34, this resulted in cold air infiltrating into the home at this uninsulated location.

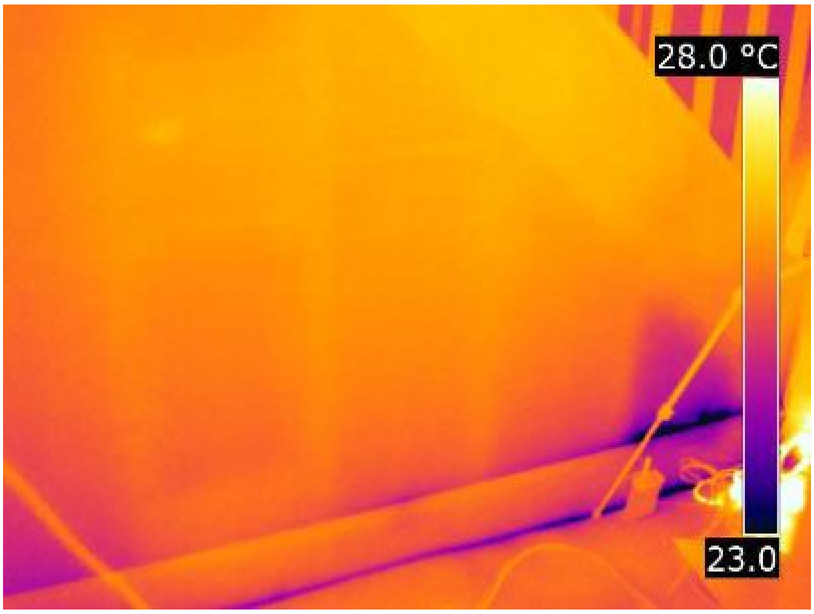

Figure 3-34 Understairs cupboard ground floor insulated in 55AD (left) but not in 57AD (right)

Both homes had their external wall below the damp proof course (DPC) insulated externally, though XPS was used as a more water-resistant alternative to mineral wool boards (air vents to the sub floor void were maintained), as shown in Figure 3-35. Applying insulation below the DPC is recommended to extend to the ground level, while previous guidance was to continue the insulation 400 mm below ground level. The new guidance means installations should be easier and cheaper to install. However, as can be seen, some groundwork was still required to accommodate the below DPC insulation, as existing drainage needed to be pulled away from the external wall edge. The impact of installing XPS below the DPC on heat losses and surface condensation risk was explored in Section 3.3.

Figure 3-35 XPS insulation below DPC requiring drainage to be relocated underground

All these differences cumulatively resulted in the retrofit at 55AD (whole house approach) achieving significantly more HTC reduction than the piecemeal 57AD retrofit, by an additional (40 ± 16) W/K, or (14 ± 9%), as shown in Figure 3-36.

The findings show that retrofits to the loft floor and external walls, applied piecemeal, and without changing a home's external glazing or doors, could reduce heat loss in these two solid walled homes by between a third to a half, with the majority of the savings being achieved by EWI.

The additional benefit from fitting new glazing, upgrading bay window roofs and continuing the EWI beyond the soffit, means that the heat loss from these solid walled homes was reduced by (56 ± 6) % in 55AD while it was only (42 ± 7) % in 57AD which did not have these additional measures.

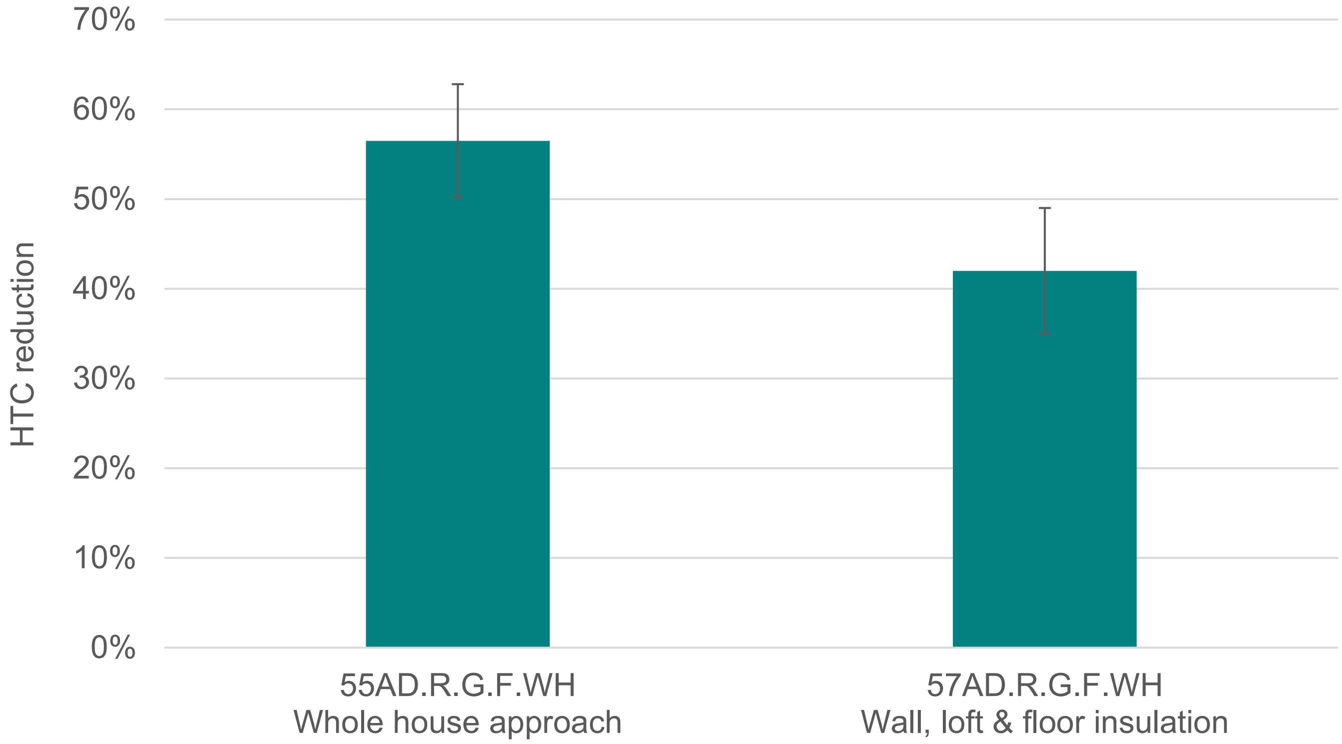

Figure 3-36 Measured heat loss savings from the retrofits

3.4.2 Whole house consideration for bay windows and EWI

Adding EWI to bay windows presented a challenge in integrating it with the installation of the new windows. As the existing window frame was not wide enough at 57AD, it was not possible to run the EWI neatly into the window as it would clash with the glazing. Instead, the EWI installers cut the insulation back at an angle so that it met the edge of the existing frame and could be easily rendered. However, this meant that there was less insulation present at the jambs of the bay window in 57AD and consequently a larger thermal bridge than at 55AD, where the EWI overlaps the frame (Figure 3-37).

Figure 3-37 57AD bay window (left) where EWI has been cut back in anticipation of a new window, and 55AD bay window (right) where the EWI overlaps the side of the window frame

At 55AD, plywood boxes were installed within the structural openings into which the external windows and sills were installed, so that they were flush with the EWI. This meant the sills provided an appropriate overhang, so no rainwater dripped onto the render (see Figure 3-38). However, the bay window at 55AD was built, and the windows fitted, in advance of the EWI. This meant that the EWI depth was not anticipated, and the bay did not have adequate overhangs.

Figure 3-38 Window sill at 55AD bay window (left), dining room (centre), and bedroom (right)

Conversely, at 57AD, where, to investigate an alternative approach, the external windows and doors were not replaced or moved forwards into the insulation before the EWI was installed for the post-retrofit test. However, after the post-retrofit tests had been completed, the external windows and doors were eventually replaced before handover to the landlord, i.e. after the EWI had been added. Here, the new external windows (except for the bay window) were fitted closer to their original position, and more in-line with the brick wall. For all of the external windows, except the bay window, this meant that the sills did not provide an adequate overhang (Figure 3-39). The installer had more flexibility with the bay window and was able to adjust where each window sat within the plywood box, therefore installing it with an appropriate sill depth.

Figure 3-39 Window sill at 57AD bay window (left), kitchen/diner (centre), and bedroom (right)

At 55AD, a new bay roof covering was fitted into the external brickwork prior to the EWI being installed, since the roof was also being rebuilt and insulated at the same time. In 57AD (where the bay was not being refurbished until after the EWI was installed), the decision was taken to also fit the new roof covering into the external brickwork prior to the EWI and left on top of the existing bay roof, until the roof was ready to be replaced prior to handover. Without doing this, the installer may have had to remove some EWI to access the bay roof. In true piecemeal retrofits, where EWI is installed without consideration of bay windows, this could be costly and disruptive.

Additionally, the installer left a larger gap than expected between the top of the bay roofs and the EWI. This was to enable access to this area should anything go wrong with the roof covering, (see Figure 3-40) causing a strip of uninsulated external wall in both properties.

Figure 3-40 Bay window of 57AD being replaced before handover (left) and completed bay window roof of 55AD (right) both showing the large gap between roof and underside of EWI

3.4.3 QUB and the coheating test HTC results

The QUB method is an alternative way of measuring the HTC of a building, and is described in the DEEP Methods 2.0 Report. Multiple QUBs were undertaken in both homes across both retrofit stages to compare against the coheating test. In total, 33 QUB tests were performed on the two houses, 27 on 55AD and six on 57AD. This was done to investigate the reliability and accuracy of the QUB test under a host of different conditions.

For 55AD, 16 tests were completed for the baseline stage and 11 for the whole house retrofit stage. For 57AD three tests were completed for each stage. The baseline tests were undertaken in September and November 2021: the whole house retrofit tests were completed in April 2022. For both houses the tests had a 10-hour duration for the baseline stage and seven hour for the retrofit stage. All attempted tests had a compliant α value (heat loss / heat gain ratio), as described in the DEEP Methods 2.01 Report, which can impact the accuracy of measurements. A reference HTC is required to compute α. A provisional BREDEM-modelled HTC was used for the baseline stage and a provisional result of the coheating test was used for the retrofit stage. Use of a secondary set of timers and thermostatically controlled heaters ensured the starting temperature remained constant for repeated tests and the α value was within the recommended range. The α value was recalculated based on the final coheating HTC measurement and remained compliant for all tests. The individual QUB HTC measurements are shown against the upper and lower uncertainty boundaries of the corresponding coheating measurements in Figure 3-41. As the houses are semi-detached, they are separated by a party wall: no adjustment for party wall losses was performed on these measurements.

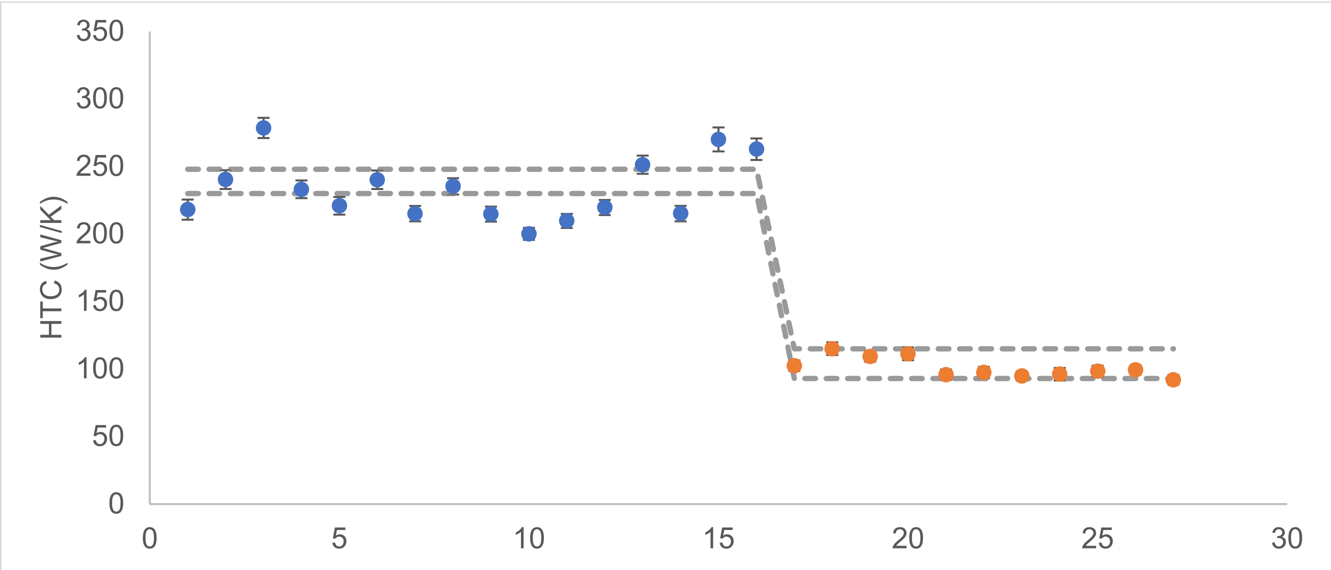

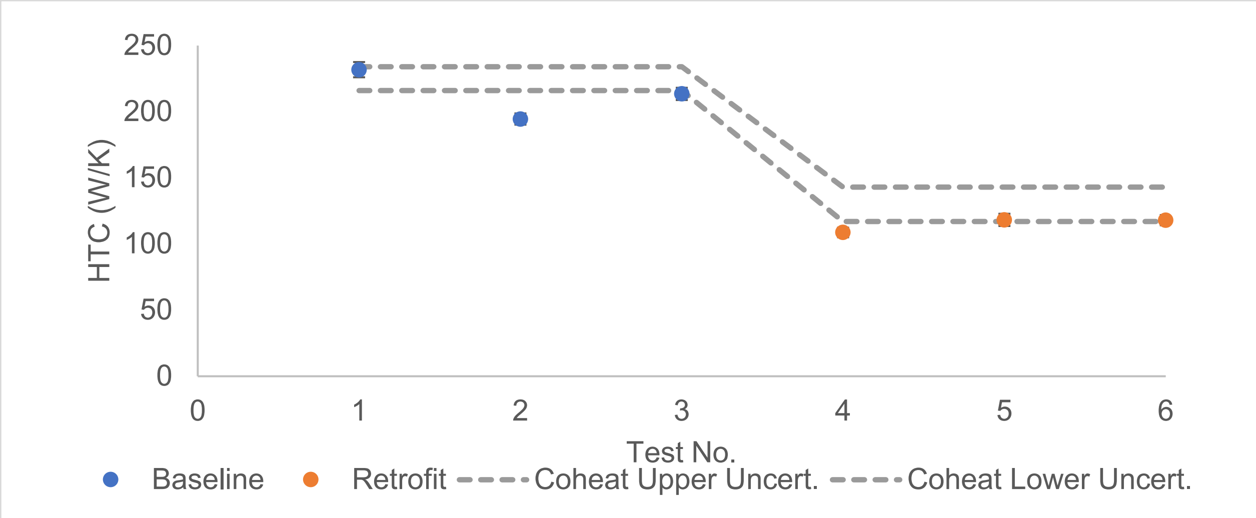

Figure 3-41 Comparing individual QUB HTC and coheating measurements (55AD top, 57AD bottom)

For both houses, results from the retrofitted stage show closer agreement than that of the baseline. Across both houses, seven out of the 19 QUB tests completed in the baseline stage have overlapping confidence intervals with coheating. Comparatively, 13 out of 14 QUB tests completed in the retrofit stage overlap with the coheating measurement. The dispersion of the QUB tests also improved following retrofit. For 55AD, the range of results relative to the mean was 35 % and 23 % for the baseline and retrofit stages respectively. For 57AD the range improved from 18 % to 8 % post-retrofit. This is possibly a result of reduced infiltration losses that are likely to vary with factors such as internal to external temperature difference and wind.

The overall uncertainty-weighted average for the QUB measurements compared against coheating is presented in Figure 3-42. When taking the average of the QUB tests, the agreement between the two tests appears even closer, with relative differences across the baseline and retrofit stages of 5 % and 4 % for 55AD and 7 % and 12 % for 57AD. These are in-line with published works that have identified a difference of between 1 % and 15 % when comparing the two methods [5, 6].

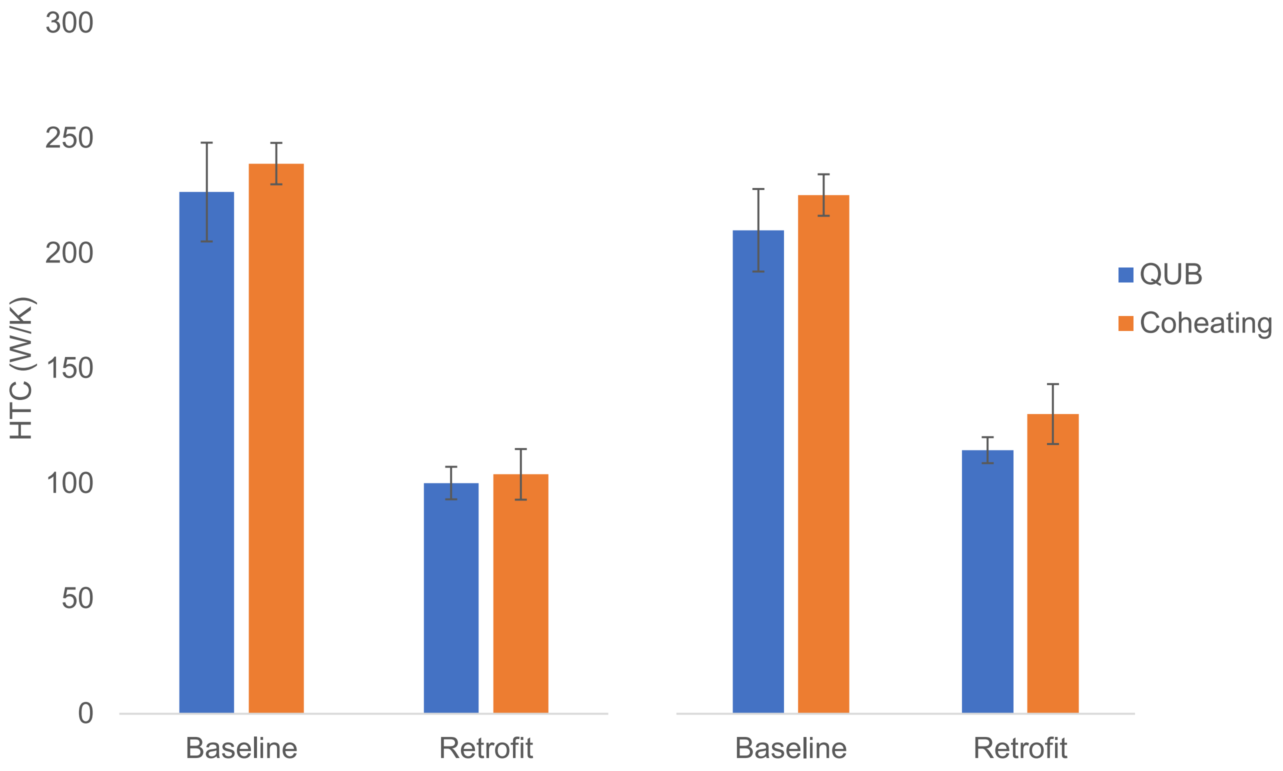

Figure 3-42 Average QUB HTC measurement vs coheating measurement (55AD Left, 57AD Right)

These results show that in these homes the QUB method was largely consistent with the coheating tests.

3.4.4 Aggregated and disaggregated HTC

The aggregate whole house HTC has been measured using the coheating test but can also be disaggregated into the three individual components:

HTC_v (infiltration heat losses) can be estimated by applying the n/20 rule to the blower door test results.

HTC_f (plane element heat losses including repeated thermal bridging) can be approximated by measuring heat flow via HFPs on all elements and summing the area.

HTC_b (non-repeating thermal bridging heat losses) can be calculated by modelling each junction in thermal bridging software; though it is erroneously often assumed to be the remainder once the HTC_v and HTC_f are subtracted from the whole house measured HTC.

According to Equation 2, the equivalent HTC saving achieved from airtightness improvements in 55AD is approximately 12 W/K. which combined with the new external glazing and doors could account for the difference in the respective HTCs.

Equation 2 Estimating background ventilation heat loss (HTC_v) via the n / 20 rule

$$HTC_v = \left(\frac{Permeability\ (m^3\ per\ m^2.hr\ @50\ pa) \times Volume\ (m^3)}{20 \times specific\ heat\ capacity\ of\ air\ (3\ MJ\ /\ m^3 K)} \right) \times Shelter\ factor\ (0.85)$$

Notwithstanding the above result, more research to investigate the n / 20 rule of thumb is needed, and any attempt to disaggregate the whole house HTC into fabric and background ventilation heat loss using the n / 20 should be treated with caution. This has been demonstrated in a recent publication, where this rule of thumb is shown to be inappropriate for a sample set of 21 buildings [7]. Investigation using a larger sample set would be required to identify an alternative rule of thumb for a range of UK archetypes.

The measured HTC from the coheating test and the HTC calculated from summing the disaggregated HTC_v, HTC_f and HTC_b are presented in Figure 3-43. As can be seen, the disaggregated method consistently predicts a higher HTC than measured by the coheating test.

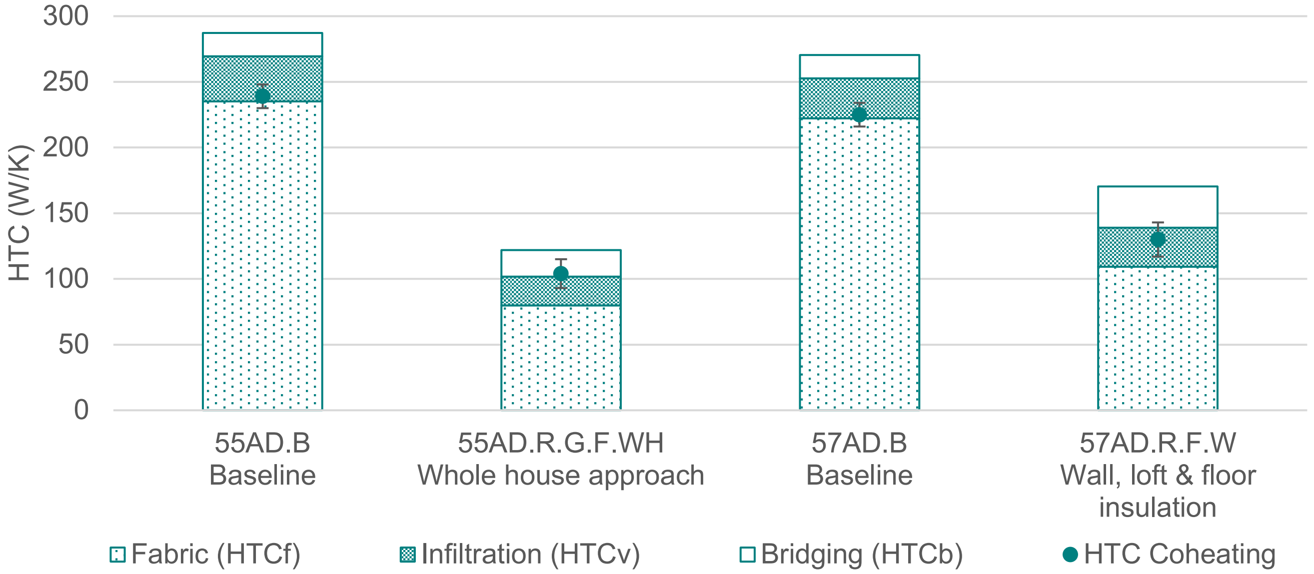

Figure 3-43 Aggregated vs. disaggregated measured HTC

The reasons for the discrepancy are likely due to:

- The n / 20 rule is an average annual approximation which may not be appropriate for different building types or for different levels of wind exposure, geography, or topography.
- HFP placements may not be representative or comprehensive of whole element heat loss, which will impact on the representativeness of the HTC_f that is estimated.
- Thermal bridging simulations contain simplifications in geometry and use default data on construction material properties, so may not be representative of actual HTC_b. The calculations also do not consider point thermal bridges.
- Systematic uncertainty in the coheating test cannot be perfectly accounted for, e.g. party wall heat exchange, solar gains, and wind. In addition, only quasi steady-state conditions are possible.
- The default U-values for the pre-retrofit external windows were assumed because specific performance details were not known.

Although the coheating and disaggregated absolute values for the HTCs differ, they agree on the scale of HTC reductions achieved by the retrofits. The disaggregated approach predicts a 58 % and 37 % savings for 55AD and 57AD respectively, while the coheating test measured a (56 ± 6) % and (42 ± 7) % reductions.

According to the disaggregated measurements, 55AD had (32 ± 17) W/K less plane element fabric heat loss than 57AD, 12 W/K lower infiltration heat loss, and 11 W/K lower thermal bridging heat losses. When combined, this means that 55AD had (55 ± 17) W/K lower heat losses than 57AD according to the individual disaggregated measurements. This is much higher than the (26 ± 17) W/K measured by the coheating tests.

Table 3-11 shows the relative heat losses in both homes pre- and post-retrofit. While the plane element fabric heat losses were responsible for most of the heat loss pre- and post-retrofit, after the fabric upgrades, the background ventilation heat losses become relatively more important, even though they fall in absolute terms in 55AD. Similarly, the thermal bridging heat losses (which slightly increase) also become relatively more important, especially in 57AD, where large thermal bridges were left around the eaves, the external windows, and doors.

Table 3-11 Whole house heat loss via disaggregated methods

Retrofit stage	HTC_f (W/K)	HTC_v W/K	HTC_b W/K
55AD.B Baseline	235 (82 %)	33 (12 %)	18 (6 %)
55AD.R.G.F.WH Whole house approach	80 (66 %)	21 (17 %)	20 (17 %)
57AD.B Baseline	222 (82 %)	29 (11 %)	18 (7 %)
57AD.R.F.W Wall, loft & floor insulation	109 (65 %)	29 (17 %)	31 (18 %)

Whole house heat loss improvement summary

The retrofits in both homes achieved significant reductions in heat loss: 135 ± 14 W/K ((56 ± 6) %) in 55AD and 95 ± 16 W/K ((42 ± 7) %) in 57AD, according to the coheating tests.

55AD achieved (14 ± 9) % more savings because its retrofit took a whole house approach and replaced the external glazing and doors. The benefit in HTC that may derive from taking a whole house approach is dependent on the specific details. For instance, the new external glazing and doors may have been responsible for up to 18 W/K of the savings (according to U-value measurement); the bay window roof as much as 3 W/K; insulating the suspended ground floor area under the stairs around 5 W/K; extending the EWI to the eaves and behind the eaves soffit around 10 W/K, and reducing the infiltration rate as much as 12 W/K. Finally, the thermal bridging heat losses were calculated to be around 8 W/K higher.

Interestingly, topping up the existing insulation in 57AD resulted in loft heat losses of (4 ± 1) W/K, and was much more successful than replacing the loft insulation in 55AD, which resulted in loft heat losses around (8 ± 1) W/K.

Combined, the individual disaggregated estimates of heat losses suggest (55 ± 17) W/K more heat loss taking place in 57AD than 55AD, double the (26 ± 17) W/K difference measured by the coheating tests. The reasons for the disaggregated approach predicting a larger difference is thought to be attributable to uncertainties around quantifying individual heat loss mechanisms. For instance, the applicability of the n/20 rule of thumb is poorly understood. Relying on spot heat flux density measurements to interpret U-values for entire elements means it is difficult to capture heterogeneous heat loss, and thermal bridging calculations rely on assumptions for construction materials, as well as construction make-up, which may not match actual conditions. Additionally, the external glazing and door baseline U-values were based on defaults and may not have represented what was installed.

Thus, although disaggregated methods can be useful in highlighting heat loss hotspots, they have high levels of uncertainty associated with them, which makes summing their individual contributions to attain a whole house value problematic. The aggregated heat loss assessment provided by the coheating test may be less susceptible to these errors, though it has its own inherent uncertainties related to variables such as accounting for solar radiation and party wall heat losses, which are not perfectly accounted for. There is also the potential for variable quasi-steady-state conditions to occur.

Despite these uncertainties, the case studies have shown that EWI, loft, and suspended ground floor insulation have the potential to reduce heat losses by more than a third. When new external glazing, doors, and bay roof insulation are added, and thermal bridging from eaves minimised, heat loss can be reduced by up to two thirds.

The QUB measurements show good agreement with the coheating tests pre- and post-retrofit, indicating QUB measurements can be successfully undertaken in semi-detached houses such as 55AD and 57AD. The dispersion of measurements improved for both houses following retrofit.

3.5 Measured vs. modelled retrofit performance

3.5.1 Measured vs. modelled HTC calibration step 1

In this step, the default input values for airtightness and U-values were used. The measured HTC values for each retrofit stage were plotted against the HTC values predicted by the uncalibrated models using default RdSAP input data in Figure 3-44.

- Each model predicted a near identical baseline HTC for each home, which was expected, as they were a pair of semis with similar geometry and construction.
- In 55AD, the steady-state predictions were near identical pre- and-post-retrofit, while in 57AD the post-retrofit prediction was assumed to be lower in RdSAP because of a slight difference in the way suspended ground floor U-values were applied in the models.
- The steady-state models predicted higher HTC values in the uninsulated home compared to the measured HTC, and DSM predictions were closer to the measured HTC, as had been found in other DEEP case studies.
- DSM and steady state predicted similar post-retrofit HTCs to one another for each home, i.e. the difference between the modelling approaches caused differences in heat loss predictions for uninsulated homes, but less so for insulated homes.
- Steady-state models predicted a 53 % reduction in HTC for 55AD, similar to that measured by the coheating test (56 ± 6) %, while DSM predicted slightly lower savings (44 %).
- Steady-state models predicted 44 % reduction in HTC for 57AD, again, similar to the coheating test (42 ± 7) %, while DSM predicted a smaller 36 % reduction.
- All models predicted higher heat losses than were measured post-retrofit, which suggested the default U-value, airtightness, and thermal bridging heat losses may not reflect those taking place in these homes.

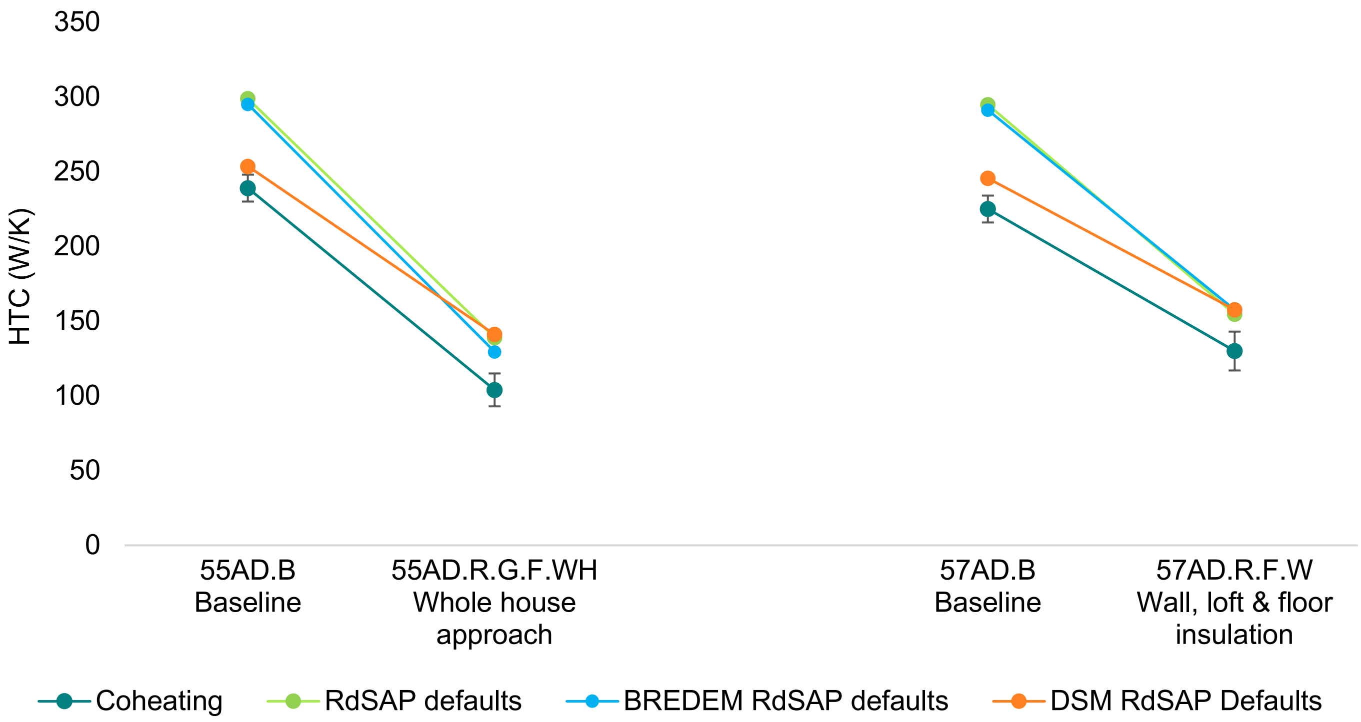

Figure 3-44 Measured vs modelled HTC calibration step 1: default data

3.5.2 Measured vs modelled HTC calibration step 2: measured infiltration

In this calibration step, the models used average annual infiltration rates derived from the blower door test, as this data is the most likely to be acquired in practice. The impact of this compared to the previous calibration stage can be seen in Figure 3-45.

- RdSAP is not shown since it was not possible to alter the infiltration rate in the software.
- The measured airtightness of both homes was lower than the RdSAP estimates. Correspondingly, when this was incorporated, both DSM and BREDEM predicted a lower HTC.
- The HTC predictions of both models became more aligned with the coheating HTC.
- In the pre-retrofit homes, the DSM HTC was now within the error of the coheating measurement, though it remained slightly higher than the coheating test post-retrofit.
- In 55AD post-retrofit, the BREDEM HTC was now within error of the coheating measurement, though not in 57AD.
- Pre-retrofit, BREDEM had significantly higher HTC indicating the RdSAP default U-values and thermal bridging heat loss may not be appropriate for this house.

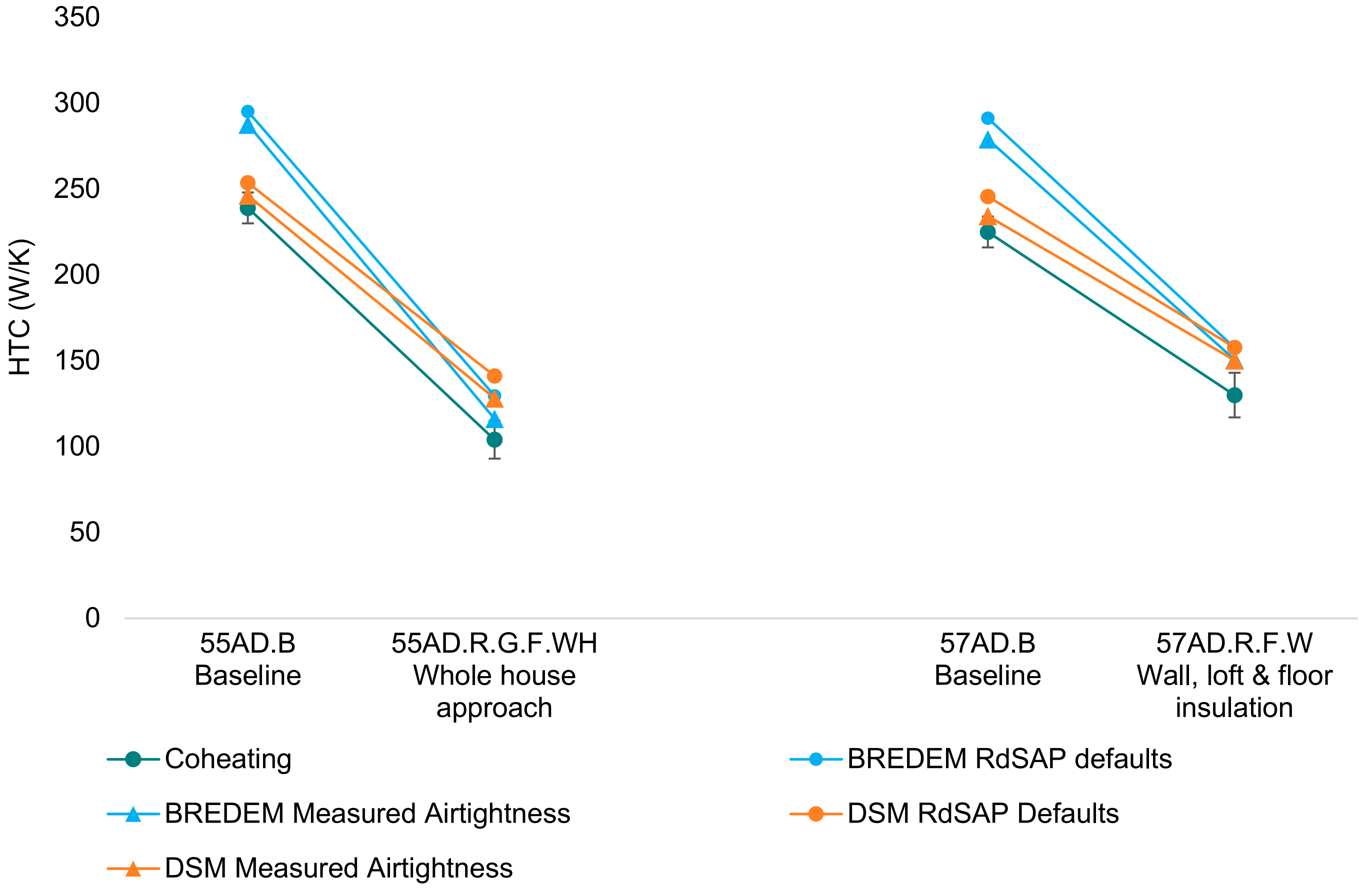

Figure 3-45 Measured vs modelled HTC calibration step 2: measured infiltration

3.5.3 Measured vs modelled HTC calibration step 3: calculated U-values

In this step, the models included U-values defined using the BRE calculator, based on detailed surveys. It often requires assumptions or destructive investigations to establish the nature and thickness of construction layers. The impact of this compared to the previous calibration stage can be seen in Figure 3-46.

- RdSAP is not shown since it was not possible to include calculated U-values in the software.
- The calculated external wall U-values for the uninsulated home were higher than the RdSAP defaults predicted, resulting in the pre-retrofit HTC predictions in both BREDEM and DSM increasing by between 3 % and 4 % respectively.
- Post-retrofit the calculated and default U-values were much closer and the difference in their HTC predictions less pronounced.
- Incorporating calculated U-values into the models moved the predicted HTCs further away from the coheating test, suggesting either the calculations were inappropriate or the default thermal bridging in the models was not appropriate for these homes.

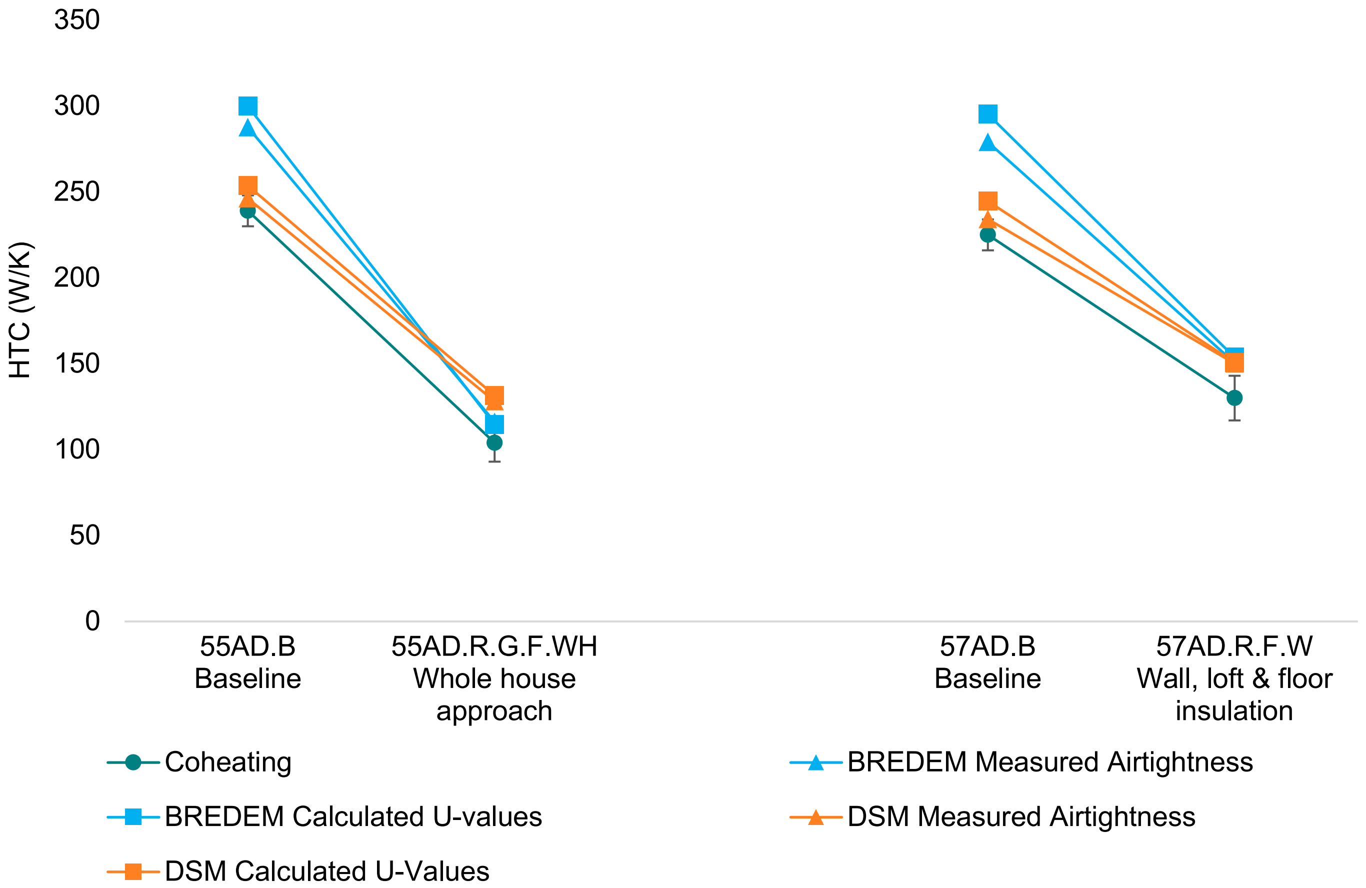

Figure 3-46 HTC calibration step 3: calculated U-values

3.5.4 Measured vs modelled HTC calibration step 4: measured U-values

In this step, the models used measured U-values which required resource intensive in-situ testing. The impact of this compared to the previous calibration stage is shown in Figure 3-47.

- The measured external wall U-values for the uninsulated home were higher than both the RdSAP default and BRE calculator predictions. Thus, in this step, the HTC predictions increased by 9 % and 21 % in RdSAP for 55AD and 57AD respectively; by 6 % and 16 % in BREDEM; while in DSM the increases were 3 % and 11 %.
- This took all the HTC predictions further away from the coheating value.
- This suggests that the home exhibited markedly heterogeneous heat flow which was not captured via the spot heat flux density measurements and may illustrate the uncertainty associated with elemental U-values measurements in the field. Alternatively, it may be that the thermal bridging heat loss default assumptions in the models were not appropriate.
- There could also be some effect on the coheating test, which was not perfectly accounted for in the coheating test and uncertainty assessments (e.g. solar).

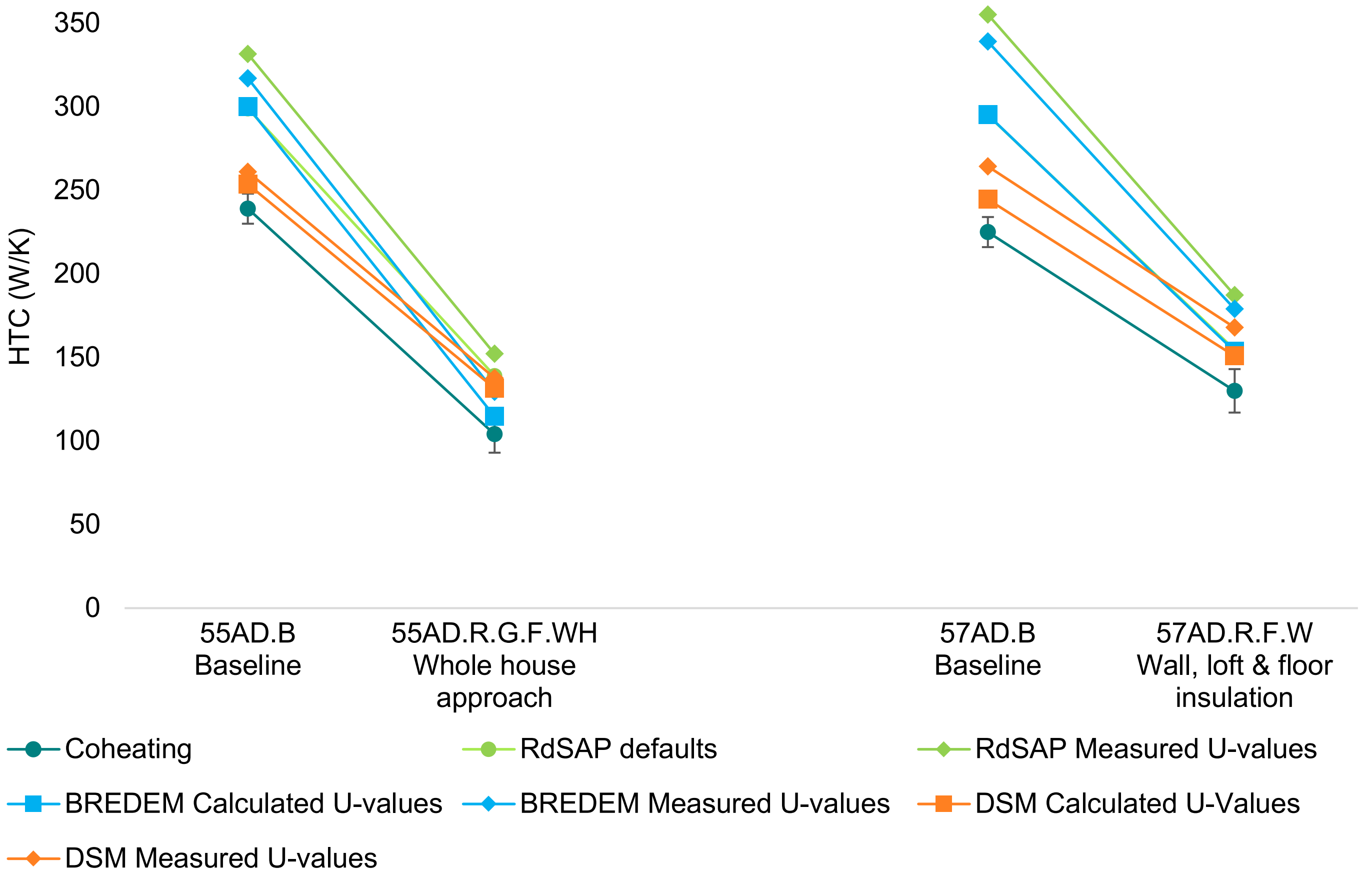

Figure 3-47 HTC calibration step 4: measured U-values

3.5.5 Measured vs modelled HTC calibration step 5: calculated thermal bridging

In this step, the models used calculated HTC_b from elemental thermal modelling to update default values. This is a highly specialist and rarely undertaken exercise. The impact of this compared to the previous calibration stage is shown in Figure 3-48.

- RdSAP is not shown since it was not possible to change default bridging heat losses in the software.
- Including the calculated thermal bridging heat losses substantially reduced the HTC predicted by DSM models, though it only slightly reduced the HTC predicted by BREDEM.
- Pre-retrofit in both homes, the calculated thermal bridging was seen to be lower than the default values and so HTCs in both models dropped (substantially for DSM).
- Post-retrofit thermal bridging in 55AD was lower than default values so HTC predictions reduced.
- In 57AD, however, post-retrofit, the bay roof, external windows and doors, and eaves junctions had large discontinuities in insulation. This caused the bridging to be higher than the defaults in BREDEM. Despite this, in DSM, the total bridging was still lower than the default value.
- Including calculated thermal bridging brings the DSM HTC very closely in-line with the results of the coheating tests, especially for 57AD.

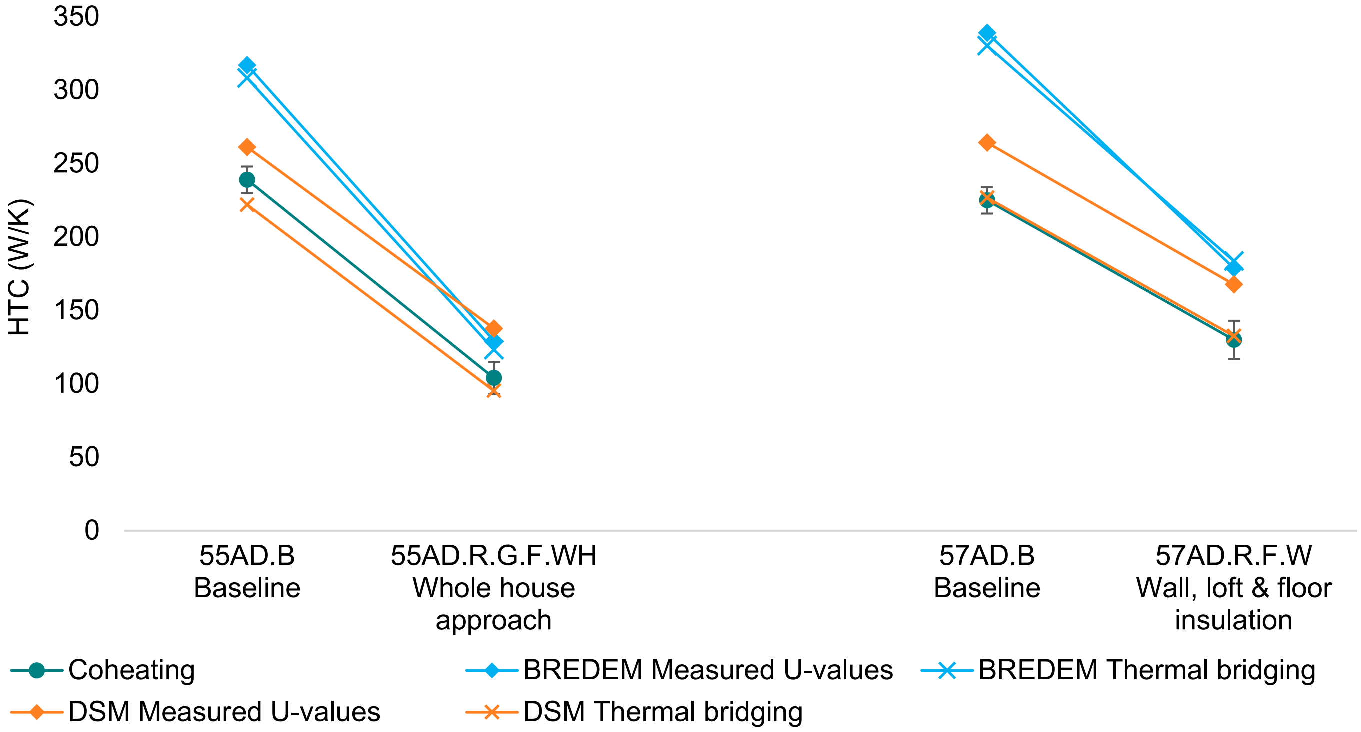

Figure 3-48 HTC calibration step 5: calculated thermal bridging

The reason why updating the thermal bridging defaults affects BREDEM marginally, but DSM significantly, concerns how they are accounted for in the models. In BREDEM, a whole house y-value is used, while DSM applies individual bridging heat loss to specific junctions based on Ψ-values. In the default case, Ψ-values based on Appendix K and the actual geometry of the junctions are used.

Converting the Appendix K default values into a y-value (dividing total heat loss by total heat loss area) gives a value of 0.25 compared to 0.15 used in RdSAP. This falls to 0.10 post-retrofit, i.e.

there is a larger reduction in DSM than BREDEM. This was exacerbated in the AD case study homes due to the presence of bay windows, which have very high Appendix K Ψ-values (1.00 W/(m·K)) compared to other junctions. This shows that use of default y-values can have a relatively large impact on the accuracy of EPCs.

Measured versus modelled HTC summary

RdSAP and BREDEM predict much higher HTC values than DSM in all the calibration models and DSM is more aligned with the measured coheating values in all models.

The models predict the two homes to have very similar starting HTCs to each other (as did coheating tests), and they predict a similar level of HTC reductions will be achieved, as was predicted by the coheating tests.

As with many of the DEEP case studies, the airtightness of the homes was much better than the defaults, and so including measured infiltration rates brings all the model predictions in better alignment with the coheating tests.

Conversely, the default U-values were assumed to be lower than they were calculated, and measured to be, meaning replacing default U-values made the predicted HTCs increase and be less aligned with the coheating test.

The thermal bridging was calculated to be lower than the RdSAP defaults in the uninsulated homes meaning that in both models, the HTC of the pre-retrofit homes reduced when defaults were updated. In BREDEM this was only a marginal change; for DSM, it was significant.

Post-retrofit in 55AD, the thermal bridging was again lower than the defaults suggested, and so updating these resulted in lower predicted HTC in both models. However, in 57AD which had more exposed thermal bridges, the thermal bridging was calculated to be higher than the default and this meant that the BREDEM HTC increased post-retrofit. Conversely, in the case of DSM, even though the thermal bridging increased marginally post-retrofit in 57AD (piecemeal approach), including the calculated values still resulted in a reduction to the HTC. This is because the other junctions in the home (especially lintels) had very high thermal bridging heat loss default values, compared to their calculated values.

More research is needed to understand the appropriateness of y-values and how these relate to Appendix K Ψ-values, the geometry of homes, thermal bridging heat losses calculated by software, and how these change as a result of adding insulation into homes.

Having a wider range of default y-values for different property characteristics would mean assessors could choose more appropriate y-values for EPCs. For instance, selecting specific building features that are particularly significant for thermal bridging heat loss (e.g. bay windows, or the presence of insulation) rather than relying on simple age band defaults.

3.6 Predicting EPC band, annual space heating, and carbon emissions

EPC bands, space heating requirements, carbon reductions, and fuel bill savings are commonly used for retrofit policy evaluation. DEEP did not perform any longitudinal monitoring of energy consumption pre- and post-retrofit in the case study homes, however, the energy models can predict the impact of the retrofits on these metrics.

To do this, all models shared matching occupancy profiles and internal heat gain inputs as defined in the RdSAP conventions. These are described in detail in the DEEP Methods 2.01 Report. Matching occupancy profiles were used to provide a comparison between the modelling approaches, based on changes to fabric inputs only. However, despite having matching assumptions for gains and occupancy, the resulting space heating demand from the RdSAP, BREDEM, and DSM models differed substantially.

Dynamic and steady-state models are fundamentally different, in that DSM calculates heat balances and demand at an hourly timestep; whereas RdSAP and BREDEM calculate these for a typical day of each month and extrapolate results for an annual prediction. Thus, the complex interactions between heat gains and heat demand that take place over a diurnal cycle are only captured in DSM. It is beyond the scope of this project to confirm which approach is more accurate, but it is clear that the RdSAP and BREDEM models consistently predict higher space heating demand than DSM. This is significant when considering the success of retrofits and calculating paybacks or impacts on EPC levels and fuel poverty for policy evaluation. RdSAP age-band default data underestimated baseline EPC scores, and thus overestimate retrofit savings.

3.6.1 Potential reasons for differences in annual model outputs

Fundamental differences between steady-state and DSM models led to discrepancies in the predicted heat loss and energy calculations for the DEEP case studies. The differences between the models are discussed in the DEEP Methods 2.01 Report, and are summarised here:

Internal heat gains from occupants, lighting and equipment
The total heat gain from each of these sources in DSM is adjusted to closely match that in BREDEM, however, as they are hourly heat balance calculations, there may be periods when useful gains may offset some fuel use as they align with periods of heating.

Heating set points and schedules
These have been adjusted to match those used in BREDEM, however, the hourly resolution of the weather data means that in some instances heating demand can occur in warmer daylight hours within DSM models. Equally, some heating may occur during periods of lower temperatures in the morning and evening.

Hourly vs daily average external temperature
The external air temperature used in the hourly heat balance calculations naturally differ from the total daily average.

Solar gain through glazing
BREDEM limits glazing orientation to the cardinal and ordinal directions whereas the dwelling is modelled in its true orientation within DSM. This can lead to differences in internal solar gain, particularly during daylight hours in heat demand periods.

Hourly vs daily average solar irradiance (external surface temperatures)
External surface temperature is an important part of the dynamic hourly heat loss calculations through all plane elements in DSM. Higher external surface temperatures will lead to lower heat loss; this will be more pronounced in dwellings with a greater area of south facing plane elements. The reverse can occur during darker winter months although the thermal mass of the constructions can retain some heat after sundown.

Geometry
DSM models exclude areas and volumes for chimney breasts, partition walls, and intermediate floors in the total heated space. This inherently means a smaller volume of air is conditioned than that used in the RdSAP calculations.

Weather
Due to the temporal resolution and variability of weather, it is not possible to match to the BREDEM inputs in the same way as the internal gains. The weather file used in the DSM was selected due to the close similarities between monthly average external temperature values (CIBSE Test Reference Year file for Leeds [8]) as discussed in the DEEP Methods 2.01 Report.

Differences specific to 55AD and 57AD
For the baseline scenarios, using measured infiltration rate and U-values, BREDEM predicts a space heating demand that is 5,503 kWh/year higher than DSM for 55AD, and 6,078 kWh higher than DSM for 57AD. As with all DEEP case studies, it is the HTC value that has the greatest influence on the annual space heating demand estimates. BREDEM (and therefore SAP/RdSAP) uses a bottom-up method to calculate the HTC used in the heat balance calculations, based upon the thermal transmittance and area of constructions, and background infiltration rates.

The DSM models mimic the coheating test conditions and therefore use a top-down method to calculate the HTC. Using an unrestricted version of the BREDEM software, it is possible to overwrite the HTC with that calculated in the DSM model.

Following this adjustment, the normalised annual space heating demand in BREDEM is 8,174 kWh, compared with the DSM estimate of 6,892 kWh for 55AD: a difference of 1,282 kWh. For 57AD, the normalised BREDEM prediction is 8,861 kWh, compared to 7,903 kWh in DSM: a difference of 957 kWh. The BREDEM calculations can be further normalised by using the DSM volume of conditioned space (23.99 m^3 less in the DSM model for 55AD, and 23.69 m^3 less for 57AD). Following this final adjustment, the BREDEM estimate is 341 kWh higher than the DSM output for 55AD but 49 kWh lower for 57AD. These results suggests that the other differences between the two modelling approaches have a limited impact of space heating demand predictions.

As with some of the other DEEP case study dwellings, the orientation of both buildings has an impact on the model outputs. The large gable wall in 55AD is orientated towards the south-east, and the front of both houses face the south-west. Increased external surface temperatures during sunny periods will result in reduced heat loss when compared to the steady-state calculations. There is, however, very little difference between the internal solar heat gains in RdSAP, BREDEM, and DSM in the two models.

The influence of the solar on opaque surfaces can be seen when comparing the baseline and completed retrofit models. In the baseline models, poorly insulated elements will be more affected by the higher external surface temperatures, with a difference in total space heating demand of 3,300 kWh in 55AD and 3,100 kWh in 57AD between DSM and BREDEM. This is reduced to almost zero difference at the completed retrofit stages, as the external wall insulation in particular means that the higher external surface temperatures have less influence on the heat balance calculations. There was also a much smaller difference between predicted HTCs following the whole house retrofits.

57AD was found to have a more efficient gas combi boiler; while 55AD had a less efficient boiler with a hot water cylinder (which incurs standing losses and so increases annual domestic hot water demand), while also providing additional heat gains to the home. 55AD had a greater proportion of low energy lighting, which would reduce annual electricity consumption though reducing the amount of useful space heating gains from lighting.

3.6.2 Impact of retrofits on EPC bands

Several policy mechanisms set EPC targets, and the Government has set an ambition that all homes where practically possible will achieve an EPC band C by 2035 [9]. The impact of the retrofits on EPC in this case study, as predicted by each model at each calibration stage, is shown in Figure 3-49. Space heating demand predicted by DSM is the only output that differs in the comparative EPC calculations.

- As can be seen, the uninsulated homes are predicted to be an EPC D, except for the DSM model for 57AD which predicts a Band C.
- The DSM predicts a higher EPC score, since it predicts lower space heating demand, as discussed in Section 3.6.1.
- In all the models post-retrofit, both homes are thought to achieve a Band C.
- Pre-retrofit the variability caused by using different model inputs is relatively large. Post-retrofit, there is much lower variation.
- Although 55AD is more exposed to solar, there are a couple of features that mean the EPC for 57AD is better than its neighbour: 55AD has a less efficient boiler with a hot water storage tank that significantly increases gas consumption, and 55AD includes a lower proportion of low energy lighting.

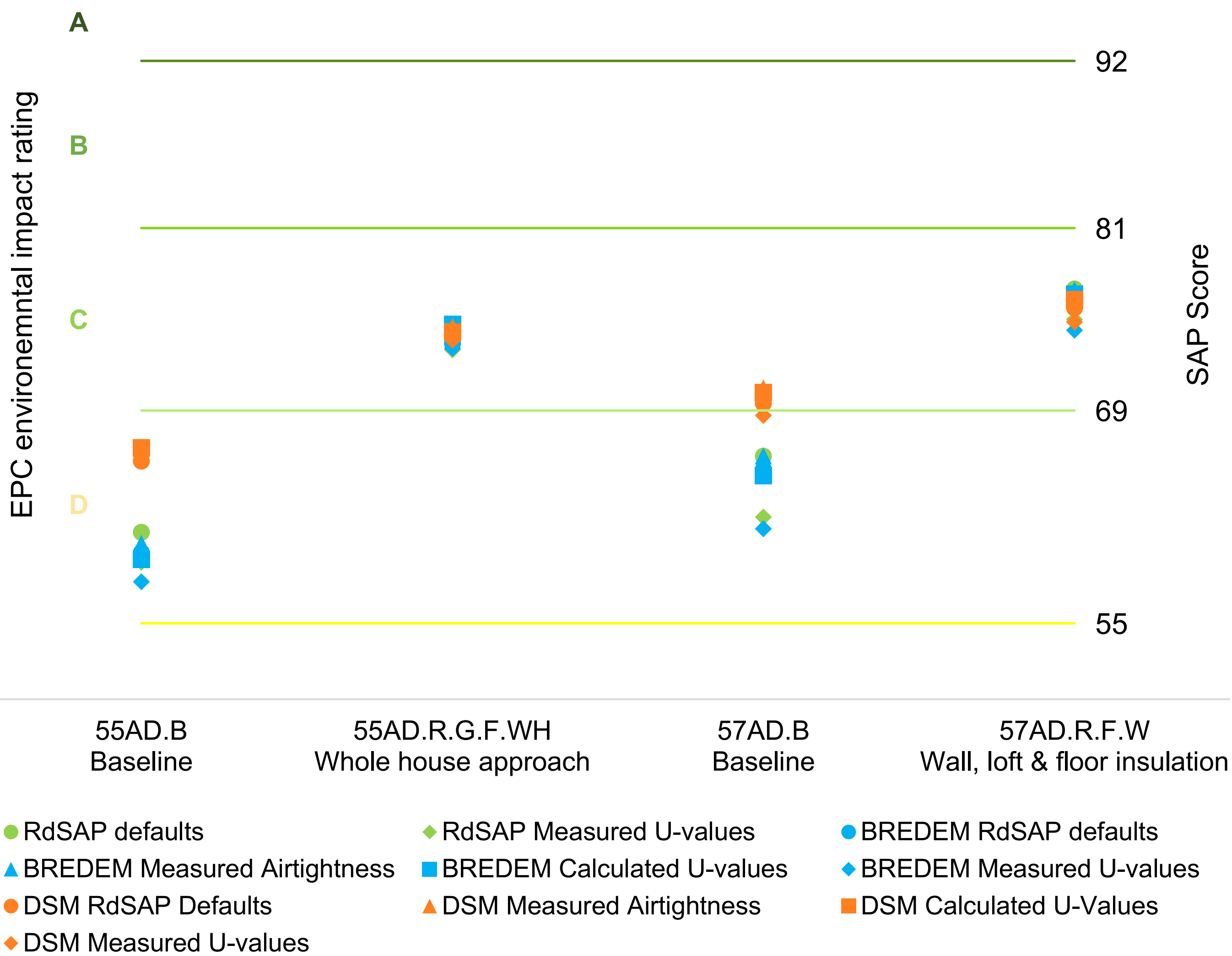

Figure 3-49 Predicted impact of retrofits on EPC band

3.6.3 Impact of retrofits on annual space heating

The Social Housing Decarbonisation Fund (SHDF) Wave 1 evaluates retrofit success by setting a target of 90 kWh per m² for annual space heating retrofits [9]. The predicted annual space heating demand attributable to the retrofit undertaken in case study dwellings is shown in Figure 3-50.

- Pre-retrofit, DSM predicts lower space heating demand than the steady-state models, primarily due to the way in which the model accounts for useful gains, hourly weather, and geometry. For example, 55AD is on the south side of 57AD, so receives more solar gains.
- 55AD has higher internal heat gains from less efficient lighting and a hot water storage tank, causing it to have lower space heating demand than 57AD.
- Including the measured airtightness level, measured U-values, and calculated thermal bridging in the pre-retrofit 55AD DSM model reduces space heating demand to 95 kWh/m²/yr, only just above the SHDF threshold.
- Post-retrofit, space heating in 55AD is reduced substantially to below the SHDF value in all the models, though the total reduction varies between 44 % and 66 % depending on the model and which inputs are used.
- Post-retrofit, all models predict space heating in 57AD to be below the SHDF threshold, except the BREDEM models which incorporated the measured U-values (which were substantially higher than the defaults) and the calculated thermal bridging scenarios. The total reduction is lower than in 55AD though, and varies substantially, between 33 % and 53 % depending on the model and the inputs used.
- Post-retrofit, 55AD's space heating demand is more aligned with 57AD, since the EWI cancels out the impact of solar.

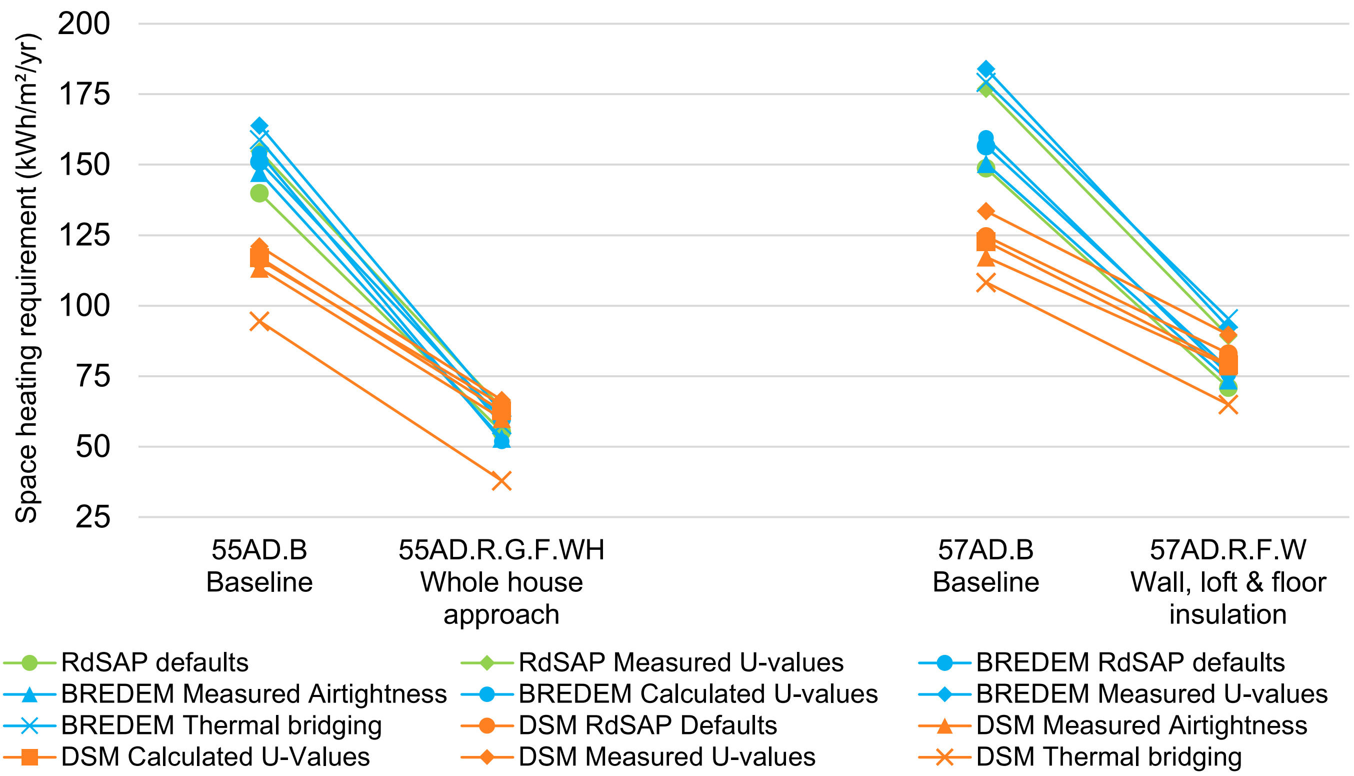

Figure 3-50 Predicted cumulative reduction in annual space heating demand

3.6.4 Impact of retrofits on CO2 emissions

Heating homes is responsible for around 15 % of the UK's CO_2 emissions [9]. The predicted reduction in CO_2 emissions achieved by the case study home retrofits is shown in Figure 3-51 based on fuel carbon emissions factors in RdSAP.

- Both retrofits substantially reduced the amount of CO_2, though the savings predicted depends on which model is being used.
- The whole house approach, which included new external glazing and doors, resulted in only marginal CO_2 reductions. This is because CO_2 emissions are also influenced by hot water and electrical use in the homes, which were higher in 55AD, and these were not affected by the retrofit.
- Updating model defaults with updated inputs only marginally reduces the proportional reduction in CO_2 achieved by the retrofits.
- DSM predicts lower annual CO_2 emissions than steady-state models and therefore also predicts that few CO_2 reductions will be made.

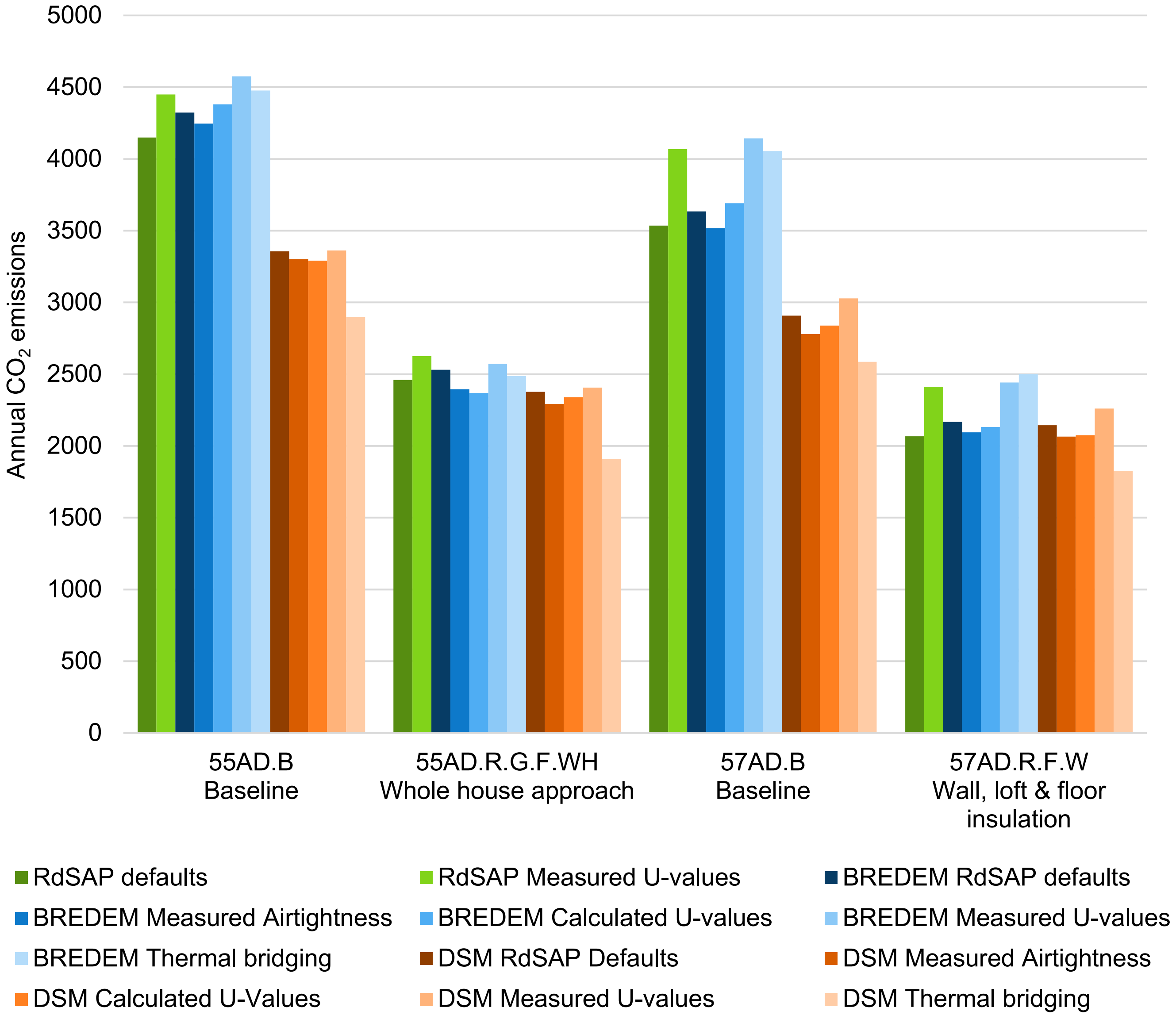

Figure 3-51 Annual CO_2 emission of homes pre- and post-retrofit

Predicting EPC band, space heating, and carbon reductions summary

The homes had similar starting EPC scores and were rated as a Band D in the steady-state models. In DSM, which considers specific impacts of hourly weather, useful solar gains and geometry and orientation, 57AD would have been predicted as EPC band C in some models. However, all DSM models that used the measured U-values (which were worse than default values) were predicted to be Band D. Post-retrofit, all the models predicted very similar SAP scores for each home and both homes were comfortably considered to have achieved an EPC grade C.

Space heating was reduced substantially in both homes by 44 % in 57AD and 66 % in 55AD. 57AD, where the external glazing, external doors, and bay roof were not upgraded, achieved slightly lower savings (between 33 % and 53% depending on which model and inputs are used).

As with other DEEP case studies, DSM predicts lower space heating savings than the steady-state models. The most significant model input update was to change the thermal bridging defaults in the DSM model, which resulted in an additional 10 % reduction in space heating demand.

The reduction in CO_2 emissions achieved in the homes was between 25 % and 46 % depending on which model and inputs were used. Again, DSM predicts lower savings due to assuming lower space heating demand. The scale of savings is lower than the space heating reductions, since the CO_2 emissions in the home are influenced by how water heating, lighting and power are provided in the dwellings, which were not changed in the retrofits.

Updating the model default inputs had a smaller effect on CO_2 emission savings than on space heating demand. Updating the thermal bridging default values in DSM caused the single largest impact on the model predictions. However, updates to this in BREDEM had a smaller impact because of the way in which thermal bridging is accounted for.

3.7 Overheating risk of retrofitting

As part of the overall DEEP project, Loughborough University has carried out parametric analysis of overheating scenarios, using a 10-year weather data file. The overheating analysis in this section is complementary to this work and uses the overheating assessment method from CIBSE TM59, which is cited in the PAS2035 guidance [10].

Two metrics are used to assess whether the dwelling will overheat Criteria A and B. Criteria A of TM59 is taken from another CIBSE publication, *TM52: The limits of thermal comfort: avoiding overheating in European buildings* [11]. The two assessment criteria are defined as follows:

A. For living rooms, kitchens, and bedrooms: the number of hours during which the ΔT (difference between the operative and comfort threshold temperature) is greater than or equal to one degree (K) during the period May to September inclusive, shall not be more than 3 % of occupied hours.

B. For bedrooms only: to guarantee comfort during the sleeping hours, the operative temperature in the bedroom from 10 pm to 7 am shall not exceed 26 °C for more than 1 % of annual hours. (Note: 1 % of the annual hours between 22:00 and 07:00 for bedrooms is 32 hours).

Overheating assessment was carried out at each stage of the retrofit. Following the TM59 guidance, the initial assessment was completed using the CIBSE Design Summer Year 1 (DSY1) file for a 2020s high emission scenario at the 50th percentile, for Leeds in this instance. There are three different DSY files available for the 14 UK regional locations. They use actual year weather data that simulate different heatwave intensities: DSY1 represents a moderately warm summer; DSY2 represents a short, intense warm spell; and DSY3 a longer, less intense warm spell [8]. Assessment was also carried out for future weather scenarios, using the DSY1 files for the 2050s and 2080s high emission scenarios at the 50th percentile. As with all naturally ventilated homes, it is the percentage of openable area in the windows that has the strongest influence on overheating risk; these are illustrated in Figure 3-52.

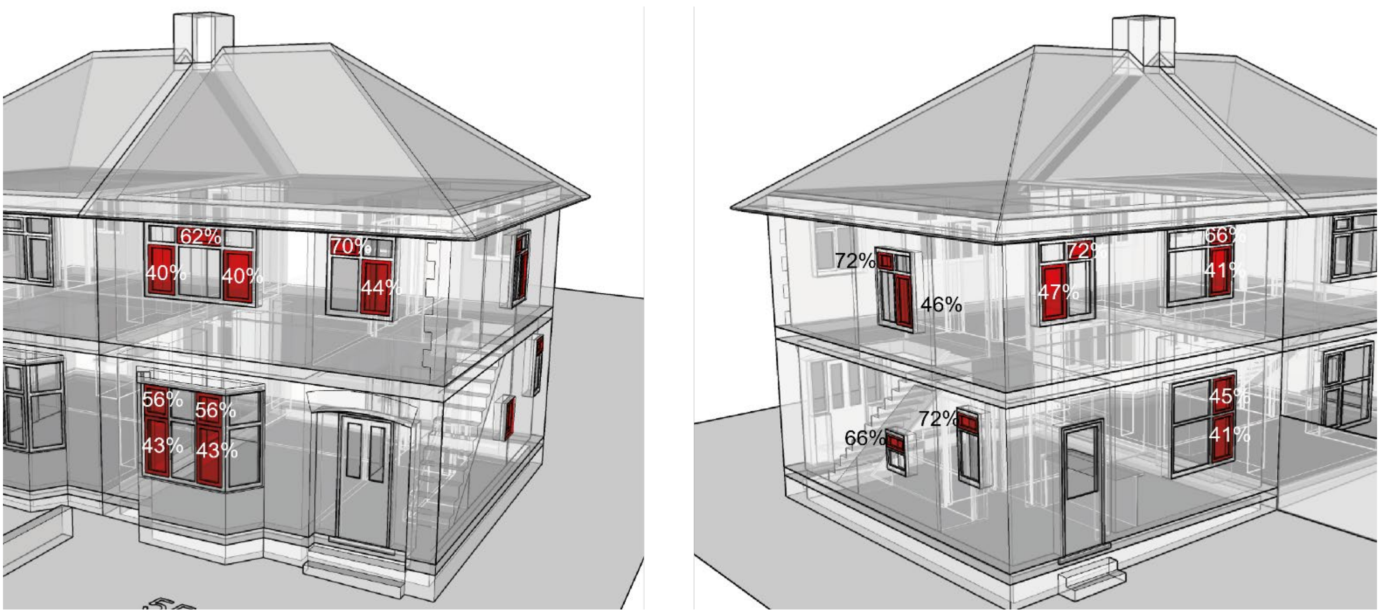

Figure 3-52 Percentage of opening area for openable windows

There is very little difference between the window opening areas in both houses, and between pre- and post-retrofit stages. The only difference between 55AD and 57AD is the small central ground floor window on the gable wall (opening area of 66 % in Figure 3-41); 57AD does not have a window in this area. This window is also the only difference between the pre- and post-retrofit stages in 55AD, with the post-retrofit window being one single unit with a revised opening area of 40 % for the total window; as opposed to having a 66 % openable area of the top light pre-retrofit. There is no difference between window openings in the pre- and post-retrofit stages for 57AD.

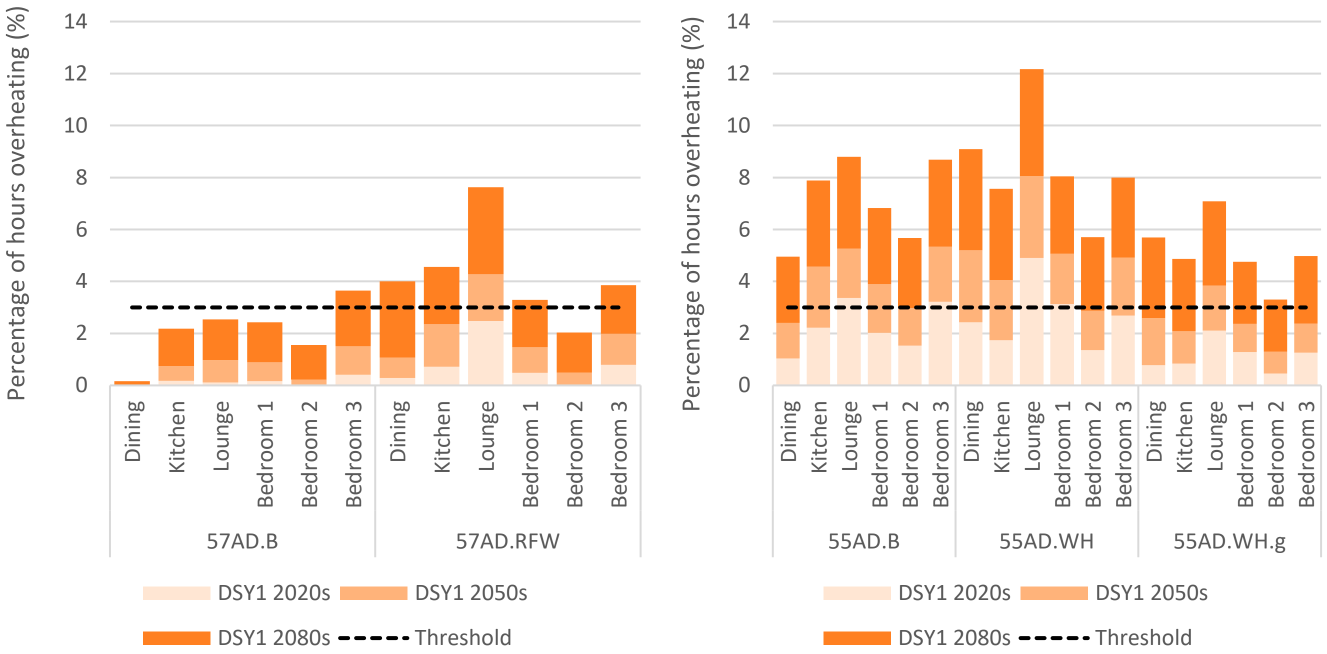

Figure 3-53 Modelled overheating under TM59 Criteria A

Under Criteria A, there is a pronounced difference in overheating in the two houses, which is due to their orientation: with 55AD effectively acting as a shade to 57AD. The large gable wall of 55AD is orientated towards the South-East, whereas the same wall in 57AD faces the North-West.The influence of this geometry is evident in the results shown in Figure 3-53. This is also emphasised by the visualisation presented in Figure 3-55. The chart for 55AD presents two sets of results for the whole house stage: the first does not include the solar control glazing that was installed in the retrofit; this has been done to illustrate the impact that a low g-value (solar transmission factor) can have on overheating. The results described as 55AD.WH.g are those that include the low g-value solar control glazing.

Even with the low g-value glazing installed, 55AD still experiences longer periods of overheating, although most spaces are deemed not to overheat excessively under the current conditions represented by the 2020 DSY1 file. The retrofitted glazing in 55AD reduced solar gains as the g-value was much lower than the glazing it replaced (0.43 compared with 0.76 for the baseline). None of the rooms in 57AD are deemed to excessively overheat under current conditions. The shading protecting 57AD actually means that predicted overheating is only evident in the 2080s weather scenario, and this is mostly in the retrofitted building.

In the ground floor spaces of 55AD, without the introduction of the low g-value glazing, overheating would have increased following the whole house retrofit. This is consistent with the results of other DEEP case study houses that have included the retrofit of suspended timber ground floors. This is due to the ground temperatures being relatively low compared with the external air temperature during summer heatwaves. Decoupling the ground from the inside of the dwelling, by insulating the suspended timber ground floor, then leads to excessive overheating. However, the low g-value glazing offsets this effect. The increased overheating following the floor retrofit is evident, but less pronounced, in 57AD. Under Criteria B, shown in Figure 3-54, both houses are predicted to experience excessive overheating, which is exacerbated by all internal doors being specified as closed overnight in the TM52 methodology. However, insulating the external walls and improving the loft insulation does help to reduce overheating slightly in the south-west facing bedrooms at the front of the house.

Figure 3-54 Modelled overheating under TM59 Criteria B

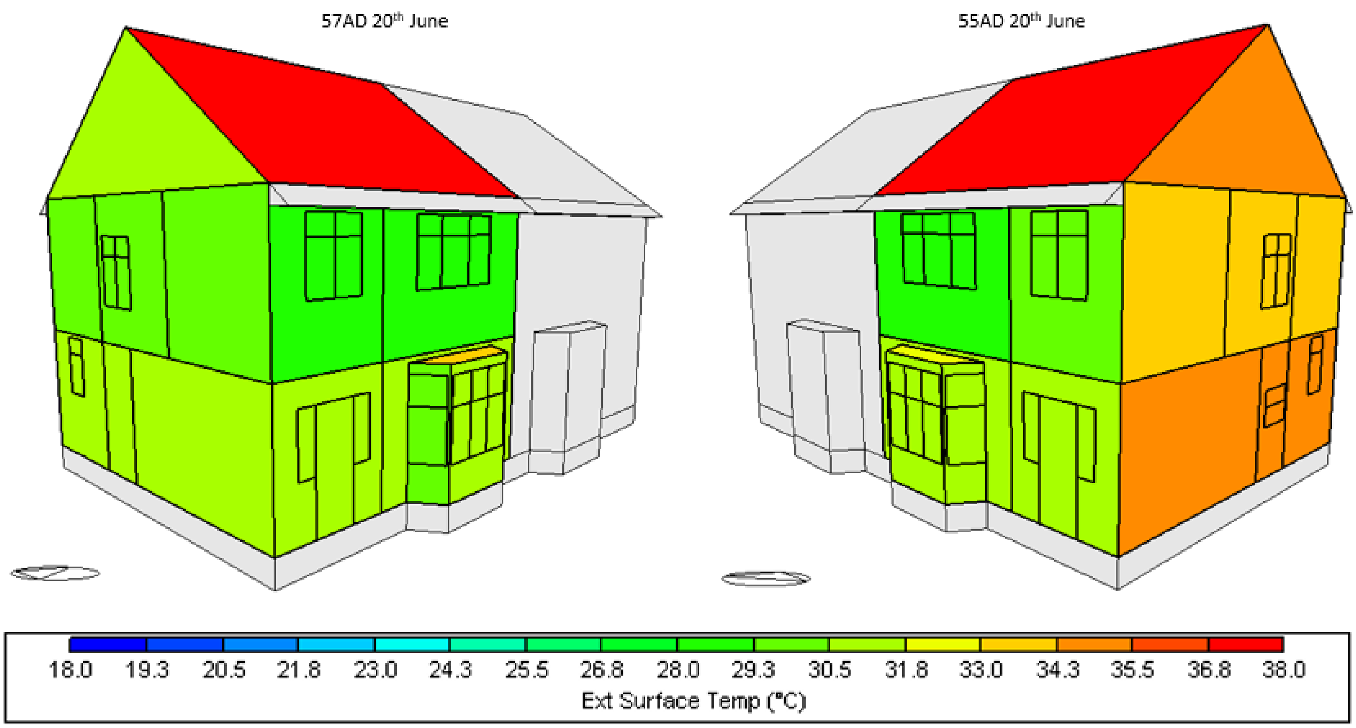

Figure 3-55 Daily mean external surface temperatures for 20th June

Overheating risk of retrofit summary

The importance and influence of building orientation on overheating risk is clearly illustrated by this pair of semi-detached dwellings. 55AD effectively acts as a large solar shading device for its neighbour, with overheating risk in 57AD modelled as being very low, even in the warmer future climate scenarios.

Although additional insulation in the external walls and loft helps to marginally reduce overheating, the retrofit measures in this instance increase the risk of overheating, although this is offset through the use of low g-value solar control glazing in 55AD.

As with most other examples in DEEP where a suspended wooden floor has been insulated, decoupling the cooler ground floor temperatures from the conditioned spaces leads to a greater overheating risk.

3.8 Retrofit moisture risks

To measure the risk of surface condensation before and after the retrofits, surface temperature measurements were undertaken at seven junctions in 55AD and 10 junctions in 57AD, at sites where thermal bridges and discontinuities of insulation were expected to pose a risk.

T-type thermocouple temperature sensors were placed on the building fabric and monitored during the coheating periods from the IWI phase onwards (See the DEEP Report 2.01 DEEP Case Studies Methods, section 2.7 for methods). The quasi-steady-state conditions of the coheating test provide comparably steady conditions for comparison with numerical thermal simulation. The sensors were removed to allow retrofit works, and subsequently replaced as close to the original positions as possible.

Temperature factors were used to indicate whether a location is at risk of surface condensation. A temperature factor below the critical value of 0.75 is a risk for a dwelling. The temperature factor (f_{Rsi}) is calculated using Equation 1, see Section 3.3.4 for the full equation.

Temperature factors are usually used in conjunction with steady-state simulations. In this study, to validate the stability of temperature factors calculated, the averaging method in BS ISO 9869: 2014 was adopted. Where a surface temperature location was unable to satisfy the validation steps, it failed.

The risk of condensation occurring does not mean condensation will necessarily manifest. Risk may be mitigated against by ensuring adequate ventilation in the dwelling, but also ensuring air circulation behind furniture and (as this project identifies) behind built-in units located on external walls. Conditions at each location are discussed in the following sections and figures.

3.8.1 55AD surface temperature measurement locations

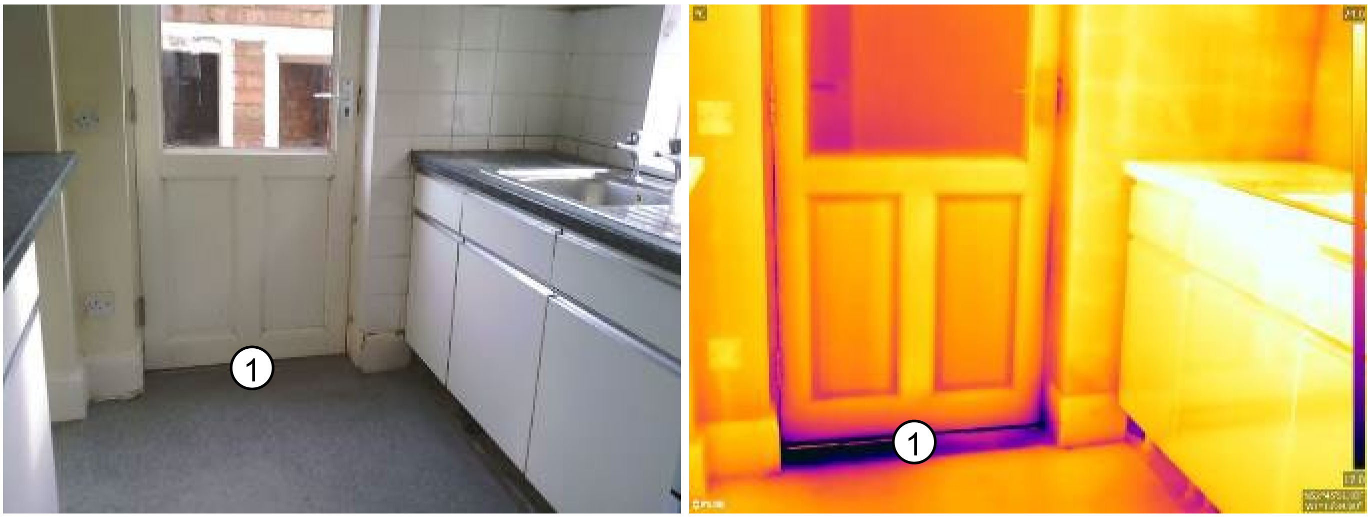

Figure 3-57: thermocouple sensor position at rear door threshold. (1)

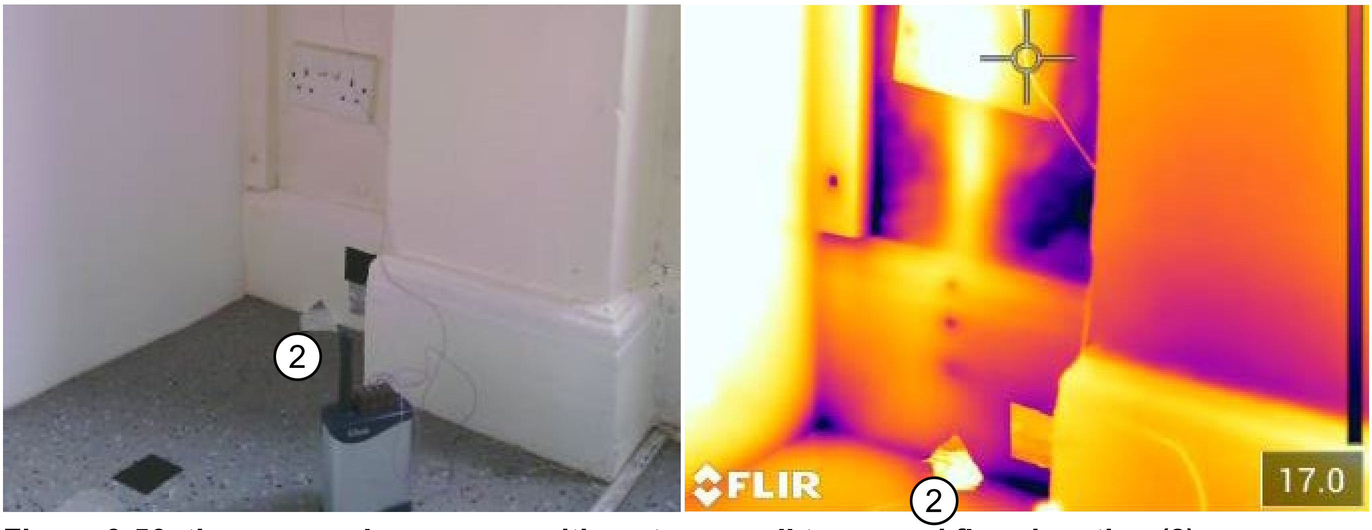

Figure 3-56: thermocouple sensor position at rear wall to ground floor junction (2)

Figure 3-58: External wall to party wall (3) and External wall to first floor ceiling (7) thermocouple sensor locations

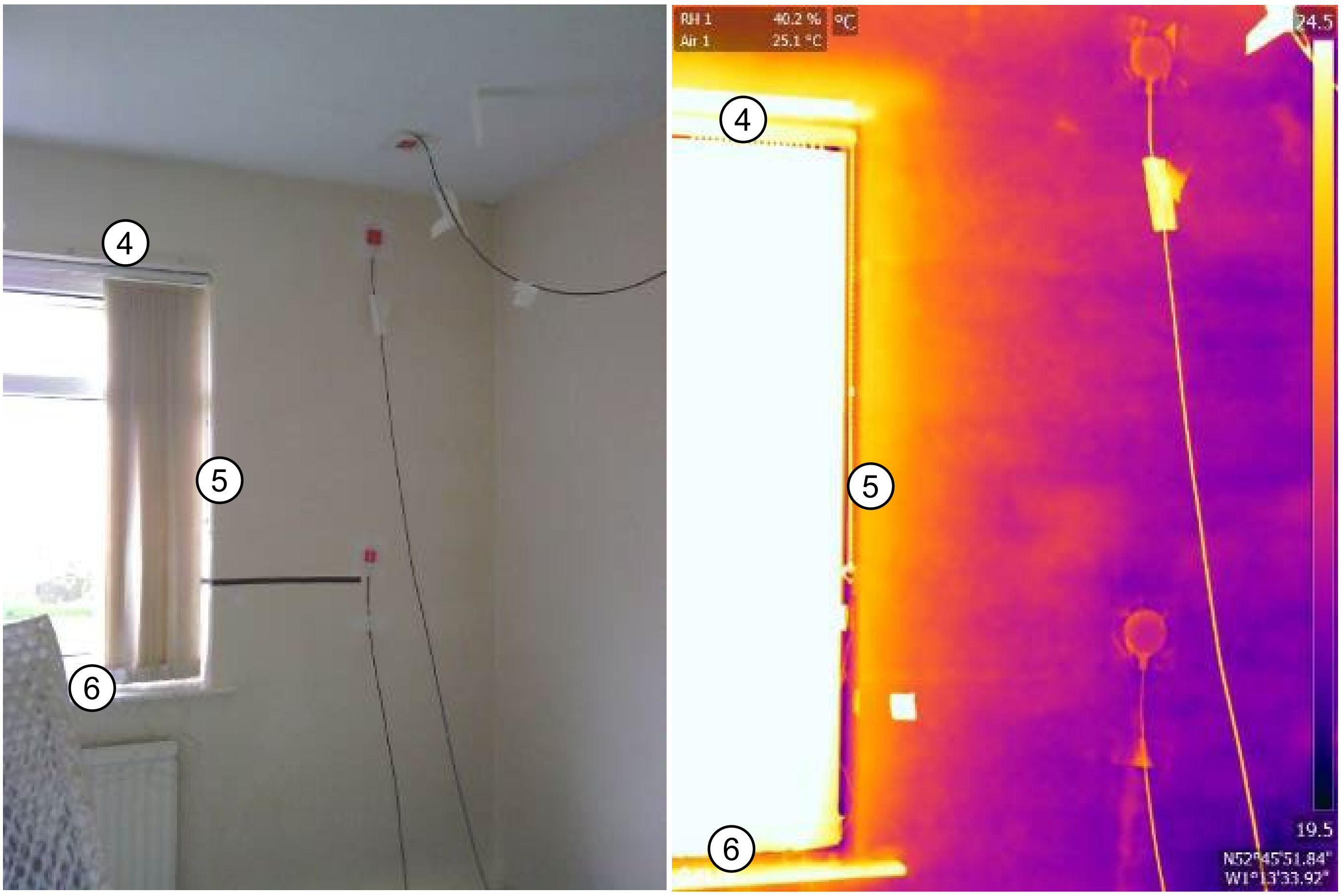

Figure 3-59: Window head (4), window jamb (5) and window sill (6) thermocouple sensor locations

3.8.2 57 AD surface temperature measurement locations

Figure 3-60: Front door threshold (1) and Door opening (9) thermocouple sensor locations.

Figure 3-61: Rear door threshold (2) thermocouple sensor location.

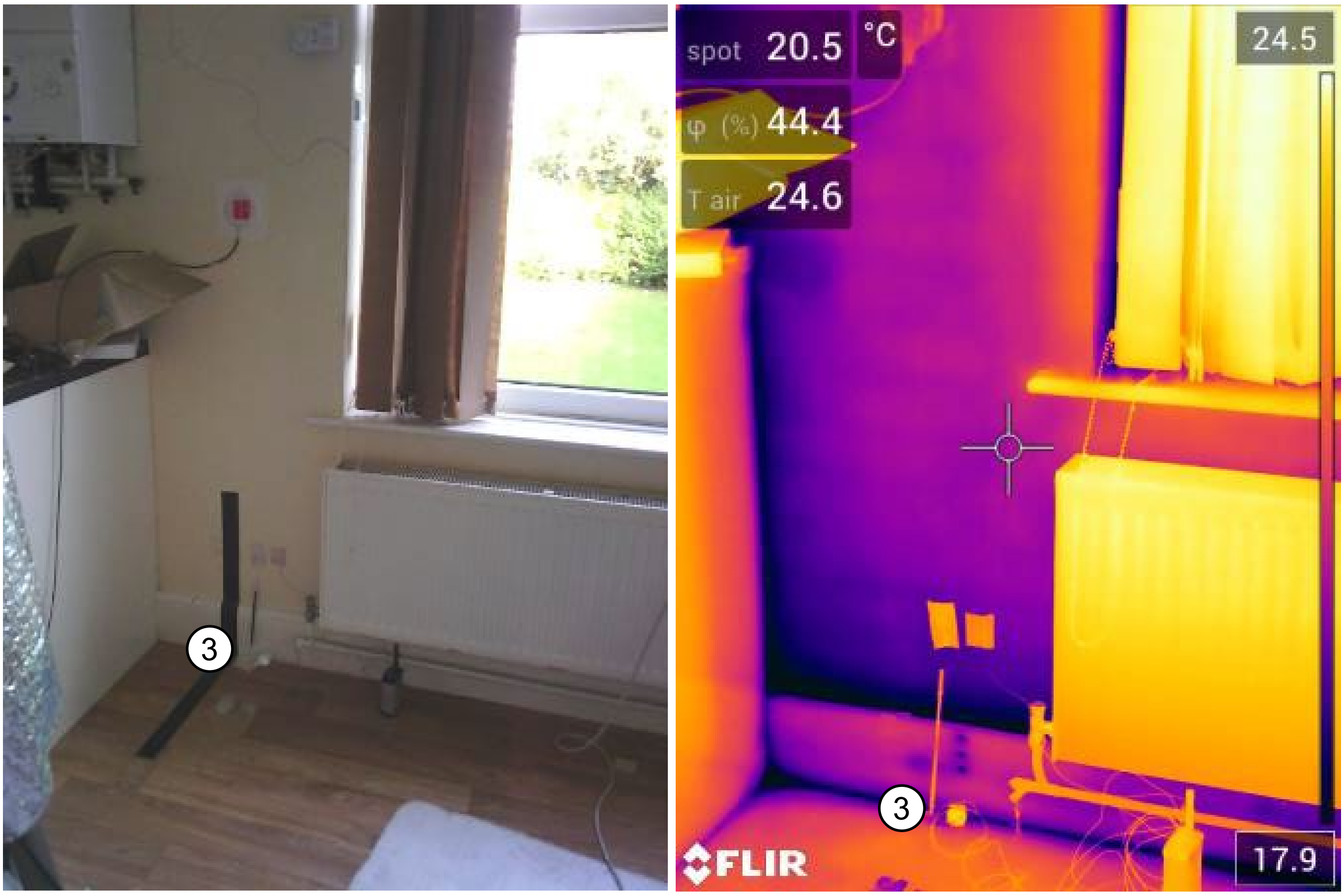

Figure 3-62: External wall to ground floor (3) thermocouple sensor location.

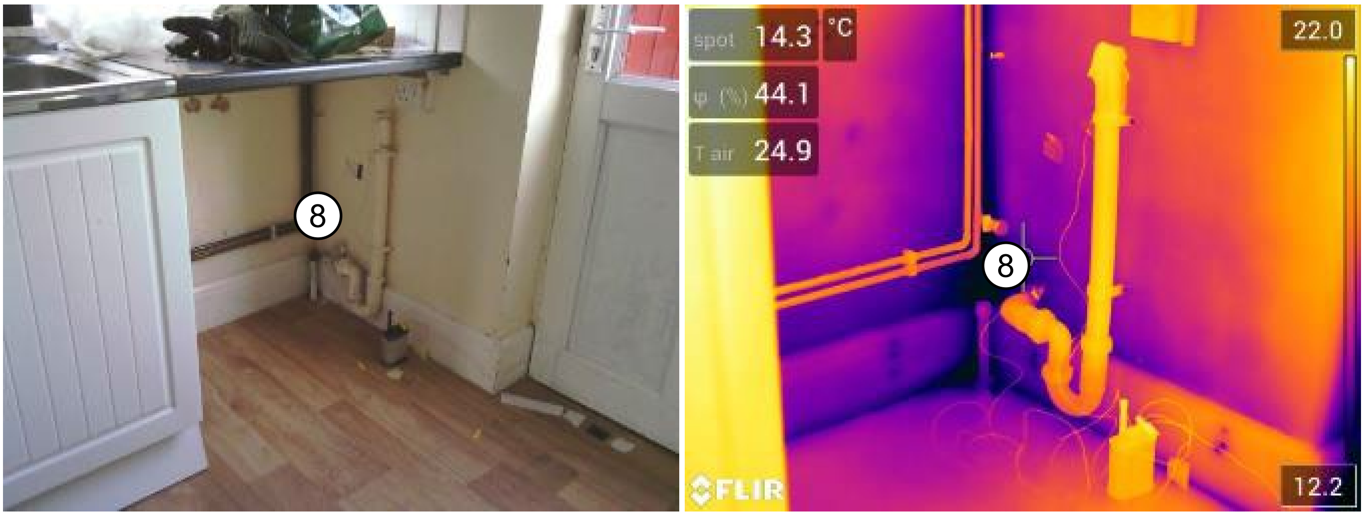

Figure 3-63: External wall waste water pipe penetration (8) thermocouple sensor location.

Figure 3-64: External wall to party wall (4) and window jamb (5) thermocouple sensor locations.

Figure 3-65: External wall to eaves (6) thermocouple sensor location

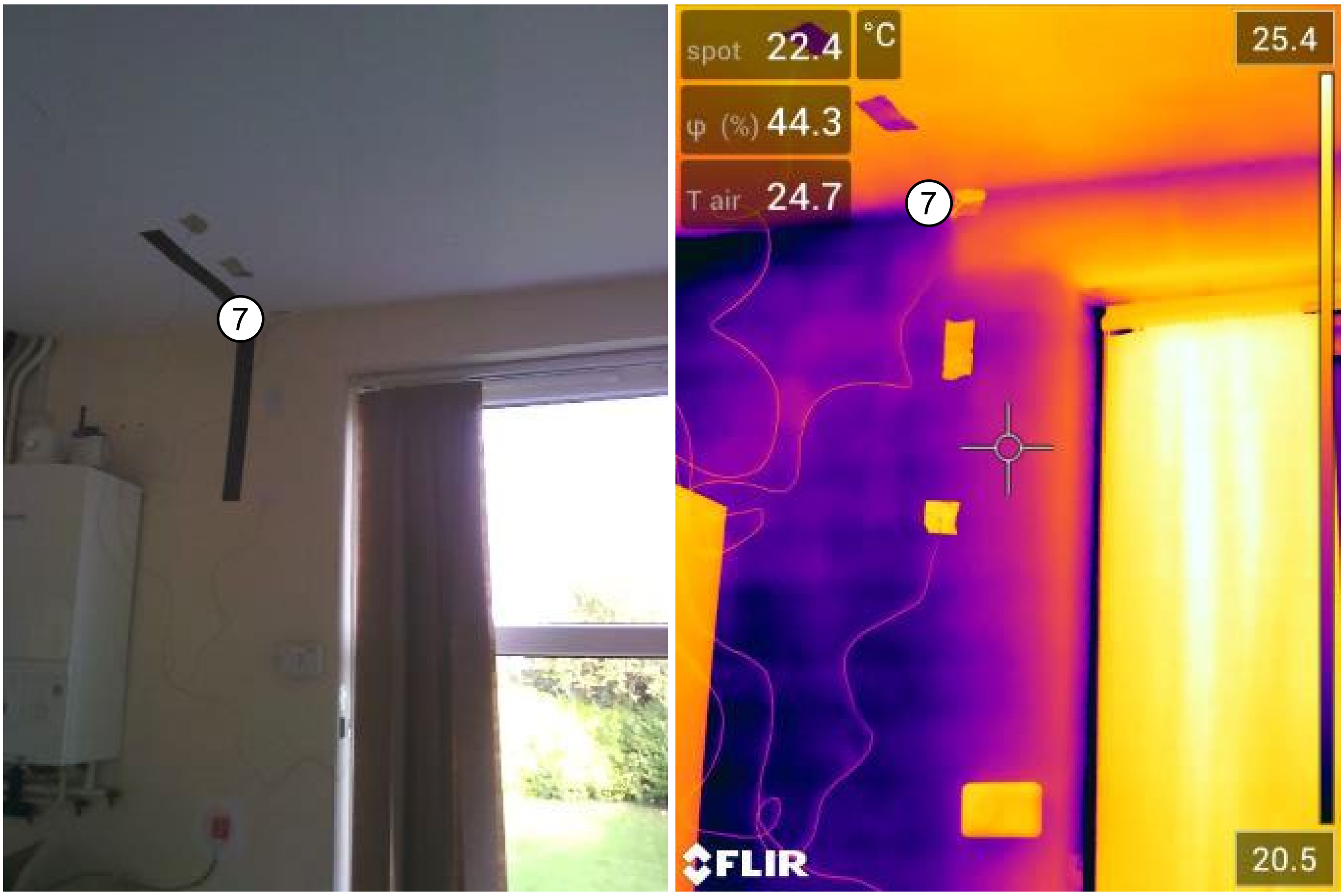

Figure 3-66: External wall to intermediate floor (7) thermocouple sensor location

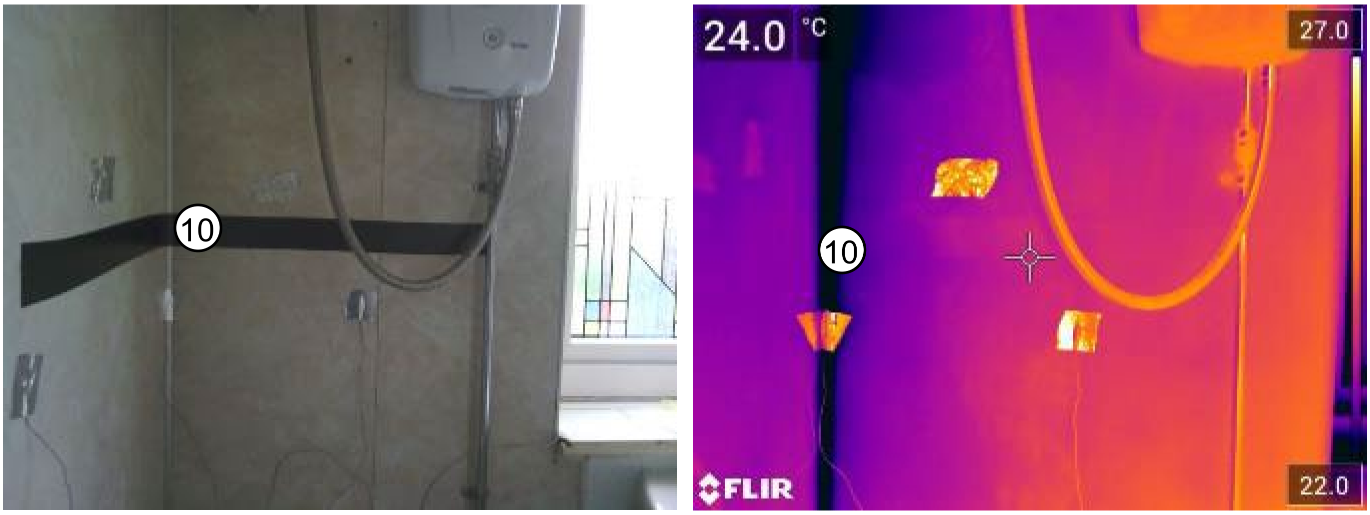

Figure 3-67: External wall corner (10) thermocouple sensor location

3.8.3 55AD & 57AD surface temperature factors

Table 3-12 summarises the surface temperature factors calculated using measured surface temperatures in 55AD and 57AD. Temperature factors below the 0.75 f_{CRsi}, which indicate a risk of surface condensation, are highlighted in red.

Table 3-12: Pre and Post-retrofit measured surface temperature factors for 55AD & 57AD

Sensor location	57 AD (Piecemeal) f_{Rsi}			55 AD (Whole house) f_{Rsi}		
	No.	Base case	Post-retrofit	No.	Base case	Post-retrofit
Front door threshold	**1**	0.39 (±0.16)	0.65 (±0.09)			
Rear door threshold	**2**	0.32 (±0.10)	0.92 (±0.02)	**1**	0.31 (±0.09)	0.77 (±0.04)
External wall - ground floor	**3**	0.70 (±0.07)	0.76 (±0.07)	**2**	0.66 (±0.06)	0.70 (±0.06)
External wall - party wall	**4**	0.88 (±0.02)	0.99 (±0.01)	**3**	0.71 (±0.08)	0.94 (±0.02)
Window head				**4**	0.83 (±0.08)	0.84 (±0.02)
Window jamb	**5**	0.77 (±0.06)	0.92 (±0.02)	**5**	0.76 (±0.06)	0.90 (±0.02)
Window sill				**6**	0.79 (±0.13)	0.84 (±0.02)
External wall - bedroom ceiling	**6**	0.92 (±0.02)	0.90 (±0.04)	**7**	0.86 (±0.03)	0.90 (±0.04)
External wall - kitchen ceiling	**7**	0.89 (±0.02)	0.96 (±0.04)			
External wall - water pipe	**8**	0.48 (±0.12)	0.54 (±0.11)			
Door opening - external wall	**9**	0.72 (±0.10)	0.85 (±0.05)			
External wall corner	**10**	0.74 (±0.07)	0.87 (±0.04)			

Not all junctions measured in the uninsulated homes were found to have a pre-existing risk of condensation: four junctions in 57AD and four junctions in 55AD were found to not pose a risk pre-retrofit.

In all but one location in both buildings, temperature factors based on measured surface temperatures increased following retrofit. This suggests the addition of the EWI may generally reduce surface condensation risk, whether a whole house or piecemeal approach is taken.

However, these results are specific to the retrofit designs, constructions, and test conditions for these case studies. For instance, the one exception where a marginal worsening of condensation risk (resulting from the EWI) was measured was in the bedroom external wall to ceiling junction in 57AD. Here, there was a discontinuity in the EWI i.e. there was no insulation behind the soffit, leading to an area of uninsulated external wall at the eaves.

This discontinuity meant that condensation risk worsened, while in 55AD, where there was no discontinuity, the surface condensation risk was reduced by installing EWI. However, in neither home, pre- or post-retrofit, was this junction measured to be at risk.

Furthermore, the EWI has removed potential risk from four out of six junctions found to be at risk in 57AD and from two out of three junctions in 55AD. In 57AD the door threshold was still considered a risk; this finding is consistent with other DEEP case studies. Indeed, the door threshold for 55AD was only just above the 0.75 critical temperature factor.

Additionally, in 57AD there was a condensation risk where the water pipe penetrated the external wall. It is not known if this was due to an air leakage pathway remaining post-retrofit,;or if there was a discontinuity associate with the way the EWI was installed around the penetration; or a particular impact of the location of the sensor because it is near the external wall corner and ground floor to wall junctions.

In 55AD, the only junction which exhibited a condensation risk post-retrofit was the external wall to floor junction. Indeed, the 57AD floor to wall retrofit was also found to only marginally reduce risk, though enough to bring it above the 0.75 temperature factor. Several retrofits were affecting this junction, such as the EWI and the suspended timber ground floor insulation, and that the EWI retrofits in both homes also included EWI below the damp proof course. More investigation is needed to understand how these different retrofits each affect condensation risk individually and collectively.

Window openings in both houses were found to be close to, though above, the 0.75 f_{CRsi} and so not at risk of condensation. Following retrofit the junctions in each house experienced a temperature factor uplift, and interestingly, there was no significant difference between 55AD where the windows were replaced and repositioned and 57AD where the windows were left as they were during the base case. This indicates that it may not be necessary to relocate windows during EWI retrofits to avoid condensation risk.

The front door opening in the external wall of 57AD pre-retrofit had a temperature factor below the 0.75 f_{CRsi} indicating a condensation risk. Following retrofit, a new door opening was constructed which included removing the single glazed side panel windows and replacing them with insulated wall, which has removed the risk of condensation.

Both the retrofit approaches adopted, the piecemeal approach in 57AD and the whole house in 55AD, resulted in uplifts at most junctions. Where a discontinuity of insulation was introduced, such as at the external wall to bedroom ceiling in 57AD, a reduction in temperature factor occurred (though in this case not posing a risk of condensation). Service penetrations may continue to pose a risk of condensation after retrofit. Adopting a whole house retrofit approach in this case appears to have a small benefit in reducing condensation risk.

3.8.4 External gas pipe cut-out condensation risk

Due to scheduling constraints, it was not possible to relocate the mains gas supplies to the test houses. External wall insulation had to be fitted around the gas pipe, leaving a thermal bridge in proximity to the external wall corner and window jamb junctions.

Surface temperature measurements were taken at the end of the testing programme, while the house was undergoing QUB testing. The data was validated using the same method as surface temperature measurements taken during the coheating test. Infrared thermography of the junction was undertaken during the coheating test, as well as elemental thermal modelling.

Figure 3-68 Left: 57AD external gas pipe cut-out. Right: internal side of gas pipe cut-out.

Table 3-13 Temperature factors at internal side of gas pipe cut-out

Source	Window jamb	External wall corner
Thermocouple sensor	0.68 (±0.05)	0.69 (±0.08)
IR Thermography	0.63	0.65
Simulation	0.66	0.80

Table 3-13 above contains temperature factors at the window jamb and external wall corner adjacent to the gas pipe cut-out, calculated using surface temperature measurements from different sources. Comparing the in-situ measured temperature factors to similar locations measured in 57AD, both the window jamb and external wall corner at the gas pipe cut-out junction were lower than their equivalents. Both locations were below the 0.75 f_{CRsi} indicating that these junctions are at risk of surface condensation due to the gas pipe cut-out.

As surface temperatures would be measured during QUB testing (described in section 3.4.3) there was potential that conditions would be too unstable to validate. As such, infrared thermography of the junction was undertaken to ensure surface temperatures were observed while the building was still under coheating conditions. This analysis suggests the temperature factors were lower than those calculated from thermocouple measurements, indicating a greater condensation risk. However, this may be a transient effect of the external temperatures at the time the IR image was captured.

Elemental thermal simulation of the junction resulted in a temperature factor at the window jamb close to the value measured. However, at the external wall corner the simulation temperature factor was significantly higher than measured, above 0.75 f_{CRsi} indicating the corner is not at risk. If relying on simulation alone, the risk at the corner would not have been detected, illustrating the difficulty in comparing condensation risk using measured and modelled approaches. Post-retrofit, an additional layer of thin internal wall insulation was installed on the window reveal to remove the risk of condensation from this location.

Retrofit moisture risk summary

Both whole house and piecemeal retrofit approaches taken in 55AD and 57AD resulted in an increase in temperature factor at most of the locations where surface temperatures were measured. This indicates that both retrofit approaches can reduce surface condensation risk in some instances.

Ground floor thresholds remain a condensation risk regardless of approach. Additionally, the exception was where a discontinuity in the insulation was created by not installing EWI behind the soffit at the eaves in 57AD. While this marginally increased the risk at the external wall to bedroom ceiling junction, it was not significant enough to be considered a risk of condensation.

Where the external gas pipe could not be moved, the EWI was cut out, creating a risk of condensation. The application of internal wall insulation did remove this risk at the window reveals.

3.9 Retrofit costs and payback

This section looks at the costs of undertaking the retrofits; however, this is only a single case study, therefore these should not be used to generalise costs of retrofits nationally. Undertaking work in existing homes can have tremendously variable costs, depending on the specification of the work being undertaken as well as the condition of the house prior to retrofit. It is also important to note that the cost data presented here may not be representative for the national retrofit market; since retrofit tends to be highly labour intensive there are variations across the country based on regional differences in construction labour markets. The data discussed here originates from a single contractor in the North of England and relates to only one house type and a limited range of retrofit specifications. Additionally, the costs are expected to be higher than benchmarks (as shown in Table 3-15), as the project does not benefit from any of the economies of scales of neighbourhood schemes.

Decoration costs were excluded from the costs reported here since the landlords were undertaking their own Decent Homes repairs following the retrofits and would take on some of the decoration work. Additionally, costs associated with decorating were outside the scope of this project. These costs have been found to represent around 14 % of the cost of IWI [9], though it is recognised that they may be different for the retrofits in these case studies.

The costs of the 55AD.WH and 57AD.R.F.W retrofits are outlined in Table 3-14 and Table 3-15. The total retrofit cost was £56,161 and £28,948 respectively. Additionally, after the 57AD piecemeal retrofit was completed, the contractors returned to install the new external windows in line with the EWI, extend the EWI up into the eaves and connect it to the loft insulation, and install insulation in the bay roof to ensure no discontinuities remained. These final activities to reach parity with 55AD took the total costs of 57AD to £ 43,911.

Table 3-14 Cost of retrofits

Retrofit	i) Retrofit activity	Retrofit costs	ii) Additional enabling work required	Enabling work costs
55AD				
55AD Loft	Removing existing and installing new mineral wool	£ 568	n/a	
55AD Floor	Mineral wool and membrane insulation under floor	£ 1,815	New skirting boards and new floorboards; relocate radiators	£ 2,788
55AD Windows	A rated windows and doors	£ 13,544	New lintels and trickle vents	£ 5,327
55AD Walls	EWI insulation, plywood window boxes & internal plaster repairs, telephone cables, external fittings and rainwater goods to be relocated, bay window rebuilt and insulated	£ 26,328	Removing doorsteps, extending floor void vents, additional plastering around windows	£ 5,790
55AD.WH total		**£ 42,256**		**£ 13,905**

Retrofit	i) Retrofit activity	Retrofit costs	ii) Additional enabling work required	Enabling work costs
		57AD		
57AD Loft	Removing existing and installing new mineral wool	£ 568	n/a	
57AD Floor	Mineral wool and membrane insulation under floor	£ 1,894	New skirting boards and new floorboards; relocate radiators	£ 2,393
57AD Walls	EWI insulation, telephone cables, external fittings and rainwater goods to be relocated.	£ 23,006	Removing doorsteps, extending floor void vents	£ 1,086
57AD.R.F.W subtotal		*£ 25,469*		*£ 3,479*
57AD Windows	A rated glazing and doors	£ 10,836	New lintels and trickle vents	£ 2,265
57AD.Whole house approach extras	Return to insulate eaves and bay window roof insulation	£ 1,863	n/a	
57AD.WH additions subtotal		*£12,699*		*£2,265*
57AD Grand total		**£ 38,167**		**£ 5,744**

The grand total for all the retrofits in 57AD was approximately £12,000 (22%) lower than the costs for those for 55AD, even when the final whole house approach retrofits had been installed at 57AD. This was due to several specific reasons. 55AD had an additional window at a cost of around £2,000. Plus, its windows were installed in plywood boxes, which also meant the window boards needed replacing, and which also required substantial internal replastering to 'make good'. Conversely, 57AD's windows were installed after the EWI was fitted without plywood boxes or the need for extra internal plastering, thus it was able to save approximately £8,000 in installation costs.

The other major change was that the bay window was partly rebuilt in 55AD to allow the EWI and new windows to be aligned. In 57AD the existing bay window was retained and the EWI was angled to fit the existing window frames, resulting in more thermal bridging, but avoiding the approximately £2,000 extra for rebuilding the bay window. The enabling costs for 55AD were 25 % of the total retrofit costs, while they were only 14 % for 57AD. Some substantial savings from the enabling work for both homes was that the gas pipes and meters did not require moving. This was quoted at several thousand pounds per property, however thermal bridging calculations were used to explore surface condensation risks and internal wall insulation was used to mitigate any risk, as previously described in Section 3.3.4.1.

In both instances, the EWI part of the project was the most significant cost, being 57 % of the cost of 55AD's retrofit and around 55 % of the cost of 57AD. Second most significant was the new external glazing and doors which were 34 % and 30 % of the costs for 55AD and 57AD respectively.

Table 3-15 Breakdown of cost of retrofits

Retrofit	Cost	Proportion of total cost	Treated area (m²)	Cost per area (£/m²)	Benchmark (£/m²) [12]	Cost per W/K reduction
			55AD			
55AD Loft	£ 568	1 %	39	£ 15	£ 20 - £ 40	-
55AD Floor	£ 4,603	8 %	39	£ 118	£ 95	-
55AD Windows	£ 18,871	34 %	9 windows 2 doors	£1,716 per fenestration	£ 300 - £ 1,000 per window	-
55AD Walls	£ 32,119	57 %	79	£ 408	£ 55 - £180	-
55AD.WH total	**£ 56,161**		177	£ 318		£ 416
			57AD			
57AD Loft	£ 568	1 %	39	£ 15	£ 20 - £ 40	-
57AD Floor	£ 4,287	10 %	39	£ 110	£ 95	-
57AD Walls	£ 24,093	55 %	71	£ 338	£ 55 - £180	-
55AD R.F.W subtotal	*£ 28,948*					£ 305
57AD Windows	£13,101	30 %	8 windows 2 doors	£1,310 per fenestration	£ 300 - £ 1,000 per window	-
55AD Whole house approach bay window and EWI at eaves	£1,863	4 %	7	£ 251	n/a	-
57AD.WH total	**£ 43,912**		177	£ 249		-

An attempt has also been made to evaluate the relative costs of the retrofits according to how much they reduced heat losses (HTC). As can be seen, the 57AD.R.F.W retrofit appears to have been more cost effective than the 55AD.WH. This is partly because 55AD had an additional window, but mostly due to the costs of ensuring all the external windows were installed in-line with the EWI (i.e. having to build plywood boxes, make repairs to the internal plasterwork, and rebuild the bay window structure to avoid thermal bridging).

However, the analysis in Section 3.3.3 and 3.3.4 shows that the addition of EWI reduced surface condensation risk around the external windows, even when the windows were left in their original location. This did not have a material impact on thermal bridging heat losses either. This suggests that it may not be essential in all instances to relocate external windows when installing EWI. However, more investigation looking at different EWI designs around different external windows is needed to understand how broadly this applies to other house types and retrofits.

Conversely, in 57AD, not extending the EWI through the eaves or insulating the bay window roof caused surface condensation risks to increase. Not only did returning to correct these discontinuities in the insulation layer remove the risk of surface condensation occurring, but it also only added marginal additional costs (around 4 %) to the retrofit. The amount of thermal bridging heat loss savings this final step resulted in was also substantial (11 W/K or just under 10 % of total post-retrofit HTC). More investigations are needed to understand if this is the case in other homes with different construction details and retrofit specifications.

The results also suggest that in some cases, additional activities required to ensure that a whole house approach has been followed can be very expensive if, for instance, they involve moving external windows or damaging internal wall surfaces. Furthermore, these activities may not necessarily have a significant impact on heat loss reduction or surface condensation risk abatement. Conversely, in some instances surface condensation risks may be reduced relatively simply. In this instance, by applying internal wall insulation to compensate for discontinuities caused by cut outs of EWI, or by extending EWI behind soffits to join loft insulation or insulating bay roofs as part of EWI retrofits.

3.9.1 Predicted fuel bill savings

The impact of the retrofits on household dual fuel bills is shown using the SAP fuel prices of 3p per kWh for gas and 13p per kWh for electricity. These values are therefore substantially out-of-date at the writing of this report. The impact of this on paybacks and fuel bill savings are discussed in the DEEP Report 2, DEEP Case Studies Summary. The indicative annual fuel bills reductions, however, are shown in Figure 3-69 for context.

- Substantial fuel bill savings were achieved, primarily due to the EWI retrofit.
- Despite 57AD having discontinuities in the EWI and not having new windows and doors fitted, the fuel bill savings are similar for each home, being between 20 % and 38 % for 55AD and 20 % and 34 % in 57AD.
- As found with the space heating demand analysis, the DSM models predict lower fuel bills (and therefore savings) than the steady-state models.
- The impact of reducing thermal bridging and fabric heat loss by installing additional EWI behind the soffits at the eaves, relocating external windows to be in-line with the EWI, and installing bay roof insulation and new external windows, meant that 55AD had a lower HTC (104 W/K) than 57AD (130 W/K). However, this did not manifest in significantly lower fuel bills; indeed, 57AD had lower fuel bills post-retrofit because it had a more efficient boiler and a combi boiler, which reduced fuel use to deliver DHW. This highlights the significance of services in fuel bills, and the importance of model inputs around space and hot water heating.

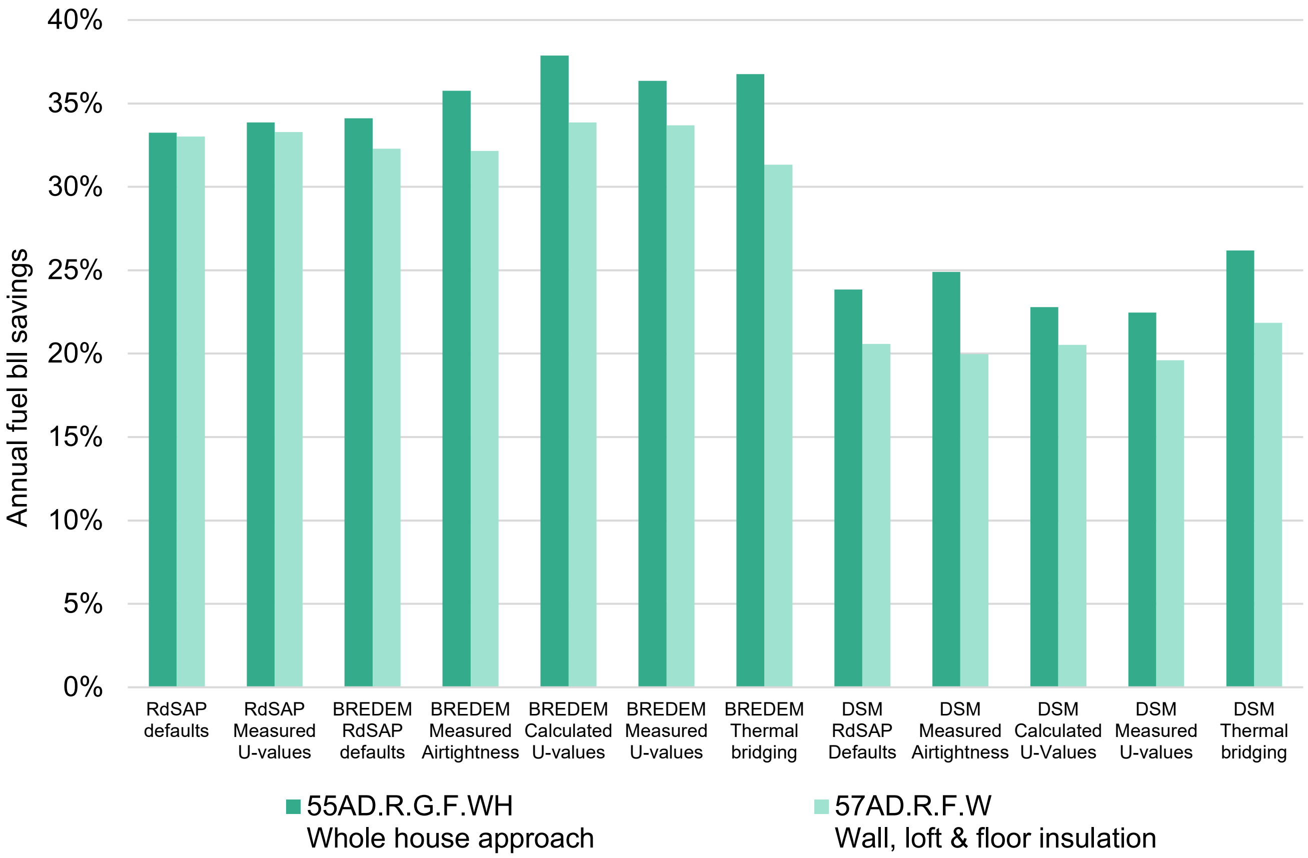

Figure 3-69 Predicted annual fuel bill savings achieved by the retrofits

3.9.2 Predicting simple payback of retrofits

The simple payback time (i.e. not considering fuel price inflation or discount rates) calculated from the retrofit costs and annual fuel bill saving estimates for this case study are shown in Figure 3-70. Recent fuel and retrofit price increases will significantly affect payback rates.

- Payback rates vary depending on which model and input data are used.
- DSM predicts lower fuel bills and lower savings; thus, the DSM payback years are predicted to be considerably higher than those predicted by the steady-state models.
- Updating model inputs to reflect measured values alters the payback predicted by around 20 years according to RdSAP, but by around 30 years in BREDEM and DSM.
- The payback between the piecemeal and whole house retrofits are similar. The greater HTC reductions achieved by 55AD are cancelled out by 57AD having higher boiler efficiency and DHW provided by a combi boiler with lower standing losses.

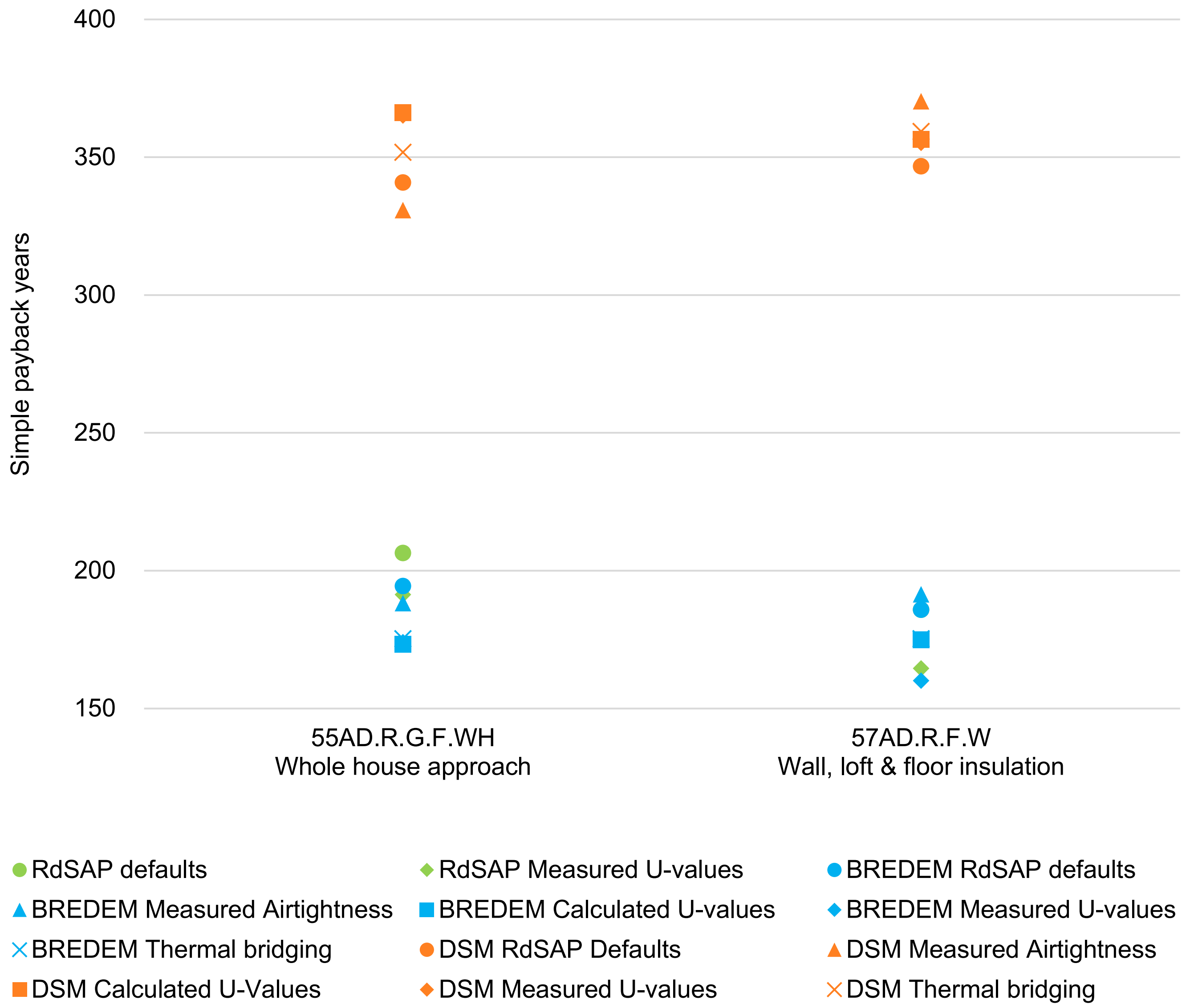

Figure 3-70 Simple retrofit paybacks

Retrofit costs summary

The piecemeal retrofit in 57AD (without the external window replacements, bay roof insulation, or EWI eaves extension) was £ 28,948, substantially lower than the retrofit in 55AD (£ 56,161), which had these additional improvements. Additionally, the 57AD retrofit was more cost effective, costing only £ 305 per W/K reduction in HTC achieved, compared to £ 416 for 55AD. Both retrofits were generally more expensive than benchmark data, though this is to be expected from one-off, small-scale projects.

The costs of revisiting 57AD to add the new external windows, bay roof insulation, and EWI eaves extension increased the cost of the retrofit to £43,912, though this was still 22 % lower than the equivalent retrofit in 55AD.

The extra cost in 55AD were mainly associated with attempts to ensure the windows were installed in-line with the EWI, i.e. fitting them into plywood boxes, and rebuilding the bay window frames. Neither of these had a significant impact on reducing thermal bridging heat losses compared to 57AD, where the original windows were left in-situ, nor did this reduce surface condensation risk.

Conversely, while insulating the bay window roof and extending the EWI through the soffits to join the loft insulation at the eaves, was marginally more expense (4 % of the retrofit cost), it substantially reduced heat losses via thermal bridges and also removed the risk of surface condensation at these locations.

More information is needed to explore the impact and costs of the design details that are the most important parts of the whole house approach to retrofit, so that those essential for promoting a risk-based approach to retrofit can be highlighted. Similarly, it may be beneficial to understand which components of a whole house approach have less of an impact on reducing risk in retrofits (and may in some instances be unnecessary) to reduce the cost barrier to whole house retrofit.

The overall payback rates were very long in both the whole house approach in 55AD (over 400 years) and in the piecemeal retrofit of loft, suspended ground floor, and external wall retrofits in 57AD (over 300 years). However, these estimates use fuel prices assumed in RdSAP. Thus, these costs require updating to be able to evaluate cost effectiveness of the retrofits more accurately.

The results also highlighted that the greater fabric improvements achieved in 55AD were offset by the higher efficiency boiler and lower DHW demand in 57AD: i.e. both homes had similar fuel bills post-retrofit, even though the 55AD fabric retrofit was far more effective. This shows the importance of the performance of services in overall retrofit savings, and for the success of whole house approaches to retrofit.

The DSM models assumed substantially lower savings and longer paybacks than the BREDEM and RdSAP models, as found in other DEEP case studies, since they include hourly calculations for useful gains etc.

4 Conclusions

This case study has identified important findings about the performance and risks associated with retrofitting solid walled homes, and investigated the models used to predict performance and risk. The main issues are discussed below:

Whole house versus piecemeal approaches

In the case study home that received the whole house approach to retrofit, the HTC was reduced by (14 ± 9) % more than its neighbour, which received a piecemeal retrofit. It also had around 10 % less space heating demand, 12 W/K less heat loss from air leakage, (32 ± 17) W/K less fabric heat loss, and around a third lower thermal bridging heat loss. However, both homes still achieved the same EPC score, and both saved roughly the same proportion of CO_2 emissions. Furthermore, most of the additional heat loss reductions are likely to be due to the whole house approach dwelling (55AD) having new external glazing and doors, while the other dwelling (57AD) did not. Thus, while it may maximise the potential heat loss reductions from any given retrofit, a whole house approach may not necessarily yield significantly more heat loss savings to similar piecemeal retrofits. However, the main driver for adopting the whole house approach is to promote a risk-based approach to retrofit and this case study confirms that this was the case. In 55AD, fewer surface condensation risks existed around the bay roof, external windows and eaves, external glazing, and external doors, than in 57AD.

Aggregated and disaggregated heat loss measurements

According to the disaggregated approach, when the measured airtightness, in-situ U-values and calculated thermal bridges were summed, 55AD's HTC was (55 ± 17) W/K lower than 57AD's. Conversely, the coheating test suggested that the difference was only (26 ± 17) W/K. Thus, caution is required when undertaking the disaggregated approach and direct whole house heat loss measurements may be preferable. Areas of uncertainty in these case study homes were that no details about the performance of the original external glazing and doors were available and so default values had to be assumed. In addition, the in-situ U-value measurements of the ground floor and bay wall were affected by ground loop issues, meaning they were excluded from the heat loss calculations. Additionally, HFPs cannot perfectly represent whole element heat loss, and the n/20 approximation cannot perfectly estimate infiltration heat losses.

Importance of Solid Wall Insulation (SWI)

The HTC of the homes was reduced by (135 ± 14) W/K, or (56 ± 6) %, in 55AD and (95 ± 16) W/K, or (42 ± 7) %, in 57AD according to the coheating tests. This is a significant amount and between 70 % and 77 % of it was achieved by the EWI. The impact of all the other retrofit measures, including the ground floor, loft, bay roof, and the installation of new external windows and doors, was therefore unimportant in terms of achieving the policy targets of an EPC band C or the SHDF 90 kWh/m²/yr target. Likewise, if all the other retrofits took place, except the EWI, the homes would not achieve an EPC band C according to RdSAP. The importance of SWI (in this instance EWI) for retrofit policy targets for solid walled homes cannot be understated.

Impact of retrofits on airtightness

The RdSAP model predicts the airtightness of homes based on building characteristics and age-band defaults. In both homes, like many of the other DEEP case study houses, the estimate (16 $m^3/(h\cdot m^2)$ @ 50Pa) was much higher than that which was measured for 55AD and 57AD (13.12 $m^3/(h\cdot m^2)$ @ 50Pa and 11.67 $m^3/(h\cdot m^2)$ @ 50Pa, respectively).

RdSAP also assumes that suspended timber ground floor retrofits will improve the airtightness of homes, yet this was not the case in these case study homes. Instead, it appears that retrofitting the bay roof, windows, and doors was mainly responsible for improving the overall airtightness (by 16 %); factors not included in the piecemeal approach taken in 57AD.

Co-pressurisation

Co-pressurisation tests were carried out in both homes prior to and following the retrofit. While airtightness tests on individual dwellings induce pressure differences on all elements of the building envelope, co-pressurising removes drivers for inter-dwelling air exchange across the party wall. When inter-dwelling air exchanges were removed, the air permeability in 55AD reduced from 12.03 to 10.15 $m^3/(h \cdot m^2)$ @ 50Pa. Post-retrofit, the air permeability reduced from to 8.29 to 5.58 $m^3/(h \cdot m^2)$ @ 50Pa. Similarly, in 57AD pre-retrofit, the air permeability reduced from 13.82 to 10.02 $m^3/(h \cdot m^2)$ @ 50Pa under co-pressurisation and again, post-retrofit reduced from 7.95 to 5.87 $m^3/(h \cdot m^2)$ @ 50Pa.

Thus, these results suggest that inter-dwelling air exchange was responsible for approximately 16 % to 33 % of the air leakage reported by the blower door test. This is significant since the inter-dwelling air exchange with the attached house is not external air but is air that has already been conditioned by the neighbour. This level of inter-dwelling air leakage could raise questions about the adequacy of the chosen ventilation strategy. More importantly in this case, it means that there may be less background ventilation heat loss taking place than the blower door tests are suggesting.

This result may have wider implications relating to those blower door tests that have taken place on attached homes across the UK housing stock, where inter-dwelling air exchanges are being reported as part of the total internal to external air leakage. Moreover, post-retrofit, air exchange with the outside was only just above the 5 $m^3/(h \cdot m^2)$ @ 50Pa threshold for which mechanical ventilation is recommended, which would not have been anticipated without the co-pressurisation tests. If the infiltration rate had been more substantially improved by the retrofit, there may have been a risk of inadequate fresh air being delivered to the homes post-retrofit for the purpose provided ventilation strategy adopted.

y-values

The non-repeating thermal bridging heat losses (HTC_b) were calculated for the homes pre- and post-retrofit. It was found that the default y-value contained within RdSAP and used in EPCs of 0.15 was overestimating the actual heat loss taking place in the uninsulated home. Analysis indicated that the y-value was more likely to be 0.10 pre-retrofit. Post-retrofit, the y-value in 55AD, where care was taken to reduce thermal bridging, was estimated to increase to 0.11. In contrast, in 57AD where EWI did not extend to the eaves and where the bay roof was not insulated, the y-value increased to 0.18. It may be beneficial therefore if more default y-values existed to represent homes in different states of insulation and with specific building characteristics that attract more thermal bridging such as bay windows.

Minimising condensation risk

Reducing condensation risk is important since this reduces risk of mould, which adversely affects health. In the uninsulated homes, almost all the junctions were at risk of surface condensation. Post-retrofit in 55AD, all of these were removed except at the door threshold. 57AD was slightly less successful in reducing risk: although it eliminated risks around the external windows, surface condensation risk remained at the eaves and first floor window heads (where EWI did not extend to the soffits), and at the bay window heads (which was left uninsulated). Thus, the whole house approach taken in 55AD may be a lower risk approach to retrofit, though it may not always be necessary to move windows in-line with EWI.

A common approach to cutting-out EWI around existing gas pipes was also investigated to discover if this caused a surface condensation risk. This was a safe approach where it took place for a short stretch and where there were no other nearby features affecting thermal bridging. Where this took place near a wall corner and a window, the risk of surface condensation was observed due to the EWI cut-out. This was, however, remedied by installing thin internal wall insulation at the window reveal, which is a more cost-effective solution to removing risk than requesting utility companies to move the gas pipes.

Model inputs and uncertainty around thermal bridging

BREDEM and RdSAP predicted substantially higher heat losses than measured or predicted by DSM. This is similar to other DEEP case studies. Additionally, the impact of replacing default model inputs with calculated and measured values only has a substantial effect on uninsulated homes. When the homes are retrofitted the divergence is reduced and models agree more closely.

Updating the model defaults with measured airtightness values, and calculated or measured U-values, changed the predicted HTC by up to 11 % in DSM and BREDEM. Updating the thermal bridging defaults with calculated values changed the predicted HTC in DSM by up to 33 %, but only 5 % in BREDEM. The reason behind this difference in impact is due to the different way in which thermal bridging is accounted for in the different models.

In BREDEM and RdSAP, HTC_b is applied as a y-value. In DSM, HTC_b is applied per junction type according to the Ψ-value and junction length. More investigation is needed into the relationship between default y-values and default Ψ-values in Appendix K. Bridging heat loss is directly influenced by building characteristics and if insulation has been installed. Thus, it may be useful to reconsider the use of age-bands in determining appropriate thermal bridging heat losses in EPCs.

Overheating

The findings identified that local shading significantly affects overheating risks. 55AD, to the south-east, substantially shades 57AD, to the north-west. This means, pre-retrofit, that the latter's risk of overheating was very low, even in the warmer future climate scenarios. In contrast, 55AD was at risk pre-retrofit. Post-retrofit the homes are at increased risk of overheating, mostly due to the insulation applied to the suspended timber ground floor, which means they no longer benefit from the cooler sub-floor temperatures in summer.

Costs

The costs of the 55AD whole house retrofit were £ 56,161, likely higher than other whole house retrofits that can benefit from economies of scale (which a standalone case study cannot). At this price, the payback time for the retrofit extends beyond the life expectancy of the homes, by a significant margin, though this analysis used outdated gas and electricity prices that are included in SAP. The costs of the piecemeal 57AD retrofit without the glazing and additional EWI insulation at the eaves or the bay window roof insulation was £ 28,948. Post-retrofit both homes had similar fuel bills. However, the reasons that 57AD appears more cost-effective is because it has a more efficient boiler, lower fuel use to deliver DHW, and substantially higher solar gains. Thus, the payback of the retrofits was not solely driven by reductions to the HTC.

Specific costs of the 55AD whole house retrofit made it much more expensive. For instance, installing windows in plywood boxes cost around £ 8,000 (14 % of the retrofit) and rebuilding the bay window frames to accommodate the new windows in line with the EWI cost approximately £ 2,000.

These activities yielded only small reductions in heat loss, via reduced thermal bridging, and were not necessary to reduce surface condensation risk, since installing the EWI and leaving the external windows in-situ in 57AD was also successful in reducing surface condensation risk in this case study. More research is needed to understand if this will be the case in homes with differing constructions and junction details.

Conversely, it was relatively cheap (£1,863) to revisit 57AD and insulate the bay roof, as well as extend the EWI behind the soffits at the eaves. Both measures were successful in substantially reducing surface condensation risk and heat losses. Thus, more investigation is needed to explore which aspects of a whole house approach to retrofit in different houses are essential and cost-effective.

References

1. Government., H., *English Housing Survey, Energy Report, 2020-21* D.f.L.U.H.a. Communities, Editor. 2021: London.

2. BSI, *BS EN ISO 10456: 2007 - Building materials and products — Hygrothermal properties - Tabulated design values and procedures for determining declared and design thermal values*, in *British Standards Institute*. 2007.

3. Anderson, B. and L. Kosmina, *Conventions for U-value Calculations. BR 443.* 2019, Building Research Establishment: Watford.

4. INCA, *Best Practice Guide External Wall Insulation*. 2015, Insulated Render and Cladding Association.

5. Sougkakis, V., et al., *Evaluation of the precision and accuracy of the QUB/e method for assessing the as-built thermal performance of a low-energy detached house in UK.* Energy and Buildings, 2022. **255**: p. 111643.

6. Meulemans, J., et al., *QUB/e: A Novel Transient Experimental Method for in situ Measurements of the Thermal Performance of Building Fabrics*, in *Building Information Modelling, Building Performance, Design and Smart Construction*, M. Dastbaz, C. Gorse, and A. Moncaster, Editors. 2017, Springer International Publishing: Cham. p. 115-127.

7. Pasos, A.V., et al., *Estimation of the infiltration rate of UK homes with the divide-by-20 rule and its comparison with site measurements.* Building and Environment, 2020. **185**.

8. CIBSE. *CIBSE Weather Data Sets*. 2016 11/02/2020]; Available from: https://www.cibse.org/weatherdata.

9. Brooke-Peat, M. and D. Glew. *Unintended Consequences of Internal Wall Insulation; Increased Risk of Mould Growth for Uninsulated Neighbours*. in *1st International Conference on Moisture in Buildings (ICMB21)*. 2021. UCL London.

10. Bonfigli, C., et al., *TM59: Design methodology for the assessment of overheating risk in homes*, K. Butcher, Editor. 2017, CIBSE: London.

11. CIBSE, *TM52: The limits of thermal comfort: avoiding overheating in European buildings*. 2013: London.

12. Palmer, J., M. Livingstone, and A. Adams, *What does it cost to retrofit homes? Updating the Cost Assumptions for BEIS's Energy Efficiency Modelling*, Department for Business Energy and Industrial Strategy, Editor. 2017, HM Government: London.

This publication is available from: https://www.gov.uk/government/publications/demonstration-of-energy-efficiency-potential-deep

If you need a version of this document in a more accessible format, please email: alt.formats@energysecurity.gov.uk
Please tell us what format you need. It will help us if you say what assistive technology you use.